2013-11-15

Novel Liposomes for Targeted Delivery of Drugs and Plasmids

Marjan Javadi
Brigham Young University - Provo

Novel Liposomes for Targeted Delivery of Drugs and Plasmids

Marjan Javadi

A dissertation submitted to the faculty of
Brigham Young University
in partial fulfillment of the requirements for the degree of

Doctor of Philosophy

William G. Pitt, Chair
Morris D. Argyle
Brad C. Bundy
Alonzo D. Cook
Randy S. Lewis

Department of Chemical Engineering

Brigham Young University

November 2013

ABSTRACT

Novel Liposomes for Targeted Delivery of Drugs and Plasmids

Marjan Javadi
Department of Chemical Engineering, BYU
Doctor of Philosophy

People receiving chemotherapy not only suffer from side effects of therapeutics but also must buy expensive drugs. Targeted drug and gene delivery directed to specific tumor-cells is one way to reduce the side effect of drugs and use less amount of therapeutics.

In this research, two novel liposomal nanocarriers were developed. This nanocarrier, called an eLiposome, is basically one or more emulsion droplets inside a liposome. Emulsion droplets are made of perfluorocarbons which usually have a high vapor pressure. Calcein (as a model drug) and Paclitaxel were used to demonstrate drug delivery, and plasmids and siRNA were used to exemplify gene delivery. Drugs or genes were encapsulated inside the interior of the liposomes along with emulsion droplets; targeting moieties were attached to the outside of the phospholipid bilayer. Ultrasound was used to break open the bilayer by changing the liquid emulsion droplets to gas, which released the content of the eLiposomes.

Transmission electron microscopy (TEM) was used to prove the formation of eLiposomes and confocal microscopy showed the uptake of drugs and genes *in vitro*. Cell viability was measured to show the effect of uptake in cancer cells.

Results indicate that eLiposomes were successfully made and that they were endocytosed into the cell. It was observed that the emulsion and the targeting moiety in combination with ultrasound are the essential elements required to produce release from eLiposomes.

Keywords: Marjan Javadi, emulsion, liposomes, eLiposomes, drug delivery, gene delivery, ultrasound, Doxorubicin, Paclitaxel, siRNA, calcein, perfluorocarbon.

ACKNOWLEDGEMENTS

I would first like to thank my mother without whose continuous support and encouragement I never would have been able to achieve my goals. She has always been there for me whenever I needed help. My mother has sacrificed her life for me and my siblings and provided unconditional love and care. Words cannot describe how much I love you Mom. I also would like to thank my sisters and brother. You are not only my siblings but my best friends and mentors in life. I thank all of you.

My life would not be so nice if Dr. Pitt would not have accepted me in his lab. I will always be so appreciative for having such a wonderful advisor. He changed my whole life by trusting in me and letting me study under his direction, and forever and ever I am grateful for having the best advisor in the world. I want to thank him for taking my hand and teaching me everything step by step, for being always patient and being eager to teach me everything that he knows. He has been always available for me and has guided me. Aside from being my advisor and my mentor in school, he has always been like a father for me. I am delighted for having such an awesome advisor. It was one of the sweetest moments in my life when I received the acceptance from Brigham Young University. Along with my advisor I would like to thank the other members of my committee, Dr. Argyle, Dr. Bundy, Dr. Cook and Dr. Lewis.

I wish to thank my amazing friends who have spent this period of my life with me who made me feel that I am not far away from my home. I also wish to thank my coworkers.

Finally, I would like to thank the Chemical Engineering Department staff and other professors in BYU for being always helpful and friendly. I also would like to thank Brigham Young University for this wonderful opportunity to study chemical engineering.

Table of Contents

LIST OF TABLES ..... **IX**

LIST OF FIGURES ..... **XI**

1 INTRODUCTION ..... **- 1 -**

2 LITERATURE REVIEW ..... **- 5 -**

2.1 TARGETED DRUG DELIVERY ..... - 5 -
2.2 NANO-SIZED DRUG DELIVERY VEHICLES ..... - 8 -
2.2.1 Nanoparticles ..... - 8 -
2.2.2 Micelles ..... - 9 -
2.2.3 Solid Nanoparticles ..... - 9 -
2.3 LIPOSOMES ..... - 10 -
2.3.1 Liposome Structure ..... - 10 -
2.3.2 Cationic Liposomes ..... - 10 -
2.3.3 Liposomes Production ..... - 11 -
2.3.4 Vesosomes ..... - 13 -
2.4 EMULSIONS ..... - 13 -
2.4.1 Perfluorocarbons ..... - 14 -
2.5 CHARACTERIZATION OF NANOPARTICLES USED IN DRUG AND GENE DELIVERY ..... - 15 -
2.6 ULTRASOUND ..... - 16 -
2.7 ACOUSTIC DROPLET VAPORIZATION ..... - 18 -
2.8 LAPLACE PRESSURE ..... - 19 -
2.9 POLYETHYLENE GLYCOL (PEG) ..... - 20 -
2.10 TARGETING VESICLES TO CELLS ..... - 21 -
2.11 THERAPEUTICS ..... - 23 -
2.11.1 Drugs ..... - 23 -
2.11.2 Plasmid ..... - 27 -
2.11.3 siRNA ..... - 27 -
2.11.4 Drug Loading ..... - 30 -
2.11.5 Endocytosis and endosomes ..... - 30 -
2.11.6 Drug Release from Carriers ..... - 32 -
2.12 PREVIOUS WORK WITH ELIPOSOMES ..... - 32 -

3 OBJECTIVES ..... - 35 -

4 MATERIALS AND METHODS ..... - 37 -

4.1 MATERIALS AND EQUIPMENT ..... - 37 -

4.1.1 Materials ..... - 37 -

4.1.2 Transmission Electron Microscopy ..... - 38 -

4.1.3 Dynamic Light Scattering ..... - 38 -

4.1.4 Confocal Microscopy ..... - 39 -

4.1.5 Ultrasound ..... - 39 -

4.1.6 Fluorometer ..... - 40 -

4.2 METHODS AND PROCEDURES ..... - 40 -

4.2.1 PFC6 Emulsion Droplet Formation ..... - 40 -

4.2.2 PFC5 Emulsion Droplet Formation ..... - 41 -

4.2.3 1-step eLiposomes Formation with PFC6 and PFC5 Emulsions ..... - 41 -

4.2.4 eLiposomes Made by Ultra Method ..... - 42 -

4.2.5 Encapsulating Calcein ..... - 43 -

4.2.6 Encapsulating doxorubicin ..... - 43 -

4.2.7 Encapsulating Paclitaxel ..... - 45 -

4.2.8 Encapsulating Plasmid ..... - 45 -

4.2.9 Encapsulating siRNA ..... - 46 -

4.2.10 Separation by Pillow Density Method ..... - 47 -

4.2.11 Folate incorporation ..... - 49 -

4.2.12 Cell Culture ..... - 49 -

5 NEW TECHNIQUES OF ELIPOSOME FORMATION ..... - 51 -

5.1 INTRODUCTION ..... - 51 -

5.2 RESULTS ..... - 52 -

5.2.1 1-Step eLiposomes ..... - 52 -

5.2.2 Ultra eLiposome ..... - 58 -

5.2.3 Characterization of eLiposomes Containing Calcein ..... - 59 -

5.2.4 Calcein Delivery to Cells ..... - 60 -

5.2.5 Discussion ..... - 63 -

6 CALCEIN AND PLASMID DELIVERY USING ELIPOSOMES ..... - 69 -

6.1 INTRODUCTION ..... - 69 -

6.2 RESULTS ..... - 70 -
6.2.1 Effect of Ultrasound ..... - 70 -
6.2.2 Effect of Emulsion ..... - 73 -
6.2.1 Effect of Folate ..... - 74 -
6.2.2 Effect of Time and Intensity of Ultrasound ..... - 78 -
6.3 DISCUSSION ..... - 79 -
7 OTHER PARAMETERS CONTROLLING OF ULTRASONIC RELEASE FROM ELIPOSOMES ..... - 87 -
7.1 INTRODUCTION ..... - 87 -
7.1.1 Effect of Ultrasound Intensity on Release from eLiposomes ..... - 88 -
7.1.2 Effect of Insonation Time on Release from eLiposomes ..... - 89 -
7.1.3 Effect of Temperature on Release from eLiposomes ..... - 92 -
7.1.4 Effect of Perfluorocarbon Composition on Release from eLiposomes ..... - 94 -
7.1.5 Effect of Storage Time on Release from eLiposomes ..... - 96 -
7.2 DISCUSSION ..... - 97 -
8 DELIVERY OF PACLITAXEL, DOXORUBICIN AND SIRNA USING ELIPOSOMES .... - 101 -
8.1 INTRODUCTION ..... - 101 -
8.2 DELIVERY OF PACLITAXEL TO CELLS USING ELIPOSOMES ..... - 102 -
8.2.1 Effect of Ultrasound in Delivery of eLipoTax ..... - 102 -
8.2.2 Effect of Emulsion on PTX release ..... - 103 -
8.2.3 Effect of Folate ..... - 105 -
8.3 DELIVERY OF DOXORUBICIN TO THE CELLS USING ELIPOSOMES ..... - 107 -
8.4 DELIVERY OF SIRNA TO HELA CELLS USING ELIPOSOMES ..... - 108 -
9 CONCOLUSIONS AND RECOMMENDATIONS ..... - 111 -
9.1 CONCLUSIONS ..... - 111 -
9.2 RECOMMENDATIONS ..... - 114 -
10 REFERENCES ..... - 117 -

LIST OF TABLES

Table 1: Impact of particle size on biological systems, table taken from [5] with permission. ..... - 7 -

Table 2: Combination of surfactants attempted in forming 1-step eLiposomes ..... - 57 -

LIST OF FIGURES

Figure 1: Illustration of the ideal eLiposome. The bilayer vesicle contains targeting ligands. Inside the bilayer are drug molecules (round spheres) and emulsion droplets (green spheres) stabilized with phospholipids. The surface structures represent targeting ligands molecules (dark blue spheres) and polyethylene glycol chains. ..... - 2 -

Figure 2: Various liposomal structures. Taken from [11] with permission. ..... - 10 -

Figure 3: Structure of antibody and antibody fragments. Taken from [63] with permission..... - 22 -

Figure 4: Structure of Paclitaxel. ..... - 23 -

Figure 5: Structure of Doxorubicin. ..... - 26 -

Figure 6: Production of eLiposomes by the 1-step process; A) Phospholipid is deposited on the flask. B) Emulsion is added. C) eLiposomes form while rotating the flask. Sizes are not to scale in this illustration. Taken from [106] with permission..... - 42 -

Figure 7: This illustrates the pillow density method, which uses sodium chloride, glucose and sucrose solutions with the same osmolarity and different densities to separate the empty liposomes, eLiposomes and free emulsions based on their differences in density. Taken from [106] with permission. ..... - 48 -

Figure 8: Pillow density method. Top layer (clear) contains sodium chloride. Bottom layer (blue) contains sucrose. Middle layer (red) contains eLiposomes. This is a two- layer pillow density technique. .... - 48 -

Figure 9: Light scattering results showing (A) distribution of DPPA emulsions of PFC6; (B) bimodal distribution of eLiposome suspension made by hydrating a DMPC film with the emulsion characterized in 9A. Taken from [106] with permission..... - 53 -

Figure 10: Light scattering data showing (A) distribution of DPPA emulsions with PFC5; (B) bimodal distribution of the eLiposome suspension made by hydrating a DMPC film with the emulsion characterized in 10A. Taken from [106] with permission..... - 54 -

Figure 11: Negatively stained 1-step eLiposomes, made from PFC6 emulsions stabilized with DPPA surfactant inside liposomes made from DMPC. L: eLiposome membrane. E: emulsion droplet. Taken from [106] with permission. ..... - 55 -

Figure 12: 1-step eLiposomes imaged by cryo-TEM showing a DPPA emulsion inside the bilayer of DMPC liposomes and an emulsion external to the eLiposome. The microscope stage is rotated to +40° (A), 0° (B) and -40°(C) to demonstrate the encapsulation of emulsion droplet inside the liposome. L: eLiposome membrane. E: emulsion droplet. Taken from [106] with permission. ..... - 56 -

Figure 13: cryo-TEM images of an ultra eLiposome made from a DMPC-stabilized emulsion inside the bilayer of a DMPC liposome. The microscope stage was rotated to +45° (A), 0° (B) and -45° (C) to demonstrate the encapsulation of an emulsion droplet inside the liposome. L: eLiposome membrane. E: emulsion droplet. Taken from [106] with permission. ..... - 59 -

Figure 14: Cartoon pictures of eLiposomes with A) 1 B) 2 and C) 3 emulsion droplets inside. Cryo-TEM picture of eLiposomes with D) 1 E) 2 and F) more than 2 emulsion droplets inside. White bar in each picture indicates 100 nm. ..... - 60 -

Figure 15: Images of HeLa cells exposed for 2 hours to ultra eLiposomes containing 15 mM calcein, followed by application of 20 kHz ultrasound at 1W/cm^2 for 2 seconds. (A, B) eLiposomes were not folated. (C, D) eLiposomes contained folate in their phospholipid membrane. A and C are light images, B and D are confocal fluorescent images. Taken from [106] with permission. ..... - 62 -

Figure 16: (A) Confocal image of HeLa cells exposed to calcein-containing folated liposomes (no emulsion within) for 2 hours after which ultrasound was applied at 1W/cm^2 for 2 seconds. (B) Confocal image of a similar experiment except that folated eLiposomes (containing PFC5 emulsions) were used. Taken from [106] with permission. ..... - 63 -

Figure 17: Light (A) and confocal images (B) of HeLa cells exposed to PFC5 folated-eLiposomes containing calcein but not insonated. Light (C) and confocal (D) images of cells exposed to ultrasound at 1W/cm2 for 2 s. (E) Average fluorescence intensity from confocal images of HeLa cells. Error bars represent 95% confidence intervals. Taken from [136] with permission. ..... - 71 -

Figure 18: (A) Confocal image of HeLa cells exposed to plasmid-containing folated eLiposomes 48 hours after adding eLiposome droplets. (B) Confocal image of the same experiment except that ultrasound was applied. C) Average fluorescence intensity from confocal images of HeLa cells. Error bars represent 95% confidence intervals. Taken from [136] with permission. ..... - 72 -

Figure 19: (A) Confocal image of HeLa cells exposed to folated liposomes (containing 15 mM calcein but not emulsion droplets) for 2 hours after which ultrasound was applied. (B) Confocal image of the parallel experiment except that folated eLiposomes (containing calcein and emulsion droplets) were used. (C) Average fluorescence intensity from confocal images. Error bars represent 95% confidence intervals. Taken from [136] with permission. ..... - 74 -

Figure 20: (A) Confocal image of HeLa cells exposed to folated liposomes containing plasmid (but not emulsion droplets) 48 hours after ultrasound was applied. (B) Confocal image of the parallel experiment except that folated eLiposomes (containing plasmid and emulsion droplets) were used. (C) Average fluorescence intensity from confocal images of HeLa cells. Error bars represent 95% confidence intervals. Taken from [136] with permission..... - 75 -

Figure 21: Confocal images of HeLa cells after being exposed to eLiposomes containing 15 mM calcein for 2 h, followed by application of 20 kHz ultrasound for 2 s at 1W/cm^2. (A) Cells incubated with non-folated eLiposomes. (B) Cells incubated with folated eLiposomes (C) Cells that were exposed to free folate (6-8 mg/mL) prior to adding folated eLiposomes. (D) Average fluorescence intensity from confocal images of HeLa cells. Error bars represent 95% confidence intervals. Taken from [136] with permission..... - 77 -

Figure 22: Confocal image of HeLa cells after being exposed to eLiposomes containing AFP plasmid and followed 2 h later by application of 20 kHz ultrasound. (A) Non-folated eLiposomes. (B) Folated eLiposomes. (C) Folate receptors were blocked with free folate (6-8 mg/mL) prior to adding the folated eLiposomes. All images were collected 48 h after applying the ultrasound at 1W/cm^2 for 2 seconds (D) Average fluorescence intensity from confocal images of HeLa cells. Error bars represent 95% confidence intervals. Taken from [136] with permission..... - 78 -

Figure 23: Confocal images of HeLa cells exposed to eLiposomes containing calcein after applying ultrasound as follows:(A) 0 J/cm^2 , (B) 0.25W/cm^2 × 2s = 0.5 J/cm^2, (C) 0.25W/cm^2 × 4s = 1 J/cm^2, (D) 0.75W/cm^2 × 2s = 1.5 J/cm^2, (E) 1W/cm^2 × 3.2s = 3.2 J/cm^2, and (F) 1W/cm^2 × 6.4s= 6.4 J/cm^2. (G) Average fluorescence intensity from confocal images of HeLa cells. Error bars represent 95% confidence intervals. Taken from [136] with permission..... - 80 -

Figure 24: Confocal images of HeLa cells exposed to eLiposomes containing plasmid after applying ultrasound as follows: (A) 0 J/cm^2 , (B) 0.25W/cm^2 × 2s = 0.5 J/cm^2, (C) 0.25W/cm^2 × 4s = 1 J/cm^2, (D) 0.75W/cm^2 × 2s = 1.5 J/cm^2, (E) 1W/cm^2 × 3.2s = 3.2 J/cm^2, and (F) 1W/cm^2 × 6.4s= 6.4 J/cm^2. (G) Average fluorescence intensity from confocal images of HeLa cells. Error bars represent 95% confidence intervals. Taken from [136] with permission..... - 81 -

Figure 25: Calcein release from conventional liposomes (▲) and eLiposomes (●). Error bars indicate the standard deviation of repeat experiments (n≥3). Ultrasound was applied for 200 ms. eLiposomes and conventional liposomes were about 200 nm and had PEG in their bilayer..... - 89 -

Figure 26: Calcein release from liposomes (Δ) and eLiposomes (o) at 23°C, and liposomes (▲) and eLiposomes (●) at 37°C, and negative control (■). A) 0.5 W/cm^2, B) 1 W/cm^2 , C) 1.5 W/cm^2. Error bars indicate the standard deviation of repeat experiments (n≥3). eLiposomes and conventional liposomes were about 200 nm and had PEG in their bilayer. E, F and G are replotted of A, B and C respectively which indicate rate of release from eLiposomes (Δ) and eLiposomes (o) at 23°C, and liposomes (▲) and eLiposomes (●) at 37°C, and negative control (■). E) 0.5 W/cm^2, F) 1 W/cm^2 , G) 1.5 W/cm^2. In E, F and G, x axis indicates average time interval in which release happened..... - 92 -

Figure 27: Calcein release from liposomes (Δ) and PFC5 eLiposomes (o) at 23°C and liposomes (▲) and PFC5 eLiposomes (●) 37°C. Error bars indicate the standard deviation of repeat experiments (n≥3). Ultrasound was applied for 200 ms to eLiposomes and conventional liposomes were about 200 nm and had PEG in their bilayer. ..... - 93 -

Figure 28: Calcein release from eLiposomes containing droplets of various mole ratios of PFC5/PFC6: 100/0 (●), 75/25 (o), 50/50 (▲), 25/75 (Δ), and 0/100 (■). Error bars indicate the standard deviation of repeat experiments (n≥3). Ultrasound was applied for 500 ms to eLiposomes that were about 200 nm in diameter and had PEG in their bilayer. ..... - 95 -

Figure 29: Calcein release from eLiposomes as a function of the calculated vapor pressure of the PFC droplets and the ultrasound intensity. 1.25 W/cm^2 (●) 2.5 W/cm^2 (□), 3.75 W/cm^2 (▲) and, 5 W/cm^2 (■) Error bars indicate the standard deviation of repeat experiments (n≥3). Ultrasound was applied for 500 ms. The eLiposomes were about 200 nm in diameter and had PEG in their bilayer. - 95 -

Figure 30: Premature release (without any insonation) of calcein from eLiposome at 4°C (▲) and 23°C (●). Error bars indicate the standard deviation of repeat experiments (n≥3). eLiposomes and conventional liposomes were about 200 nm in diameter and had PEG in their bilayer. ..... - 96 -

Figure 31: Effect of ultrasound on cell viability of HeLa cells after incubation with various formulations for 15 min before insonation. Insonation was done at 1 W/cm^2 for 2 seconds. Error bars show the standard deviations (n≥ 3). ..... - 103 -

Figure 32: Effect of emulsion droplets on cell viability of HeLa cells after incubation with various formulations at various times. Insonation was done at 1W/cm^2 for 2 seconds. Error bars are standard deviations (n=3). ..... - 104 -

Figure 33: Effect of folate on cell viability of HeLa cells after incubation with eLiposomes at various times. Insonation was done at 1 W/cm^2 for 2 seconds. Error bars are standard deviations (n=3).... - 106 -

Figure 34: PhLP blot. First column on left is the ladder (molecular-weight size marker), columns 2-4 are non-specific siRNA encapsulated in eLiposomes, columns 5-7 are specific siRNA encapsulated in eLiposomes, column 8 is the negative non-specific Lipofectamine control, and column 9 is the positive Lipofectamine control..... - 110 -

1 INTRODUCTION

Drug delivery is a process by which humans or animals receive pharmaceutical compounds. Drug delivery technology is modification of the release, absorption and circulation of drug in the body to improve effectiveness and safety of the drug and also entails a more convenient way for a patient to receive the drug. Some common routes for delivering drugs are through the mouth, skin, nose, eyes and mucosal surfaces.

Some of the gene-based drugs, vaccines and antibodies (such as polynucleotides and polypeptides) cannot be delivered by those routes; they are digested in the stomach or are not absorbed into the circulatory system because of their size or charge. Injection is the best way to deliver these kinds of drugs, either directly into the target tissue or into the circulatory system. Immunizations are usually done by injection of proteins into tissue. Chemotherapy is usually done by injection into the circulatory system.

My dissertation research was centered on developing a new therapeutic delivery system that employs ultrasound to accomplish the delivery at a specific site. The delivery system consists of liposomes and perfluorocarbon emulsions, and is designed to securely sequester the therapeutic and then release it only when activated by ultrasound. The disadvantage of oral delivery or injection into the circulatory system is its broad distribution. Often it is desired to confine the effect of the drug to a specific region or tissue.

Controlled delivery a specific region or tissue istermed “targeted drug delivery”.

Figure 1 shows an ideal drug delivery vehicle called an eLiposome. An eLiposomes is defined as one or more emulsion droplets inside a liposome. The thin shell of the eLiposome is a

phospholipid bilayer that may contain targeting ligands. Inside the bilayer are drug molecules (round spheres) and emulsion droplets (large spheres) stabilized with phospholipids. Sizes are not to scale in this illustration.

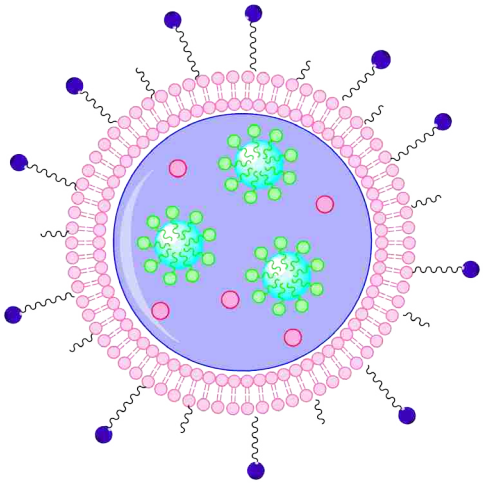

Figure 1: Illustration of the ideal eLiposome. The bilayer vesicle contains targeting ligands. Inside the bilayer are drug molecules (round spheres) and emulsion droplets (green spheres) stabilized with phospholipids. The surface structures represent targeting ligands molecules (dark blue spheres) and polyethylene glycol chains.

The overall objective of this research is to improve the design and manufacturing of eLiposomes so they could be used to deliver specific drugs, plasmids and siRNA. The eLiposomes may have targeting ligands on their surface so they can be directed to the cancerous cells and be endocytosed. The emulsion droplets are made of perfluorohexane (PFC6) and perfluoropentane (PFC5) which are nontoxic and can be converted to gas by applying ultrasound (US). The ultrasound causes emulsion droplets to change their phase from liquid to gas and rupture the eLiposomes to release the payload. Calcein and Paclitaxel (PTX) were studied as

model therapeutic agents. Plasmid and siRNA were studied for gene delivery purposes. The scope of this research included eLiposome formation and characterization and also the release of the drug and expression of genes.

2 LITERATURE REVIEW

2.1 Targeted Drug Delivery

The objective of targeted drug delivery is to confine the effect of the drug to specific tissues, cells, and cellular structures. In this process the drug is released only in a particular region and the concentration of drug is higher in that region compared to other regions. Such confinement improves the efficiency of the drug and reduces the side effects of the drug on other tissues. Targeted drug delivery can also include temporal control of when the drug is released. Targeted drug delivery is often used in treatment of cancer because it can localize drug delivery to tumors and not to adjacent healthy tissues or tissue throughout the body. For example, in chemotherapy it is preferred that drug is delivered to the targeted tissue instead of injecting and circulating it to the whole body. In addition to reducing side effects, targeted drug delivery requires less amount of drug, which is economically preferable. The best possible scenario is to release the drug only inside of the targeted cell. Drug released outside the cell can diffuse away and damage other cells.

Designing the best system to deliver drugs to cancerous cells is one of the challenging steps in cancer treatment. Passive and active techniques are two general categories of methods employed for targeted drug delivery [1].

In passive delivery there are no targeting ligands; drug carriers accumulate within tumors that have leaky vasculature [2]. This phenomenon is generally called the enhanced permeation and retention (EPR) effect. Certain sizes of molecules (apparent molecular size larger than 50 kDa), typically liposomes or macromolecular drugs, tend to accumulate in tumor tissue much more than they do in normal tissues. This occurs because tumor cells often stimulate the production of new and rapid capillary growth, and these capillaries are often poorly formed. They have holes in them which allow the passage of submicron particles out of the capillaries and into the cancerous tissue. Poor lymphatic drainage of the tissue also contributes to the passive accumulation of submicron particles [3, 4]. See Table 1.

Active targeting occurs through specific binding interactions between the carrier and the cell. Ligands bind specifically to complementary receptors and play a key role in active delivery to the cells. Furthermore the sub-micron size of the nanovehicles can allow them to be taken into the cells via endocytosis, particularly if the particles have ligands that induce endocytosis when bound [6]. In an ideal scenario, nanocarriers passively enter tumor tissue via the EPR effect, bind to selected tumor cells via specific ligands, and are endocytosed into tumor cells. All that remains is to actuate the release of the drug from the carrier once it has been endocytosed.

Table 1: Impact of particle size on biological systems, table taken from [5] with permission.

Size	Biological systems and remarks
4.5 nm	Abundant small pores present in normal tissue endothelium
25 nm	Relatively few large pores present in normal tissue endothelium
20–50 nm	Average size of polymeric micelles without loaded drugs
100 nm	Frequently tested size of drug-loaded polymeric micelles
150 nm	Proposed cutoff size for particle extravasation in liver
200 nm	Nanoparticles less than 200 nm have significantly longer circulation time due to low uptake by the reticuloendothelial system (RES)
380 nm	A tumor-dependent functional pore cutoff size ranges from 200 nm to 1.2 μm, but the pore cutoff size of porous blood vessels in majority tumors is known to be 380–780 nm. Thus, the range for the EPR effect should be similar.
400 nm	Sterically stabilized liposomes of 400 nm in diameter were able to penetrate into tumor interstitium. Accumulation of hyaluronic acid-coated nanoparticles (400 nm) in the tumor tissue
500 nm	The maximum size of nanoparticles allowing penetration through cell membranes is known to be 500 nm
1 um	Particles below 1 um were taken up by Peyer's patches and then migrated to mesenteric lymph nodes
5 um	The upper limit for rigid particles circulating within the smallest capillaries
40 um	Particles larger than 40 um have been used for embolization therapy

2.2 Nano-sized Drug Delivery Vehicles

2.2.1 Nanoparticles

Nanoparticles include structures known as nanocapsules or nanospheres. Nanocapsules are vesicular systems in which a drug is confined to a cavity surrounded by a polymer membrane, whereas nanospheres are matrix systems in which the drug is physically dispersed in a solid [7].

By definition, nanoparticles range in size from 1 to 999 nm. The size of the nanoparticles is a strong determinant of where and how the particle will be distributed in the body. For example nanoparticles with a diameter of over 200 nm usually show a more rapid rate of clearance from blood than particles with radius under 200 nm [5]. In addition to the size, the surface chemistry of nanoparticles is very important in the distribution of the particle through the body.

When nanoparticles enter the blood system, the immune system attempts to identify and remove the particles. Opsonization involves the binding of an opsonin (a protein) or binding of an antibody (also a protein) to the nanoparticle. The opsonins signal the cells of the reticulo endothelial system (RES) to engulf and rapidly clear these particles from the blood [8].

Since most nanoparticles in the blood stream are opsonized rapidly, it is necessary to reduce the opsonization by coating the particles with hydrophilic polymers such as polyethylene glycol (PEG) chains [8]. The PEG chains reduce the rate of opsonin adsorption, which greatly reduces the clearance rate so that the particles persist in the blood long enough to release drug or to extravasate.

2.2.2 Micelles

A micelle is a colloidal collection of surfactant molecules dispersed in a liquid. Surfactants have head and tail groups; the heads are hydrophilic and are surrounded by the solvent, and the tail group is hydrophobic and is located in the center of the micelle structure. Their hydrophobic interior enables micelles to sequester hydrophobic drugs that will not be released until application of some type of drug delivery mechanism or stimulus that disrupts the micelle [9].

A normal micelle has a hydrophobic core and hydrophilic surface and is used in drug delivery. An inverse micelle has hydrophobic tails which extended out to a nonpolar solvent while the heads cluster in the interior. Most micelles are spherical, but cylinders and ellipsoids are other possible shapes. The molecular geometry of the surfactant molecules and also conditions of temperature, pH, and surfactant concentration will determine the shape and size of the micelles [8].

2.2.3 Solid Nanoparticles

Solid nanoparticles have solid cores and are not always spherical vesicles. Solid lipid nanoparticles (SLN) are made from solid lipids with diameter between approximately 50 and 999 nm [10]. Drug molecules can attach to these particles or be formulated within these particles for use in drug delivery systems.

2.3 Liposomes

2.3.1 Liposome Structure

A liposome is a small vesicle made of surfactant molecules that form bilayer sheets and fold into a spherical vesicle. Liposomes can be formed from the same natural phospholipids found in cell membranes, or they may be formed from synthetic surfactants. The surfactants most often have a hydrophobic tail and a hydrophilic head.

Liposomes are classified on the basis of their structure, method of preparation, composition and application. They can also be classified as conventional or specialty liposomes.

Based on their structure liposomes include; unilamellar vesicle (UV), small unilamellar vehicle (SUV), medium unilamellar vesicle (MUV), large unilamellar vesicle (LUV), giant unilamellar vesicle (GUV), oligolamellar vesicle (OLV), multilamellar vesicle (MLV), and multi vesicular vesicle (MVV) (See Figure 2).

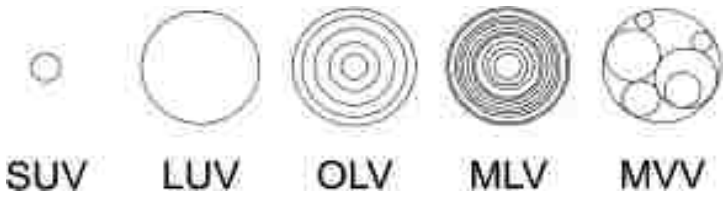

Figure 2: Various liposomal structures. Taken from [11] with permission.

2.3.2 Cationic Liposomes

Cationic liposomes represent a non-specific alternative approach to active targeting. Cationic liposomes comprise a lipid component that creates an overall positive surface charge and no specific ligand is used as a targeting moiety. It is the positively charged component of the liposome itself that binds through electrostatic interactions to negatively charged phospholipid

head groups that are on the surface of all cells, and which are preferentially expressed on tumor endothelial cells [12]. The disadvantage of cationic liposomes is that they are taken up by all cells because all cells express some negatively charged phospholipids. Cationic lipids are also toxic [13]. While they may be used beneficially for delivery *in vitro* in cell culture, their use *in vivo* is problematic because of non-specificity and toxicity.

2.3.3 Liposomes Production

The three different strategies for the preparation of liposomes are as follows:

a) Mechanical methods

b) Methods based on replacement of organic solvent

c) Methods based on size transformation or fusion of prepared vesicles

Mechanical methods consist of film methods and ultrasonic methods. The film method is the simplest procedure for preparing liposomes but has some limitations. In this method liposomes are prepared by depositing a thin lipid film from an organic solvent onto the surface of a flask. The organic solvent is removed under vacuum. When all the solvent is removed, the mixture was hydrated by adding water or some aqueous buffer. The lipids swell and hydrate to form bilayer sheets which close upon themselves to form liposomes. In this method most of the liposomes are MLV and over 1 micrometer in diameter [14], which is usually too large for drug delivery. Loading drug through the multiple layers can be complex.

The ultrasonic method is used for preparing SUVs with diameter in range of 10 nm to 25 μm in diameter. There are two ultrasonic methods; probe sonication and bath sonication. The probe sonication is used for small volumes while the bath is employed for large volumes. Increasing the time and/or intensity of ultrasonication reduces the size of the liposomes [15].

Sonication reduces the size and complexity of particles, reducing OLVs, MLVs and MVVs to SUVs [15].

In methods based on replacement of organic solvents, lipids are co-solvated in organic solution and then dispersed into an aqueous phase containing some chemicals (usually therapeutics) to be entrapped within the liposomes.

Methods based on size transformation or fusion of preformed vesicles include freeze thaw extrusion and dehydration-rehydration. The freeze–thaw method consists of repeated cycles of quickly freezing (in liquid N_2) and thawing (in warm water) of a liposome dispersion formed with the film method [16]. Complex vesicles are broken into SUVs during the freeze-thaw cycles. Dehydration-rehydration method is another process which starts with 'empty' (buffer-containing) SUVs, which are mixed with a marker- or drug-containing solution. This mixture is either dried by vacuum or freeze-dried. In this process the small vesicles fuse to form large aggregates with the marker or drug enclosed [17, 18].

Biocompatibility, versatility and biodegradability are some of the advantages of using liposomes as drug carriers. The lipids that are used to form the liposomes can be custom tailored for a specific application to control the surface charge, chemical properties, rigidity, and stability of the liposome. Over the past decade liposomes have been investigated as drug carriers in a wide variety of applications, including transdermal delivery and intravenous delivery of a wide range of therapeutics [19]. Inclusion of PEG on the surface of the liposome has been shown to decrease opsonization and increase the time that the liposomes remain in the body compared to non-PEGylated liposomes [19, 20].

Because of their small size, liposomes have been used in passive targeting for cancer therapy. Liposomes can be made sufficiently small to extravasate via the EPR effect, which produces a high drug concentration in cancerous tissues.

2.3.4 Vesosomes

Liposomes reformed from lipid sheets will be referred to as vesosomes [21]. Vesosomes may be empty or may contain nanosized structures such as small liposomes, micelles, emulsions, or nanoparticles. Vesosome sizes range from about 0.1 μm to greater than 1.0 μm.

To make vesosomes, very small liposomes (about 30 to 50 nm) are first formed. Then EtOH is added (about 3M) to open these vesosomes (which possess high bending stress) into bilayer lipid sheets. Once the sheets are formed, they are very stable, and EtOH can be removed by centrifugation and washing. These sheets are stable below the transition temperature (T_m) of the phospholipid. To form the vesosome, a suspension of nanoparticles (with or without drugs or other chemicals) is mixed into the sheets, and the mixture is heated above T_m. In the absence of EtOH, the sheets spontaneously fold back into large liposomes, entrapping the nanoparticles inside. External particles are removed by centrifugation, and the vesosomes can be extruded to reduce their size.

2.4 Emulsions

An emulsion is a colloidal suspension of liquid droplets in an immiscible liquid. The difference between an emulsion and a solid suspension is that in an emulsion both the dispersed and continuous phases are liquid and the emulsion droplets are usually <10 microns in diameter. For drug delivery with emulsions, the continuous phase is usually aqueous, and the drug is often

carried in the dispersed phase (the emulsion droplets) which is usually composed of non-polar hydrocarbons. Emulsions are usually unstable and do not form spontaneously. Surfactants are used to stabilize the emulsions and prevent the dispersed phase from coalescing into larger droplets. Small emulsion droplets can be formed by high mechanical shear stress (extreme stirring or shaking) or by low frequency ultrasound radiation (called insonation).

Emulsions of perfluorocarbons have been used previously as oxygen carriers in artificial blood substitutes and as ultrasound contrast agents for imaging [22, 23]. Common surfactants for these emulsions are phospholipids [24].

2.4.1 Perfluorocarbons

Fluorocarbons and perfluorocarbons are organic chemical compounds that contain carbon and fluorine bonded in the polarized and remarkably strong carbon-fluorine bond. They can be gases, liquids, waxes, or solids, depending upon their molecular weight. Fluorocarbon liquids are colorless. They have high density, due to their high molecular weight (fluorine instead of hydrogen). They have low viscosities when compared to liquids of similar boiling points. They have very low solubility in water, and water has very low solubility in them. The number of carbon atoms in a fluorocarbon molecule determines physical properties. The greater the number of carbon atoms, the higher the boiling point, density, viscosity, surface tension, critical properties, vapor pressure and refractive index.

PFC6 (perfluorohexane, C_6F_{14}) is a perfluorocarbon used in this research. It is a derivative of hexane in which all of the hydrogen atoms are replaced by fluorine atoms. It is considered inert and stable. Its normal boiling point is 56°C. Perfluorohexane dissolves gases, including oxygen, to a higher concentration than is found in other liquids. Animals can be

submerged and breathe in a bath of oxygen-saturated perfluorohexane without drowning, as there is sufficient oxygen available in the solvent to allow respiration to continue.

PFC5 (perfluoropentane, C_5F_{12}) is also another perfluorocarbon used in this research. It is a derivative of pentane and its normal boiling point is 29°C. Both PFC5 and PFC6 are biocompatible and are used in making emulsion droplets for this research. Perfluorocarbons are eliminated from the body through the lungs by exhalation.

2.5 **Characterization of Nanoparticles Used in Drug and Gene Delivery**

Particle size is one of the most important characteristics of nanoparticles because it influences the amount of drug loading, drug release, stability of the nanoparticles and most importantly the location of distribution in the body. Smaller particles have a larger surface area to volume ratio, so using nanoparticles for drug delivery allows for shorter transport distances and thus faster release rates. Large particles (> 1 μm) are quickly identified by the immune system (RES) and become localized in the liver and inside macrophages. Very small particles (< 5 nm) are quickly cleared by the kidneys. Medium-sized particles (500 nm < d < 1 μm) remain in the blood but are slowly removed by the RES. Small particles (5 nm < d < 500 nm) can extravaste into tumors [25, 26].

Electron microscopy and photon-correlation spectroscopy are two common ways of measuring the size of the nanoparticles. In photon-correlation spectroscopy, also called dynamic light scattering (DLS), the size of nanoparticles are determined from their Brownian motion. When the viscosity of the medium is known, the hydrodynamic radius can be determined from Stokes law [27].

Cryo-TEM and negative staining TEM are two common ways for visualizing nanoparticles. Cryo-TEM is a form of transmission electron microscopy (TEM) in which the sample is quickly frozen, usually using liquid ethane. Another TEM method visualizes nanoparticles by negative staining in which heavy metals (osmium, titanium or lead) is coated on the nanostructures to provide contrast. For example, lead salicylate shows up as an electron dense black dot in TEM and collects in hydrophobic environments, allowing it to be used to stain the non-polar emulsion droplets.

2.6 **Ultrasound**

Ultrasound consists of a stream of high frequency pressure waves, and is similar to audio sound except that it is above 20 kHz, the threshold of human hearing. For medical applications, the face of ultrasonic transducer is placed in contact with gel or some aqueous media that can transfer the sound waves to the body tissues. Ultrasound is commonly used for medical imaging, and is being considered for drug delivery [28-30]. One of the advantages of using ultrasound is that there is no need for surgery and the treatment can be done without any pain. There are reports of increased drug activity when drugs are administered along with the application of ultrasound, particularly for cytotoxic drugs [31]. As the frequency of the ultrasound increases, the depth of penetration into the tissue decreases.

Thermal and non-thermal effects are two main categories of the interaction between the ultrasound and body tissues. The absorption of acoustic energy by the tissues produces heat and causes thermal effects. Non-thermal (mostly mechanical) effects are produced by the oscillation of gas bubbles, which is called cavitation [32].

Cavitation phenomena also include the formation of bubbles when the local pressure of the liquid is reduced below its vapor pressure. Bubbles may also form from dissolved non-condensable gases (O_2, N_2) in the fluid. Two main categories of cavitation are inertial (also called collapse cavitation) and non-inertial cavitation (also called stable cavitation) [33].

In inertial cavitation a bubble in the liquid collapses and produces a shock wave, whereas in non-inertial cavitation bubbles oscillate for long times without collapse. If collapse cavitation occurs near to the surface, the asymmetric collapse of the bubble results in the formation of a high-velocity jet of liquid [34]. These bubble oscillations, liquid jets, and shock waves generated with ultrasound can shear and disrupt the cell membrane, creating reversible openings through which drugs, DNA plasmids or siRNA can pass [35-42]. If membrane disruptions are sufficiently large, irreversible openings are formed and the cell dies.

Ultrasound can excite bubbles of any size, but only bubbles that have the natural resonant frequency near the ultrasonic frequency can reach the highest level of oscillation required to undergo collapse cavitation. So when the ultrasonic acoustic pressure is low, bubbles oscillate with low amplitude but their size increases slowly as gases diffuse from the water into the bubble. As the acoustic pressure increases in amplitude or the size of the bubble reaches the resonance size, the bubbles collapse [28, 29]. The acoustic pressure threshold to produce collapse cavitation decreases as the frequency decreases, so more inertial cavitation is observed at lower frequencies [28, 29].

This collapse event produces a shockwave, and generates a very high pressure and temperature. The high pressure and temperature may cause cell damage. In general both inertial and non-inertial cavitation may damage the cell.

As an example, a polymer stabilized perfluoropentane (PFC5) emulsion was used to deliver Dox to tumors in mice [43, 44]. It was reported that Dox was sequestered inside polymer micelles and the mixture of polymeric nanoparticles and emulsion droplets (stabilized with the same polymer) was delivered to cells. First, heating was used to show that the droplets could be vaporized into micrometer-sized bubbles, as visualized by light microscopy. Ultrasound was then used to deliver Dox to tumor cells. Cells exposed to this treatment *in vitro* showed a higher uptake of Dox compared to negative controls. *In vivo*, tumors treated with ultrasound did not continue to grow while negative control tumors did grow.

2.7 **Acoustic Droplet Vaporization**

An alternative for pre-existing microbubbles is to use acoustic droplet vaporization (ADV), a phenomenon in which a small liquid emulsion droplet is converted to a much larger gas bubble by a pulse of ultrasound [45, 46]. Perfluorocarbons (PFCs) have been proposed for medical ADV because PFCs are non-toxic and have low solubility in blood [47]. When formulated properly and with sufficiently small size, PFC emulsions can remain stable as a liquid phase even at temperatures above their normal boiling points [45, 48, 49]. Such meta-stability is possible due to the droplet's highly curved interface that raises the internal pressure within the PFC emulsion droplet. Thus PFCs with low boiling points – such as perfluoropentane (PFC5) – could be used as a relatively stable emulsion in the human body even though its normal boiling point (29°C) is lower than body temperature (37°C).

Upon insonation the emulsion droplets can change phase from liquid to gas, and thus can be used to mechanically trigger drug delivery by gas bubble cavitation.

For example, Fabiilli et al. reported that by using ultrasound frequencies above 1 MHz and applying microsecond pulse lengths, small PFC emulsion droplets were changed from liquid to gas [50, 51].

2.8 **Laplace Pressure**

Laplace pressure is defined as the pressure difference between the inside and the outside of a curved surface.

$$\Delta P_{Lp} \equiv P_{inside} - P_{outside} = \gamma\,(1/r_1 + 1/r_2) \quad \textbf{(1)}$$

Where γ is the surface tension and r_1 and r_2 are the radii of curvature. For a sphere $r_1 = r_2$ so $\Delta P_{Lp} = 2\,(\gamma/r_1)$. Laplace pressure is another factor that affects vaporization of emulsion droplets. In general for an emulsion droplet the interior pressure (P_{inside}) is the sum of the local external pressure (P_∞) and Laplace pressure.

$$P_{inside} = P_\infty + P_{Lp} \quad \textbf{(2)}$$

In order for ultrasound to provide a driving force for emulsion droplet vaporization, a reduced local pressure must exist. The minimal amount of reduction is the difference between pressure inside the droplet and the vapor pressure of the liquid emulsion droplet.

Even though smaller emulsion droplets are more favorable for endocytosis, it is harder to vaporize them because of the Laplace pressure. The choice of surfactants employed to stabilize emulsion droplets is very important because that affects the Laplace pressure by its interfacial

energy (γ). Laplace pressure for PFC emulsion droplets can be calculated when the radius of the nanodroplets and γ are known.

Laplace pressure causes small emulsion droplets to boil at a temperature higher than their normal boiling point, which makes it suitable for our research. For example we use PFC5 with normal boiling point of 29°C, but we can still have these emulsion droplets remain thermodynamically stable at 37°C (body temperature) due to Laplace pressure [48, 52].

2.9 **Polyethylene Glycol (PEG)**

Drug therapy is more effective if the drug carriers are not rapidly cleared from blood. To increase the circulation time, nanoparticles must avoid clearance by the reticular endothelial system (RES) [53]. Usually liposomes and other nanoparticles containing drugs are quickly opsonized (coated by proteins) so they are cleared from blood very quickly, resulting in limited drug therapy. To increase their circulation time, PEG chains can be attached to the surface of the nanoparticles. PEG has been shown to increase blood circulation time and increase drug accumulation at the tumor site [54]. If prolonged circulation is desired, the drug delivery system should incorporate PEG onto the surface [54].

Even though PEG increases the circulation time, it also increases the hydrodynamic radius and thus reduces extravasation. PEG also reduces endocytosis of the liposomes [55]. To avoid this problem, the distal ends of PEG can be derivatized with ligands that bind to receptors on the cell surface that actively induce endocytosis [53], as will be discussed in the next section.

2.10 **Targeting Vesicles to Cells**

Target molecules that can be exploited to achieve selective localized attachment of drug carriers to cells can be divided into the following classes: (i) targets that are preferentially expressed on endothelial cells of tumor blood vessels (ii) targets that are overexpressed on tumor cells and (iii) lineage-specific targets that are expressed at the same level on tumor cells and on normal cells [56]. The ligand is the molecule that binds to the target, sometimes called a receptor. Ligands are attached to the carrier vesicle.

The list of ligands that are used for active targeting includes a wide range of compounds, too large to list here but which may be found elsewhere [57, 58]. This discussion will be limited to antibody fragments (Figure 3) and folic acid, since those are used with eLiposomes in our research.

Polypeptides, including polyclonal antibodies and monoclonal antibodies (mAb) and other proteins (e.g. fibrinogen and transferrin) [59, 60] have been employed as targeting ligands. mAbs, either whole mAbs [61] or mAb fragments, including Fab′ [61] and single-chain Fv fragments [61], are among the most frequently used ligands. Because mAb fragments lack the Fc domain that binds to Fc receptors on phagocytic cells (resulting in the RES scavenging particles bearing whole mAbs), particulates derivatized with mAb Fab′ fragments have increased circulation time in the blood compared to particulates derivatized with whole mAbs [62].

The frequent use of mAbs or mAb fragments as ligands for particulate drug carriers is the result of a well-established chemistry that synthesizes derivatives that retain full binding activity [64]. mAb fragments have the additional advantage that they can be expressed as recombinant proteins in prokaryotic cells, a procedure that facilitates a more cost-effective large-scale production than the production of whole mAbs in eukaryotic cells [64].

Folic acid is a natural, non-peptidic, low molecular weight vitamin that has also been employed as a targeting moiety [65]. All cells have receptors for folic acid. However, rapidly growing cells need more folic acid and usually have more receptors. Tumors of many kinds overexpress folic acid receptors and thus can be targeted with folic acid [66]. Initial *in vitro* results using liposomes derivatized with this ligand were successful in showing specific targeting [67, 68].

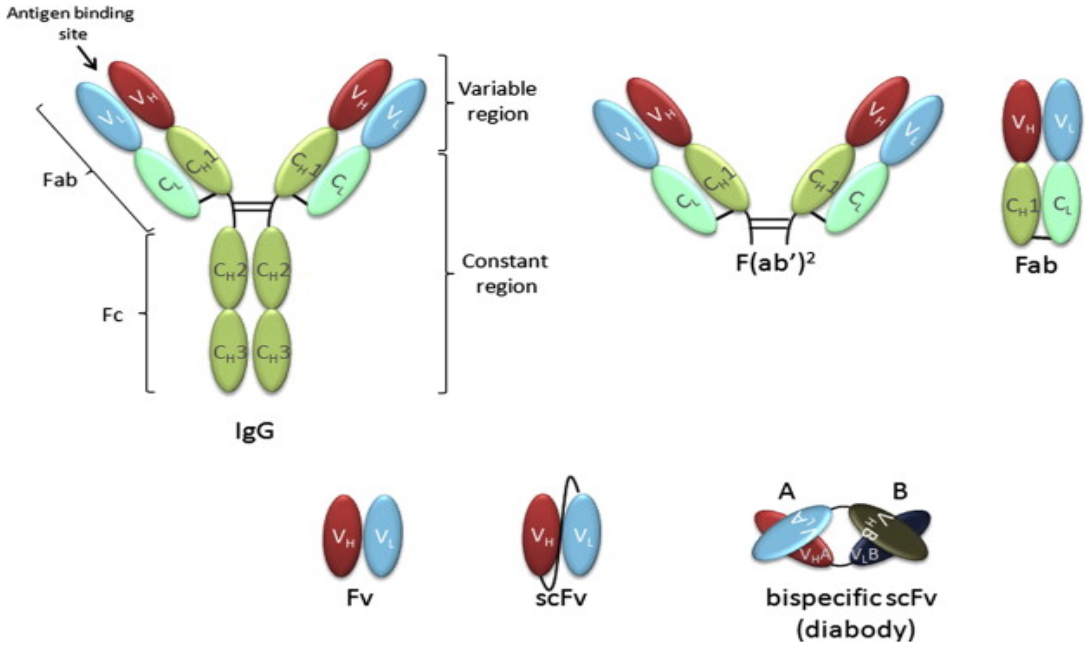

Figure 3: Structure of antibody and antibody fragments. Taken from [63] with permission.

It was also shown that upon activation of folate receptors, the folic acid (and whatever is attached to it) is taken up by clathrin-independent endocytosis, so trafficking (directed movement within a cell) is not to the digestive lysosome. It was shown that liposomes containing doxorubicin with folate on the outside increased *in vitro* cell toxicity, which suggests increased

endocytotic uptake [69]. Lee et al. observed the uptake into KB cells was 45 times higher in folated liposomes than non-targeted liposomes [70]. Folate is an attractive ligand due to its small size, tumor specificity, and ease of conjugation to PEG.

Folate has been attached to PEG using an amide bond [71]. The PEG chain provides flexible steric agility of the ligand so it can associate easily with receptors on the cell surface. Ligands attached directly to the surface of liposomes are not internalized as extensively as ligands attached to a PEG spacer [72].

2.11 **Therapeutics**

2.11.1 Drugs

2.12.1.1. Paclitaxel

Paclitaxel (PTX, trademark Taxol®) is a drug that inhibits cell division and is used in chemotherapy. PTX was extracted from the bark of Pacific yew trees and Taxus brevifolia. It was realized later than fungi in the bark synthesize the PTX. It is a pseudoalkaloid that has a taxane ring as its nucleus ($C_{47}H_{51}NO_{14}$, MW 853.93). See Figure 4.

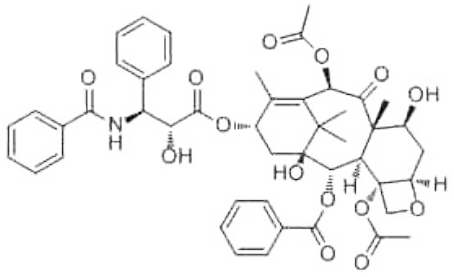

Figure 4: Structure of Paclitaxel.

PTX can be used for treatment in various cancer diseases, particularly to treat ovarian cancer, breast cancer, lung cancer, head and neck tumors, Kaposi's sarcoma, and urologic malignancies [73]. While the majority of cytotoxic drugs act by attacking the nuclear components such as the DNA, paclitaxel's toxic mechanism is different. The main site of action of paclitaxel is the microtubules in the cytosol that form the cell's cytoskeleton. PTX acts during the mitotic phase of cell division and stabilizes the polymerization of the tubulin proteins and their assembly into microtubules. They cannot depolymerize at the appropriate time, and this stops (arrests) the cell growth cycle [74]. Often the cell senses that something is wrong and undergoes apoptosis (self-destruction).

Extraction of PTX from its natural source, Taxus brevifolia, has a very low yield and requires the consumption of many trees, which is not desirable. Since PTX has a very complex structure, a fully synthetic technique of production of paclitaxel has not yet been developed [75-79]. Present industrial production of PTX is done by plant cell fermentation technology, in which PTX is extracted from a cultured Taxus cell line and purified by chromatography.

PTX is solubilized prior to use in the clinical setting (dilution before intravenous administration). The clinical formulation of drug contains polyoxyethylated castor oil (Cremophor EL) in a 1:1 v/v mixture with dehydrated ethanol. It remains stable in unopened vials for 5 years at 4°C [80].

A nanoparticle formulation for PTX was introduced in 2005 under the trade name Abraxane to reduce the toxic effects associated with the Cremophor EL in the conventional formulation described earlier, and to lessen the risk of precipitation of PTX upon dilution. Nanoparticles of biodegradable polymers and bioadhesive materials have also been considered for delivery of PTX [81].

Nanoparticles made from liposomes are also another carrier for delivery of PTX. Crosasso et al. [82] have prepared sterically stabilized PTX-containing liposomes. They compared conventional PTX-loaded liposomes with stealth or sterically stabilized (via PEG chains) long circulating paclitaxel-containing liposomes. The results showed that stealth liposomes can stay longer in blood compared to conventional liposomes [83]. Ceruti et al. also compared conventional liposome formulations of PTX with PEGylated liposomes. The PEGylated liposomes circulated for a long time, with an half-life of nearly 50 hours compared to less than 10 hours with conventional PTX liposomes [84].

The PEGylated liposomes were prepared using PTX with phospholipids and cholesterol. The formulation containing egg yolk phosphatidylcholine and phosphatidylglycerol in the ratio 9:1 and PTX and lipids in the molar ratio of 1:30 was found to have an incorporation efficiency of 95%. This formulation preserved 90% of the drug content over a period of 2 months at 4°C, during which the liposomes were physically stable [82].

2.12.1.2. Doxorubicin

The United States Food and Drug Administration (FDA) has approved about 132 anti-cancer drugs, and many of these are anthracylines; the first two anthracyclines were used early in the 1960s and are Doxorubicin (Dox) which is shown in Figure 5 and Daunorubicin (DNR). They both have aglyconic and sugar moieties. The aglycone has a tetracylic ring with a quinone-hydroquinone group adjacent to the aglycone. The daunosamine (moieties sugar) is attached by a glycosidic bond to one of the rings and has a 3-amino-2, 3, 6-trideoxy-L-fucosyl moiety. The only difference between Dox and DNR is that the side chain of Dox terminates with a primary alcohol but for DNR it terminates with a methyl group.

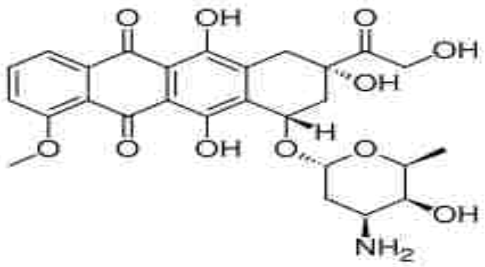

Figure 5: Structure of Doxorubicin.

Dox is one of the most used anticancer drugs, and can be used alone or in combination with other drugs. It has the widest spectrum of activity. Dox is used to treat many different cancers including breast, bile ducts, prostate, uterus, ovary, esophagus, stomach, liver and also leukemia [85].

Dox intercalates with the DNA helix and binds to proteins involved in DNA replication and transcription. This interaction causes the inhibitation of DNA, RNA and protein synthesis and finally leads to cell death, usually via apoptosis [86].

Usually Dox enters to the cancerous cells by diffusion and binds to the proteasome in cytoplasm with high affinity. Dox binds to the 20S proteasomal subunit and forms a Dox proteasome complex. This complex translocates into the nucleus with nuclear pores using an ATP-dependent process which is facilitated by nuclear localization signals. Since DNA has higher affinity for Dox than the proteasome, Dox dissociates from the proteasome and binds to DNA [87]. Thus Dox needs only delivery to the cytosol to be effective.

The clinical use of Dox is restricted because of serious side-effects like development of resistance in tumor cells or toxicity in healthy tissues, particularly the heart. The most common side effects of Dox are acute nausea, vomiting, stomatitis, gastrointestinal disturbances, alopecia, neurologic disturbances, cumulative cardio toxicity and bone marrow aplasia [88, 89].

Recently, Dox has been delivered in liposomes with improved clinical success [90]. The degree of stability of Dox and other drugs depends not only on the liposome but also on the intrinsic physicochemical properties of each specific drug and on the method of loading. Much progress has been made by using the technology of encapsulation of ionizable amphiphiles such as Dox. For example, high Dox concentrations can be achieved in the liposome internal aqueous phase, resulting in a drug-to-phospholipid molar ratio greater than 20. Because the estimated concentration in the liposome interior exceeds the solubility of Dox in water, it is thought that the drug may form a gel-like phase [91]. TEM observations of liposomal Dox show elongated crystals thought to be Dox-sulfate [92].

2.11.2 Plasmid

Plasmids are loops of DNA grown in bacteria. When plasmids are transferred to mammalian cell nuclei, they are transcribed to mRNA which enters to the cytosol and is translated to protein.

2.11.3 siRNA

Short interfering RNA (siRNA) is one of the therapeutics that we attempted to deliver in liposomal nanocarriers. RNA interference (RNAi) is a biological mechanism by which short strands of RNA can inhibit the production of specific proteins. When small double stranded RNAs (dsRNA), are introduced into the cell cytosol, they disrupt the particular messenger RNAs (mRNAs) that contain complementary sequences, and cause the mRNA to not be translated into a protein. The lack of protein production due to siRNA (or other mechanisms) is called “protein knockdown”. Any protein in any cell type or tissue can be targeted if its mRNA sequence is

known. Professors Andrew Z. Fire and Craig C. Mello received the Noble prize in 2006 for their discovery that short double stranded RNA interferes with gene activity in a homology-dependent manner. The discovery of these siRNAs revealed a new mechanism for regulating cell function by controlling protein expression, which eventually feeds back to gene control and cell function [93].

RNA interference has been observed in many organisms such as plants, invertebrate animals and even vertebrates. It has a big impact on biomedical research and is proposed to be an amazing method with potential to cure many different diseases, such as cancer, viral diseases, hematological diseases and many other genetic illnesses [94]. siRNAs have two advantages over molecular drugs: first the sequences can be designed to target any protein; second the synthesis of siRNA is not complicated. However, delivery of siRNA is still very challenging.

The first challenge is stability of siRNA [95]. The siRNA size is very small so it is cleared from blood very quickly through the kidneys. siRNA is negatively charged, which makes it more difficult to penetrate through the cell membrane (the cell membrane is negatively charged). Even if siRNA could pass through the membrane by receptor mediated endocytosis, the siRNA would still have to escape from the endosome to avoid digestion. All these factors make naked siRNA delivery very difficult. To overcome these challenges siRNA can be encapsulated inside a nanocarrier, or can be condensed with cationic lipids to form a solid nanoparticle.

Some other major obstacles in delivering siRNAs include the off-target effects, and its interferon responses. Every time that siRNA longer than 30 nucleotides is delivered to cells at high concentration, there is an up-regulation of the immune system. That includes production of interferon which leads to an inflammatory response [96].

Low transfection efficiency and poor penetration through the tissues are some of the other major problems of siRNA therapy. The lack of an efficient delivery system to target and deliver the siRNA to the specific part of the body is a challenging limitation. Another major obstacle in delivery of siRNA is the ubiquitous presence of RNAse everywhere in our environment which can degrade naked siRNA.

Almost all *in vivo* studies of siRNA have used naked siRNA in high doses through injection. This method leads to very small gene-inhibition effects because only a very small amount of siRNA can be injected directly into cells, and the rest is rapidly degraded by RNAse enzymes. The half-life of the naked siRNAs is reported to only span from several minutes to about an hour. If they are modified (such as sugar modification or backbone modifications), they become more stable. It is observed that backbone modifications, and bio-conjugation with lipids and peptides have improved the half-life, the stability, and the cellular uptake of siRNA [97].

Chemically synthesized siRNA, which is used *in vitro*, is introduced to the cell cytosol directly using electroporation, nuclear or cytoplasmic microinjection, or is conjugated with some commercially available lipid reagents such as Oligofectamine, Lipofectamine, Metafectene, or siPortAmine [98]. Most of these reagents contain cationic lipids and are cytotoxic. Due to this fact these methods are not commonly used for *in vivo* delivery. It would be very desirable to develop a targeted delivery system that does not involve cationic lipids.

The desired final destination of the siRNA delivery is the cytoplasm. The small size and high RNAse concentration in blood leads to rapid degradation of siRNA after injection, which renders injection nearly useless. Also the siRNA needs to be targeted to the specific tissue in the body. Because of its size and charge, to deliver siRNA, it has to contact the cell membrane,

become endocytosed, and after endocytosis it has to pass from the endosome to the cytoplasm without degradation.

Since we have all the information about the nanoparticle that we want to use and the kind of therapeutic that we want to deliver, now we need to discuss how to load the therapeutic into the nanocarrier.

2.11.4 Drug Loading

Having a high drug-loading capacity is a key characteristic of a successful nanodelivery system. Two different methods are commonly used for drug loading: incorporation method and absorption method.

Drug is loaded at the time of nanoparticles formulation by the incorporation method usually by forming the carrier in the presence of the drug. On the other hand, the absorption method is used for absorption of drug after formation of nanoparticles. In general drug loading depends on drug solubility. For many small molecules, ionic interaction between drug and matrix increases the drug loading.

2.11.5 Endocytosis and endosomes

Endocytosis is an energy-requiring process by which a cell takes in large molecules such as proteins. Endocytosis occurs in all cells in the body since large polar molecules cannot pass through the hydrophobic layer of a cell membrane. Different pathways are employed to endocytose different types of molecules, and these pathways are based on both size and ligands.

In all types of endocytosis, the cell membrane extends and surrounds a portion of external media. The membrane then comes together and pinches off to entrap previously external

molecules. The new vesicle (now inside the cell) is called an endosome [99]. To break down and digest the endocytosed materials, hydrogen ions are pumped in to lower the pH [100]. The endosome merges with vesicles containing lytic protein to form a lysosome where in molecules are digested into smaller pieces.

There are four different endocytosis pathways: clathrin-mediated endocytosis, caveolae endocytosis, macropinocytosis and phagocytosis. Clathrin-mediated endocytosis can be found in almost all cells and is mediated by contact with particles about 100 nm in diameter. Caveolae endocytosis is the most common non-clathrin endocytosis and it occurs on the surface of most cells, but not all. Macropinocytosis is used for particles between 0.5-5 μm in diameter and phagocytosis is used for particles larger than 0.75 μm.

Transferrin-coated gold nanoparticles were used to study the endocytotic mechanisms [101]. It was observed that particles up to 50 nm were endocytosed very easily, but as particle size increased, the rate and amount of endocytosis decreased.

For therapeutics that require intracellular delivery, the drug must escape from the endosome before it is digested. Successful escape is one of the major barriers to effective intracellular delivery. There are currently four main ways to escape from the endosome; pore formation in the endosomal membrane, pH-buffering effect, fusion in the endosomal membrane and photochemical distribution of the endosomal membrane [102].

After therapeutics are loaded into nanocarriers and are endocytosed to the cells, the content of the carrier should be released inside the cell. This is discussed next.

2.11.6 Drug Release from Carriers

When developing a nanoparticle delivery system, it is important to consider drug release from the carrier. There are numerous items that affect drug release such as drug solubility, desorption kinetics of adsorbed drug, diffusion of drug through the nanoparticles, nanoparticle degradation, and finally the combination of degradation and diffusion. In conventional nanospheres the drug is distributed uniformly, and diffusion or erosion of the matrix causes the drug to be released. If diffusion happens faster than matrix erosion, the release mechanism is controlled by diffusion.

This research investigated a novel method of releasing drugs from liposomal carriers directly to the cytosol of the cells. To release the drug from the carrier we used ultrasound. Applying the ultrasound made the emulsion droplets change phase from liquid to gas, so their volume increased and ruptured the liposome and thus released the drug. As an additional benefit, the ultrasound is proposed to also have caused escape from the endosome.

2.12 Previous Work with eLiposomes

James Lattin and Jonathan Hartley, graduate students at BYU Chemical Engineering Department, started making and developing eLiposomes [103, 104]. Below is the description of the method they developed. My methods and delivery techniques exceeded their preliminary work.

Lattin and Hartley developed an eLiposome called a "2-step" eLiposome because liposomes were formed twice. Their technique was a modification of the "vesosome" method described previously. First, small (< 100 nm) liposomes were formed and then ethyl alcohol (EtOH) was added. The alcohol interacted with the polar groups of the membrane and caused

the spherical liposomes to unfold into sheets [21, 105]. Then the alcohol was removed by centrifugal separation, but the sheets remained stable at temperatures below the transition temperature of the lipids. Next the sheets were combined with a suspension of the PFC nanoemulsion, with or without calcein or drug. The solution was heated up above the transition temperature of the lipids (usually about 50°C), and the liposomes spontaneously reformed, thus entrapping some of the emulsion inside the liposome [104].

Although eLiposomes were successfully made, the 2-step process was laborious and time-consuming. Furthermore, the heating step (to reform liposomes) limited the types of PFC emulsion that could be used. For example, perfluoropentane (PFC5) with a boiling point of 29°C might boil away during the step in which eLiposomes are formed by heating the sheets above 50°C. However, with care, Lattin was able to make 2-step eLiposomes with PFC5 emulsion droplets [104].

The goal of my research was to encapsulate the PFC emulsions inside the eLiposome in one step without the requirement of prolonged and elevated heating, so that we could place temperature sensitive emulsions and therapeutics within the eLiposomes.

3 OBJECTIVES

The overall objective of this research was to further develop and improve an ultrasonically activated system using liposomes for drug and gene delivery. Dr. James Lattin developed a "first generation" eLiposome with which he demonstrated calcein delivery. In addition to easier manufacturing, my eLiposomes may have targeting ligands on their surface so they can be directed to the cancerous cells and be endocytosed. The emulsion droplets were made of perfluorohexane (PFC6) and perfluoropentane (PFC5) which are nontoxic and can be excited by applying ultrasound (US). The ultrasound caused a phase change from liquid to gas and these small liquid droplets changed to gas and ruptured the eLiposomes to release their contents. In my research chemotherapeutic drugs such as paclitaxel and doxorubicin were loaded into and delivered from eLiposomes. The most novel aspect is making eLiposomes by 2 new methods that were not attempted previously. I also loaded and delivered DNA plasmids.

The following were objectives of my research:

1. Develop a new technique to make eLiposomes that is more practical than the previous method. The goal was to develop a technique that was faster in preparation (Lattin's method took 2 days) and did not require high temperature or low pressures. The use of non-toxic surfactants was a requirement, and incorporation of PFC5 nanodroplets was very desirable so eLiposomes could form gas bubbles at body temperature.

2. Incorporate calcein into the eLiposomes to use as a model drug. Calcein had been used by Lattin to quantitate the amount of drug release. I also desired to incorporate actual drugs, something that had not been done previously. Dox and PTX were selected since they only had to be delivered to the cytosol to be effective.

3. Verify the essential components of an effective eLiposome, such as the emulsion droplet, the folate on the surface and the types of surfactant molecules that could be used.

4. Investigate the role of other parameters controlling ultrasonic release from eLiposomes. These included the effect of ultrasound intensity, the effect of insonation time, the effect of temperature, the effect of perfluorocarbon composition and the effect of storage time.

5. Demonstrate delivery of calcein, PTX, Dox and siRNA using eLiposomes. Verification of Calcein and Dox were easy because they are fluorescent. However, for detection of PTX and siRNA some other analytical method needed to be used.

6. Demonstrate the toxicity of PTX delivery on HeLa cancer cells in vitro, with and without ultrasonic activation of the eLiposomes by using a 20 kHz ultrasound.

4 MATERIALS AND METHODS

4.1 Materials and equipment

4.1.1 Materials

1,2-dimyristoyl-sn-glycero-3-phosphocholine (DMPC), 1,2-dihexadecanoyl-*sn*-glycero-3-phosphocholine (DPPC), 1,2-didodecanoyl-sn-glycero-3-phosphate (sodium salt) (DLPA), 1,2-dioctadecanoyl-sn-glycero-3-phosphocholine (DSPC) and 1,2-distearoyl-sn-glycero-3-phosphoethanolamine-N-[amino(polyethylene glycol)-2000] (DSPE-PEG(2000)-amine) were purchased from Avanti Polar Lipids, Inc. (Alabaster, AL). 1,2-dipalmitoyl-sn-glycero-3-phosphate (DPPA) was purchased from Echelon Biosciences Inc. (Salt lake City, UT). Perfluorohexane (PFC6), perfluorooctanoic acid (PFOA), folic acid and N, N'-dicyclohexylcarbodiimide (DCC) were purchased from Sigma-Aldrich (St. Louis, MO). Perfluoropentane (PFC5) was purchased from SynQuest Labs, Inc. (Alachua, FL). Zonyl® FSN-100 fluorosurfactant was a gift from DuPont (Wilmington, DE). Phosphate buffer saline (PBS) solution was purchased from Fisher Scientific (Fair Lawn, NJ). Sodium chloride and dimethyl sulfoxide (DMSO) were purchased from Mallinckrodt (Paris, Kentucky), sucrose from Avantor Performance Materials (Phillipsburg, NJ) and glucose form United Biochemical Corp.

(Cleveland, OH). Calcein was purchased from MP Biomedicals (Aurora, OH).

Triton X-100 was purchased from Fisher Scientific (Fair Lawn, NJ). Chloroform was purchased from Mallinckrodt Baker Inc., (Phillipsburg, NJ). Gibco DMEM media, F-12 Nutrient Mixture, RPMI-1640 folate free media, and fetal bovine serum were purchased from Life Technologies (Grand Island, NY). Trypsin for cell passaging was purchased from Invitrogen (San Diego, CA). All water used was double distilled. These reagents were used without further purification.

4.1.2 Transmission Electron Microscopy

Cryogenic transmission electron microscopy (cryo-TEM) was used to image emulsions, liposomes and eLiposomes. Images were taken with FEI Tecnai F30 transmission electron microscope (Hillsboro, OR) at 300 kV. Samples were placed on 200-mesh copper (holey-carbon) grids. Grids were plunge frozen in liquid ethane using a FEI Vitrobot. To verify encapsulation of the emulsion droplets inside the bilayer, the microscope stage was rotated and the sample was viewed at -45°, 0°, and +45°.

For negative staining techniques, samples were viewed on an FEI Tecnai 12 transmission electron microscope (Hillsboro, OR) on continuous carbon grids using a Gatan single-tilt sample holder.

4.1.3 Dynamic Light Scattering

Dynamic light scattering (DLS) (90Plus, Particle Size Analyzer, Brookhaven Instrument Corporation, Holtsville, NY) was used to measure the size distribution of the emulsions, liposomes and eLiposomes. Samples were prepared at concentrations to give 500 kcounts/second

to 1.5 Mcounts/second. Ten runs with duration of 1 minute each were performed on each sample and averaged. The Conton model was used to calculate the size distribution.

4.1.4 Confocal Microscopy

Cells were imaged using an Olympus IX70 microscope FluoView FV 300 confocal laser scanning microscope. The confocal microscope is equipped with an argon laser providing excitation light at wavelengths of 458 nm, 488 nm, and 515 nm as well as green Helium-Neon and red Helium-Neon laser sources with respective excitation wavelengths of 543 nm and 633 nm. The cells were removed from wells using cell scrapper and deposited on a glass slide for imaging. To visualize the presence of calcein or expression of the AFP plasmid, the 488 nm wavelength was used. Images were analyzed with ImageJ software (NIH, Bethesda, Maryland) to obtain the average fluorescence intensity per cell.

4.1.5 Ultrasound

A 20 kHz ultrasonic probe (VCX400, Sonics and Materials Inc., Newtown, CT) of 3-mm diameter was used to form and shear emulsion droplets and liposomes. The same setting was used for release experiments (ultrasound intensity and insonation time were varied). Degased and deionized water was used to calibrate ultrasound intensity using a low frequency hydrophone (Model 8103, Bruel & Kjaer, Naerum, Denmark). For this calibration, the hydrophone was positioned 3 mm from the transducer and connected to an oscilloscope. Factory calibration parameters were used to convert the hydrophone voltage signal into intensity (W/cm^2).

With cell experiments, the probe tip was placed into the well approximately 1.5 cm above the cell monolayer and sonication was conducted. The media was removed and cells were washed

with PBS four times. Cells receiving plasmid were grown for 48 hour after insonation. Cells receiving calcein were examined immediately (within minutes) after insonation.

4.1.6 Fluorometer

A QuantaMaster fluorometer (Photon Technology International, Birmingham, NJ) was used to measure the amount of calcein release for eLiposomes. The excitation and emission wavelengths were set to 488 nm and 525 nm, respectively. In order to avoid damaging the machine, apertures were adjusted to limit the fluorescent counts per second (cps) to less than 1,000,000. Data were collected at 4 points/second and exported to Microsoft Excel for analysis.

4.2 Methods and Procedures

4.2.1 PFC6 Emulsion Droplet Formation

To make nanoemulsions, 0.6 mL of DPPA, DPPC or DMPC solution (10 mg/mL in chloroform) was vacuum dried onto a round bottom flask to remove all the chloroform and then hydrated in 1.2 mL PBS. Next 0.6 g of PFC6 was added. A 3-mm probe on a 20 kHz sonicator was used to emulsify the PFC6 (1.25 W/cm^2, 3 times, for 30 seconds each with a 1 minute pause in between sonications). To further reduce emulsion droplet size, they were extruded through a 100-nm filter (Hamilton, Reno, NV). This step was only done on samples in which the desired size was smaller than 100 nm. The same method was used to make PFC6 emulsions stabilized with Zonyl, PFOA, and other phospholipids (DLPA, DSPC, etc.). Droplet size was measured by dynamic light scattering.

4.2.2 PFC5 Emulsion Droplet Formation

A similar method was used to make PFC5 nanoemulsions, except that 1.0 mL of DPPA, DPPC or DMPC solution (10 mg/mL in chloroform) was dried onto a flask and then hydrated in 2 mL PBS; 0.5 g of PFC5 was added. During the subsequent ultrasonic mixing process, the flask was placed in an ice-water bath to reduce evaporation of PFC5. The rest of the procedure was similar to that described above, including the three 30-second sonications.

4.2.3 1-step eLiposomes Formation with PFC6 and PFC5 Emulsions

The 1-step eLiposome formation commenced by evaporating 50 mg of DMPC from chloroform solution onto a round-bottom flask using a vacuum pump. Then 1.0 mL of the PFC nanoemulsion was added to the flask with dried DMPC, and the flask was rotated to hydrate the film of DMPC with the emulsion at atmospheric pressure, as illustrated in Figure 6. For the PFC6 emulsions, the flask was rotated at 40°C for 5 to 10 minutes until dried lipid was no longer visible on the flask surface. For PFC5 emulsions, the rotation was done at room temperature (23°C) and much longer time (45 to 60 min) was required to completely hydrate (remove) the deposited liquid film. Sometimes the resulting eLiposome suspension was reduced in size by extrusion (Avestin Inc. Ottawa, ON, Canada) through a 200-nm filter 10 times. Non-encapsulated emulsions and empty liposomes were separated using the pillow density method described in 4.2.10. Droplet size was measured by dynamic light scattering.

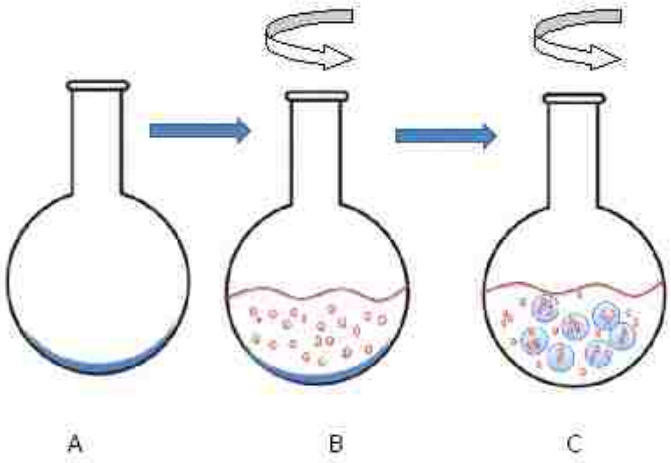

Figure 6: Production of eLiposomes by the 1-step process; A) Phospholipid is deposited on the flask. B) Emulsion is added. C) eLiposomes form while rotating the flask. Sizes are not to scale in this illustration. Taken from [106] with permission.

4.2.4 eLiposomes Made by Ultra Method

In this method phospholipid-stabilized emulsions were made as described earlier and extruded through a 100-nm filter. Liposomes were made by the hydration method as follows. Phospholipids (DMPC or DPPC, 50 mg) were deposited as a film on a round bottom flask using a rotovap. Then 1.0 mL of PBS was added to the flask and it was heated above the transition temperature of the phospholipid. Then the suspension was sonicated at 20 kHz, 1.5 W/cm^2 for 10 minutes to reduce the size of liposomes (~200 nm) [15]. Liposomes were extruded through a 200-nm filter 10 times. After cooling to room temperature, 1.0 mL of emulsion was added to 1.0 mL of the liposome suspension and the mixture was sonicated at 20 kHz, 1.5 W/cm^2 on ice, 3 times, 30 second each time with 1 minute between sonications. eLiposomes were extruded through a 200-nm filter. Non-encapsulated emulsions and empty liposomes were separated using a pillow density method described in section 4.2.10.

4.2.5 Encapsulating Calcein

To quantify the release, eLiposomes containing calcein were prepared by combining 2 mL of 30 mM calcein with 1 mL emulsion droplets and 1 mL liposomes. Sonication of this mixture resulted in 15 mM calcein solution inside and outside the eLiposomes. To remove most of the external calcein, samples were centrifuged at 500 x g for 5 minutes and washed twice.

Calcein fluorescence (excitation 488 nm and emission wavelengths 525 nm) was measured with a Quanta Master fluorometer. To quantitate the amount of released calcein, all fluorescent measurements were conducted in the linear region of the calcein concentration curve. Calcein has linear fluorescence intensity at concentrations less than 20 μM, has a maximum fluorescent at about 50 μM and is totally self-quenched at concentrations above 15 mM.

To calculate the release from eLiposomes, baseline fluorescence (without sample) was collected for 10 s using the fluorometer. An eLiposome solution was exposed to ultrasound at various values of intensity, insonation time and eLiposomes temperature. Aliquots from the insonated samples were diluted into the linear fluorescence range for measurements. Calcein that had been released was diluted and measured, while non-released calcein remained entrapped in the eLiposome and was not diluted and thus not measured. Following release, the total amount of calcein (released and non-released) was measured after lysing all vesicles with Triton X-100 and diluting to the linear region [103]. Experiments at each parameter were repeated 3 to 5 times. Pillow density (see 4.2.10) was used to remove free emulsion and empty liposomes.

4.2.6 Encapsulating doxorubicin

Two solutions were prepared: 1) 0.11 M ammonium sulfate (pH~4.5) and 2) sucrose/ascorbic acid/HEPES/NaOH. The desired final concentration for the second solution

was: 15mM HEPE, 5mM ascorbic acid (anti-oxidant) and 0.26 M sucrose. 1 M NaOH was added dropwise to adjust the pH of this solution close to 7.5. Both solutions were iso-osmotic (280-295 mOs), matching the osmotic pressure of blood and tissue.

The liposome formulation for encapsulating Dox was a little different than the commercial formulation called Doxil. Lipids of DPPC, cholesterol, DSPE-PEG (2000)-amine, and α-tocopherol (anti-oxidant) in a 3:1:1:0.004 molar ratio were dried on a glass flask. Liposomes were made by the hydration method using the ammonium sulfate buffer instead of PBS. The liposome suspension was extruded through the 800 nm and 220-nm filters. Then 1.0 mL of PFC5 emulsion in 0.11 M ammonium sulfate was added to 1.0 mL of the liposome suspension and the mixture was sonicated as described earlier. eLiposomes were extruded through a 200-nm filter. Non-encapsulated emulsions and empty liposomes were separated using a pillow density method described in 4.2.10.

Doxorubicin solution was prepared by adding Dox powder to the solution of sucrose/ ascorbic acid/HEPE/NaOH solution at pH 7.5. Doxorubicin solution (20 mg/mL) was added to eLiposomes at 1:1 v/v ratio, and incubated for 24 hours at room temperature. An ion exchange column (Dowex 50W-200, Sigma-Aldrich, MO) was used to remove free Dox from the solution. The column was prepared by passing 10 mL sucrose/ascorbic acid/HEPE/NaOH solution first. eLiposomes containing Dox passed through the column but the external free Dox adsorbed to the column. After removing external Dox, the concentration of Dox in eLiposome was measured using spectrophotometer (λ=488 nm) (Beckman Coulter DU-640 UV, Fullerton, CA).

In the technique described above, Dox was loaded into the eLiposomes by a technique called “remote lading”. Dox at pH 7.5 has neutral charge so it is diffuses through the eLiposome lipid bilayer. Once inside, at the lower pH, it is protonated by NH_4^+, forming Dox^+ which cannot

penetrate the lipid bilayer, but the neutral NH_3 diffuses out through the bilayer. Since neutral Dox is no longer in the eLiposome interior (it changed to Dox^+), there is still a concentration gradient that keeps driving neutral Dox into the eLiposomes until nearly none remains outside the eLiposomes, or until all the NH_4^+ changes to NH_3.

4.2.7 Encapsulating Paclitaxel

Paclitaxel particles were prepared as follows using an adaption of published techniques [82, 84, 107]. Soy PC (0.025 g), safflower oil (0.3 mL), commercial paclitaxel drug (0.25 mL, Hospira, Lake Forest, IL) and PBS (4.5 mL) were mixed using 20 kHz ultrasound for 2 minutes at 1.25 W/cm^2 (Sonics and materials, VCX400). Particles were passed through a 100- nm filter 10 times.

DMPC liposomes were made (200-250 nm). PFC5 emulsion droplets were prepared (using DPPA surfactant) and eLiposomes were made in the presence of emulsion droplets and PTX nanoparticles. Hillary Bringham and Mikayla Herbert (undergraduate students in Dr. Pitt's Lab) helped me develop the PTX particles. Since these nanoparticles were made from commercial paclitaxel, there are probably small amounts of Cremopher EL and EtOH present in the formulation.

4.2.8 Encapsulating Plasmid

Plasmid preparations were done in the lab of Dr. Jeffery Barrow of BYU, with the assistance of his students. A single colony of *E. coli* containing the AFP2 plasmid [108] was selected and inoculated in 500 mL LB medium. The mixture was incubated for 24 hour at 37°C with shaking at 300 rpm. The bacterial cells were centrifugally harvested (3000 x g for 30 minute

at 4°C). Plasmid DNA was separated by maxiprep (QIAGEN, Valencia, CA) according to the QIAGEN instructions and then concentrated using cold ethanol precipitation. The preparation centrifuged at 15,000 x g for 10 minutes and the supernatant was decanted. 200 μL of double distilled autoclaved water (DDAW) was added to the pellet; then 20 μL NaOAc (sodium acetate) and 550 μL cold ethanol were also added to the pellet. The mixture was centrifuged at 4°C for about 15 minutes. Finally the supernatant was gently removed and 100 μL of DDAW was added to the plasmid pellet. A spectrophotometer was used to measure the plasmid concentration. This plasmid contains a gene coding for the expression of a green fluorescent protein (GFP).

To incorporate plasmids within eLiposomes, the desired amount of plasmid along with 1.0 mL of 100-nm-emulsion droplets (PFC5, DPPA surfactant) was added to 1.0 mL of 200 nm DMPC liposomes, and "ultra" eLiposomes were prepared by sonication at 20 kHz on ice, 1.5 W/cm^2, 3 times, 30 seconds each time, with 1 minute between sonications. The resulting eLiposomes were extruded through a 200-nm filter. Non-encapsulated emulsions, empty liposomes and non-encapsulated plasmid were separated using the pillow density method described below.

4.2.9 Encapsulating siRNA

Encapsulating of siRNA inside the eLiposomes is very much similar to encapsulating plasmid. siRNA complementing a section of the PhLP mRNA was provided by Chris Tracy of Dr. Willardson's lab at BYU. The concentration of siRNA was 100 nM in 200 uL of eLiposomes. The only different thing was extreme cleanliness from RNAse enzymes. All the preparations were done in clean (without RNAs) glassware. Everything was treated with

RNaseZAP® (Sigma, St. Louis, MO) before usage. The cell culture hood was used for all the preparation. All pipet tips, centrifuge tubes, water and PBS that are used were RNAs free.

4.2.10 Separation by Pillow Density Method

A density technique was developed to separate un-encapsulated emulsions and empty liposomes from the eLiposomes. Three different solutions with the same osmolarity but different densities were prepared. Sodium chloride, glucose and sucrose were used, each with an osmolarity of 0.3 Os/kg and relative densities of 1.005 kg/L, 1.017 kg/L and 1.035 kg/L, respectively [109]. The mixture of eLiposomes, free emulsions and empty liposomes was added to the bottom of a 1.5 mL microfuge tube. Then the other 3 solutions were added to the bottom in order of increasing density. First, NaCl was added to the microfuge tube. Then using a glass Pasteur pipette, the glucose solution was slowly pipetted to the bottom of the microfuge tube, underneath the NaCl layer. Similarly sucrose was slowly pipetted to the bottom underneath the glucose. About the same volume (~ 0.4 mL) of each solution was added to each layer. The sample was spun for 10 minutes at 3000 rpm (~500 x *g*) using a fixed rotor centrifuge (Eppendorf 5415 C, Hauppauge, NY).

The unencapsulated emulsion nanodroplets have the highest density (about 1.67 g/cm^3 for PFC6 and 1.63 g/cm^3 for PFC5), so they settled at the bottom, while eLiposomes collected between the glucose and sucrose layers and empty liposomes (having the lowest density) collected between the glucose and sodium chloride layers (see Figures 7, 8). Sometimes liposome and eLiposome membranes were labeled with oil red O (Sigma-Aldrich, St. Louis, MO) for verification that the red color did indeed collect at the interfaces.

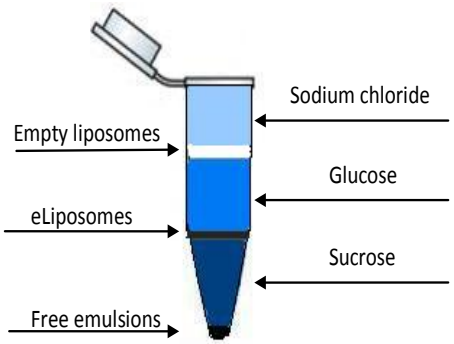

Figure 7: This illustrates the pillow density method, which uses sodium chloride, glucose and sucrose solutions with the same osmolarity and different densities to separate the empty liposomes, eLiposomes and free emulsions based on their differences in density. Taken from [106] with permission.

In order to just remove free emulsions from the mixture, sometimes a two–layer pillow density technique was used. These two layers are sucrose and sodium chloride, and the eLiposomes collected at the interface while free emulsion droplets went to the bottom.

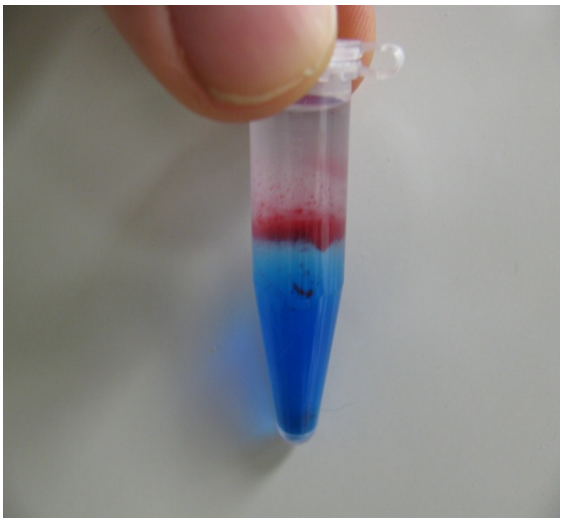

Figure 8: Pillow density method. Top layer (clear) contains sodium chloride. Bottom layer (blue) contains sucrose. Middle layer (red) contains eLiposomes. This is a two- layer pillow density technique.

4.2.11 Folate incorporation

Folate was attached to a DSPE-PEG amine spacer by adaptation of published methods [71]. First 16.7 mg of folate was dissolved in 667 μL of anhydrous dimethyl sulfoxide (DMSO) in a round-bottom flask. DSPE-PEG-amine (66.7 mg) and 333 μL of dry pyridine were added to the flask along with 21.7 mg of N,N'-dicyclohexylcarbodiimide (DCC). The reaction proceeded for 4 hours under nitrogen at room temperature in the dark. The pyridine was removed by evaporation. Then 16.7 mL of water was added to the solution. Membrane dialysis with a 3500 molecular weight cut-off was used to remove the unreacted folic acid, DCC, byproducts, and DMSO. After removal of byproducts and reactants, an equal volume of chloroform was added to extract the product (DSPE-PEG-folate). A drop of hydrochloric acid was added to the aqueous phase to protonate the product to make it more soluble in chloroform. The characteristic yellow of folate shifted from the aqueous phase to the chloroform phase. NMR was used to confirm attachment of the folic acid to DSPE-PEG-amine.

DSPE-PEG-folate micelles were formed and then mixed with the eLiposome formulation in an microfuge tube to a PEG concentration of approximately 1.2 mole %. The mixture was incubated at room temperature for one hour, during which time DSPE-PEG-folate molecules were inserted into the outer surface of the eLiposomes.

4.2.12 Cell Culture

HeLa (cervical cancer) cells were grown in DMEM (Sigma Aldrich) supplemented with 10% fetal bovine serum (FBS). Trypsin was used to passage and split the cells. Experiments were conducted on cells passaged less than 20 times after receiving them from ATCC. Cells were starved of folate by growing for 48 hours prior to addition of eLiposomes. Approximately

300,000 cells per well were seeded in a 12-well-plate and grown in RPMI 1640 folate-free media for 48 hours. eLiposome preparations were added to the wells in 200 µL aliquots. eLiposomes and cells were allowed to incubate at 37°C for 15 minutes to 2 hours before application of ultrasound. Ultrasound was applied to the cells by adding 3 mL of media to the wells and inserting the probe directly into the media. After sonication, the media was removed from all of the wells. Cells were washed with PBS or media at least two times and cells were removed from the surface with a cell scraper or trypsin. Cells were stored on ice until viewed with the confocal microscope.

With plasmid experiments, positive and negative control tests were done using a commercial transfection process called Lipofectamine (Invitrogen, Grand Island, NY) with either AFP2 plasmid or empty pcDNA3.1 plasmid, respectively.

5 NEW TECHNIQUES OF ELIPOSOME FORMATION

5.1 Introduction

An eLiposome is a liposome encapsulating an emulsion nanodroplet, and can be used for drug delivery. For example, therapeutic agents are encapsulated inside the eLiposomes, and application of ultrasound can cause the emulsion droplet to change from liquid to gas, thus increasing the volume inside the vesicle, causing rupture and release of the drug.

In this research, two new methods were developed to prepare eLiposomes. In the first method, called the one-step method, emulsion droplets were made of PFC6 or PFC5 and stabilized with DPPA. A layer of DMPC was dried in a round-bottom flask. Then the emulsion suspension was added to the flask. As the suspension hydrated the phospholipids, they formed liposomes around the emulsions. In the second method, called the "ultra" method, emulsions and liposomes were made separately and then were mixed together using ultrasound. The advantage of this second method compared to the previous one is that this is fast and easy and eLiposomes can be made with fewer restrictions due to incompatible combinations of surfactants, as will be shown. This work has been published in *Langmuir* [106].

Dynamic light scattering and transmission electron microscopy were used to measure the size of the emulsions, liposomes and eLiposomes. This size of eLiposomes is appropriate for extravasation into tumors with malformed capillary beds.

Both types of eLiposomes were constructed with folate attached via a poly (ethylene glycol) tether to induce endocytosis of the eLiposome. The latter eLiposomes were used to successfully deliver calcein as a model drug to HeLa cells.

The goal of this particular study was to encapsulate the PFC emulsions inside the eLiposome in one step without the requirement of prolonged heating required in the 2-step method of Lattin [104], so that temperature sensitive emulsions and therapeutics could be placed within the eLiposomes. Two new successful methods were developed which are presented in this chapter.

5.2 **Results**

5.2.1 1-Step eLiposomes

PFC emulsions were made by the method described previously (see 4.2.1 and 4.2.2) and their size distributions were measured by dynamic light scattering. Figure 9A shows the size distribution of PFC6/DPPA emulsions made with the one-step process, which ranges from about 90 nm to about 120 nm. Figure 9B shows the size distribution (before density separation) of eLiposomes made by the 1-step method, in which the emulsion of Figure 9A was used to hydrate a film of DMPC. This distribution is bimodal and the smaller peaks have the same distribution as the emulsion used to hydrate the lipid film to form the eLiposomes. We posit that the larger

peaks correspond to dynamic light scattering from the eLiposome surfaces. The smaller group of peaks is assumed to be scattering from PFC6 emulsions both outside and inside of the eLiposome vesicles, since the lipid bilayer is transparent to light and the sample was analyzed before separation of the external emulsion.

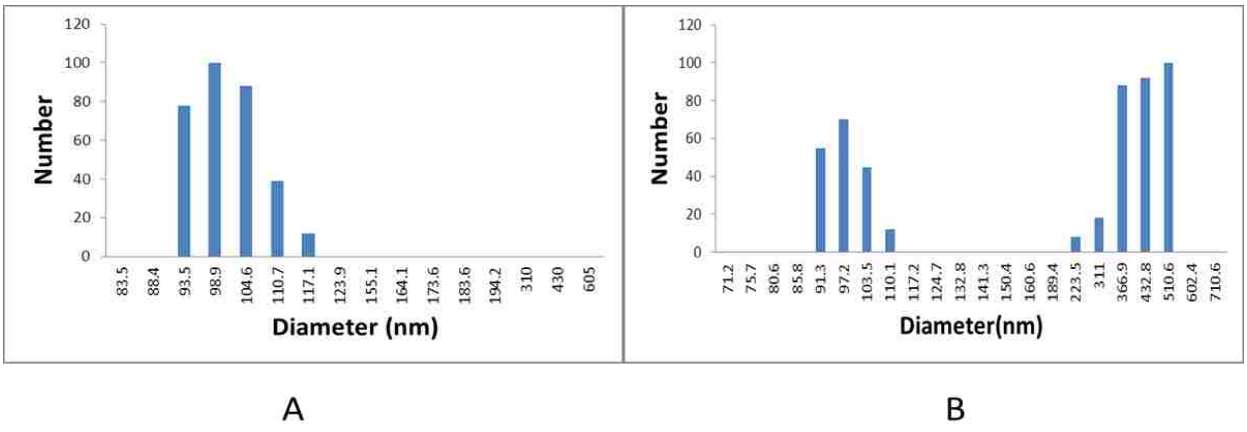

Figure 9: Light scattering results showing (A) distribution of DPPA emulsions of PFC6; (B) bimodal distribution of eLiposome suspension made by hydrating a DMPC film with the emulsion characterized in 9A. Taken from [106] with permission.

A similar preparation was done to make one-step eLiposomes with PFC5 emulsion droplets. Figure 10A shows the size distribution of PFC5/DPPA emulsions; the size range of PFC5 emulsions is from 90 nm to 190 nm, slightly larger than PFC6 emulsions. Figure 10B shows the bimodal distribution of the eLiposomes made by hydrating a DMPC film with the same PFC5 emulsion. The range of the emulsion size is about the same, and there is a set of larger peaks that we believe corresponds to the bilayer surface of the eLiposomes. The eLiposome size range is about the same with these PFC5 emulsions as with the PFC6 emulsions, which is 200 to 600 nm.

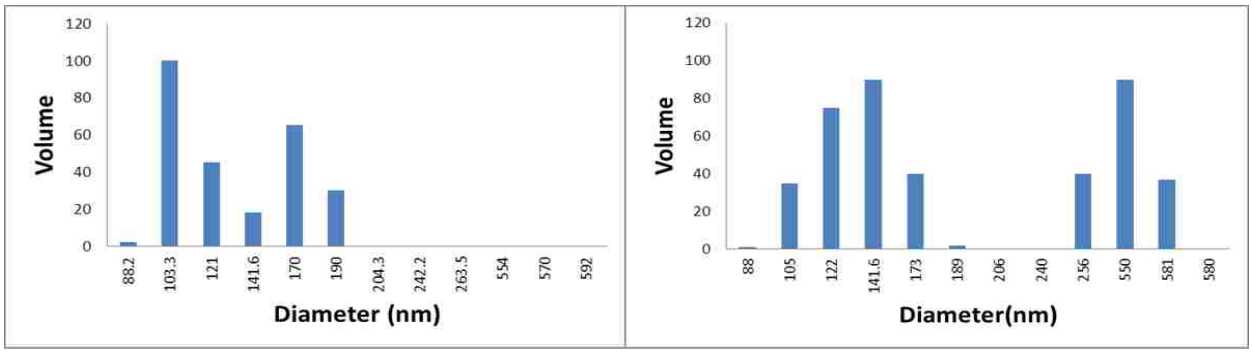

Figure 10: Light scattering data showing (A) distribution of DPPA emulsions with PFC5; (B) bimodal distribution of the eLiposome suspension made by hydrating a DMPC film with the emulsion characterized in 10A. Taken from [106] with permission.

Because a simple mixture of liposomes and emulsions would also create the size distributions observed in Figures 9B and 10B, we sought TEM evidence that some emulsion droplets had been encapsulated inside the eLiposomes.

We collected images of the 1-step eLiposomes using TEM with negative staining as described earlier. Figure 11 shows the images of 1-step eLiposomes prepared with PFC6 emulsion droplets. In each figure there appears to be membranes that are folded and sometimes peeled back. This may have occurred during the sample preparation. There also appears to be a sphere inside the larger structure that is between 100 and 200 nm in diameter, which corresponds to the DLS measurements of the emulsion size. We postulate that smaller spheres are indeed PFC6 emulsion droplets inside a larger eLiposome. However negative staining TEM images that were recorded from only one angle cannot definitely prove that the emulsion droplet is actually

inside the eLiposome. In addition, the samples are dried and may not represent the native structure; for such proof we relied on cryo-TEM images at multiple angles.

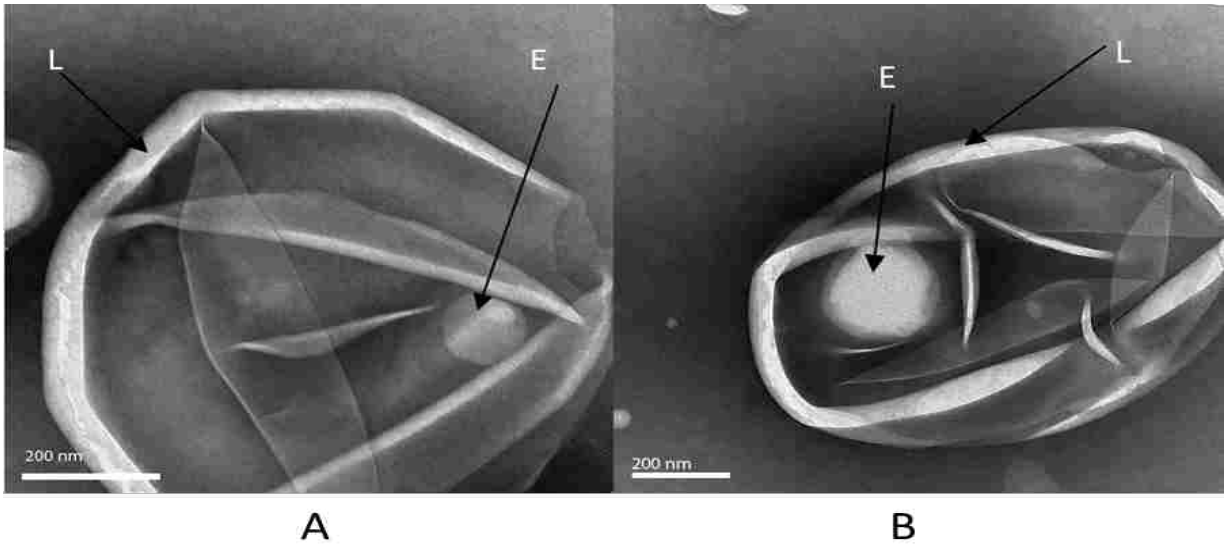

Figure 11: Negatively stained 1-step eLiposomes, made from PFC6 emulsions stabilized with DPPA surfactant inside liposomes made from DMPC. L: eLiposome membrane. E: emulsion droplet. Taken from [106] with permission.

Figure 12 shows Cryo-TEM images of 1-step eLiposomes. We verified that the emulsion droplet was inside the liposomes by rotating the TEM stage and capturing images at -40°, 0° and 40°. eLiposomes were extruded through a 200-nm filter. The emulsion droplet appears to be within a prolate-spheroid-shaped eLiposome.

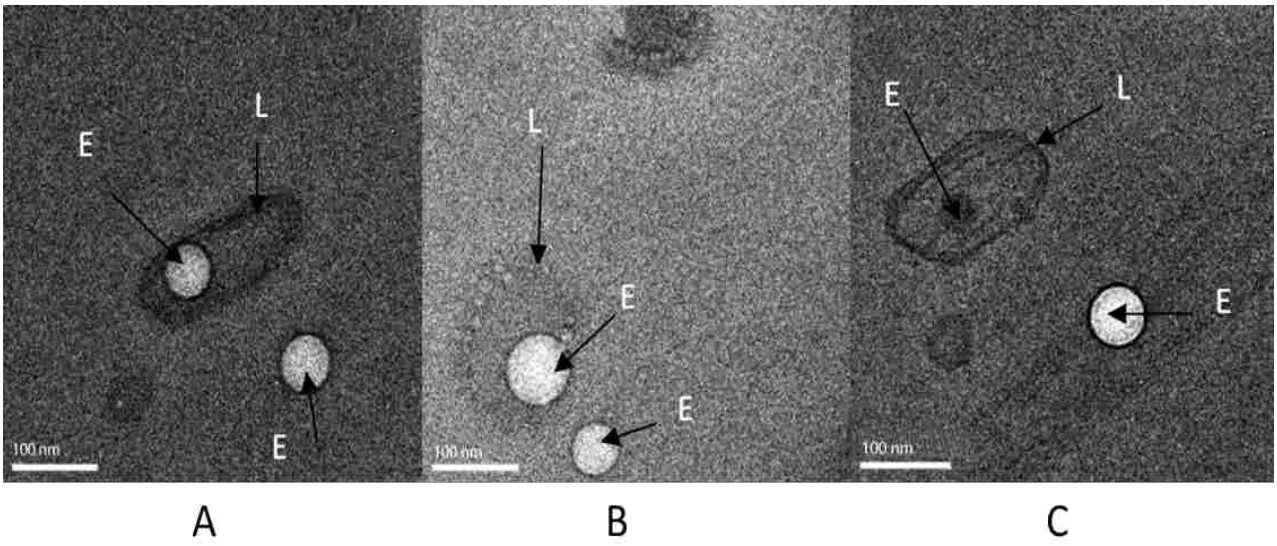

Figure 12: 1-step eLiposomes imaged by cryo-TEM showing a DPPA emulsion inside the bilayer of DMPC liposomes and an emulsion external to the eLiposome. The microscope stage is rotated to +40° (A), 0° (B) and -40°(C) to demonstrate the encapsulation of emulsion droplet inside the liposome. L: eLiposome membrane. E: emulsion droplet. Taken from [106] with permission.

We have tried constructing eLiposomes using the 1-step process with several combinations of various surfactants used to stabilize the emulsion droplets and various phospholipids used to form the liposome bilayer. Table 2 shows which combinations were found to successfully produce eLiposomes in the one-step hydration process with PFC6 emulsions. Failure to form eLiposomes was evidenced by the lack of scattering by emulsion-sized particles in dynamic light scattering. For example, if there were no particles below 200 nm observed in DLS we concluded that the emulsion droplets were destroyed and no eLiposomes were formed. In general, the data indicate that stable eLiposomes form only in the case of using a negatively charged surfactant (dialkylglycerophosphates) for the emulsion and a zwitterionically charged

dialkylphosphatidylcholine surfactant for the eLiposome bilayer envelope. Emulsions stabilized with Zonyl or PFOA did not form 1-step eLiposomes, as evidence by DLS.

Table 2: Combination of surfactants attempted in forming 1-step eLiposomes. Taken from [106] with permission.

Emulsion Surfactant	Liposome Surfactant	Successful 1-step eLiposome
DPPA	**DMPC**	**Yes**
DLPA	**DMPC**	**Yes**
DPPA	**DPPC**	**Yes**
DPPA	DPPA	No
DPPA	DLPA	No
DLPA	DPPA	No
DMPC	DMPC	No
DPPC	DPPC	No
DMPC	DPPA	No
DMPC	DLPA	No
DSPC	DSPC	No
DSPC	DPPA	No
DSPC	DLPA	No
Zonyl	DMPC	No
PFOA	DMPC	No

It is noteworthy that we were unsuccessful in forming eLiposomes employing the same phospholipid for the emulsion and the eLiposome bilayer. This is an interesting result since 2-step eLiposomes [104] can be formed using identical phosphocholines for both the emulsion and

the liposome. Although the 1-step formation of eLiposome is much easier and faster than the 2-step method, surfactant incompatibility may limit its application to a small subset of potential emulsion and liposome surfactants.

It should be mentioned that the light scattering data that were shown in Figure 9 and 10 are supporting evidence, not conclusive evidence, for making eLiposomes. The cryo-TEM images of Figure 12 are conclusive evidence. If the emulsion peak in the DLS data disappeared, this indicated that eLiposomes were not formed. So as a rule, successful eLiposomes had a DLS distribution showing an emulsion peak that was not changed compared to the original emulsion peak itself; and in unsuccessful attempts the emulsion peak was completely gone.

5.2.2 Ultra eLiposome

In the "ultra" method, we prepared emulsion droplets and liposomes separately and then we used ultrasound to encapsulate emulsion droplets inside the liposome bilayer. Interestingly when we were preparing the eLiposomes with the "ultra" method, we found that unlike the 1-step method, in which the charge of the emulsion and liposomes surfactant are important, we could successfully use combinations of liposome surfactant and emulsion surfactant with similar charge. For example, Figure 13 shows a cryo-TEM of an ultra eLiposome made from a DMPC-stabilized PFC6 emulsion droplet inside a bilayer envelope made from DMPC. We verified that the emulsion droplet was inside the envelope by rotating the TEM stage and capturing images at 45°, 0° and -45°.

The size distribution of eLiposomes can be controlled using an extruder. For example the eLiposomes shown in Figures 12 and 13 were extruded through a 200-nm filter and are 150 to

200 nm in size. The eLiposomes of Figure 11 were not extruded and are much larger. Even after extrusion, the emulsion droplets remained inside the eLiposomes.

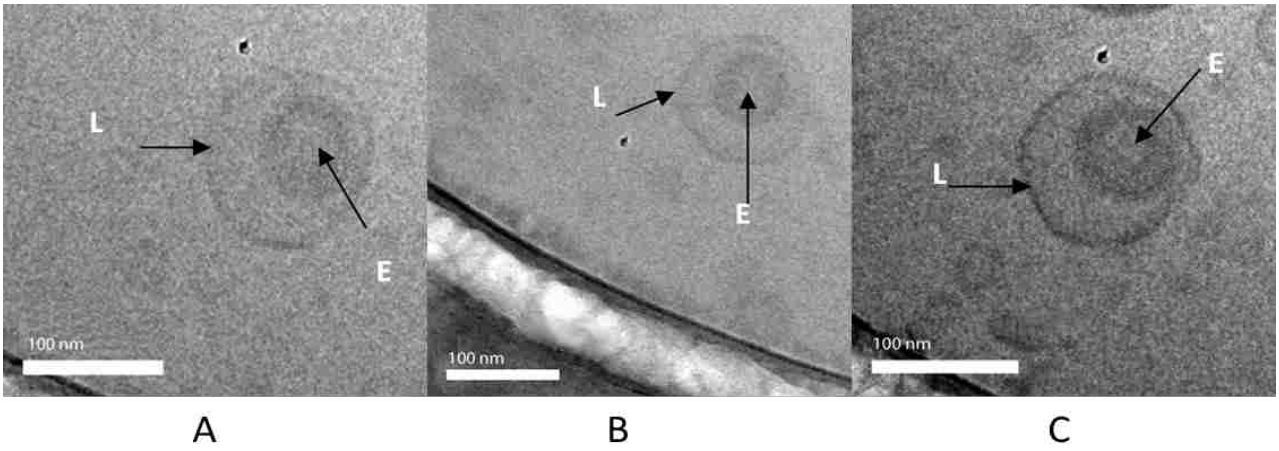

Figure 13: cryo-TEM images of an ultra eLiposome made from a DMPC-stabilized emulsion inside the bilayer of a DMPC liposome. The microscope stage was rotated to +45° (A), 0° (B) and -45° (C) to demonstrate the encapsulation of an emulsion droplet inside the liposome. L: eLiposome membrane. E: emulsion droplet. Taken from [106] with permission.

5.2.3 Characterization of eLiposomes Containing Calcein

Figure 14A is a schematic cartoon of an emulsion droplet inside a liposome bilayer envelope while Figures 14B and 14C illustrate 2 and more than 2 emulsion droplets inside the bilayer respectively. Figures 14D, 14E and 14F are the corresponding cryo-TEM images.

Of the eLiposomes imaged, those containing only 1 droplet were most common (~ 80 %), those with 2 droplets were less common (~19%) and those with more than 2 droplets were rare (~ 1%). Liposomes without nanodroplets were separated by the pillow density technique, so it is unknown what percentage of vesicles had no emulsion droplets.

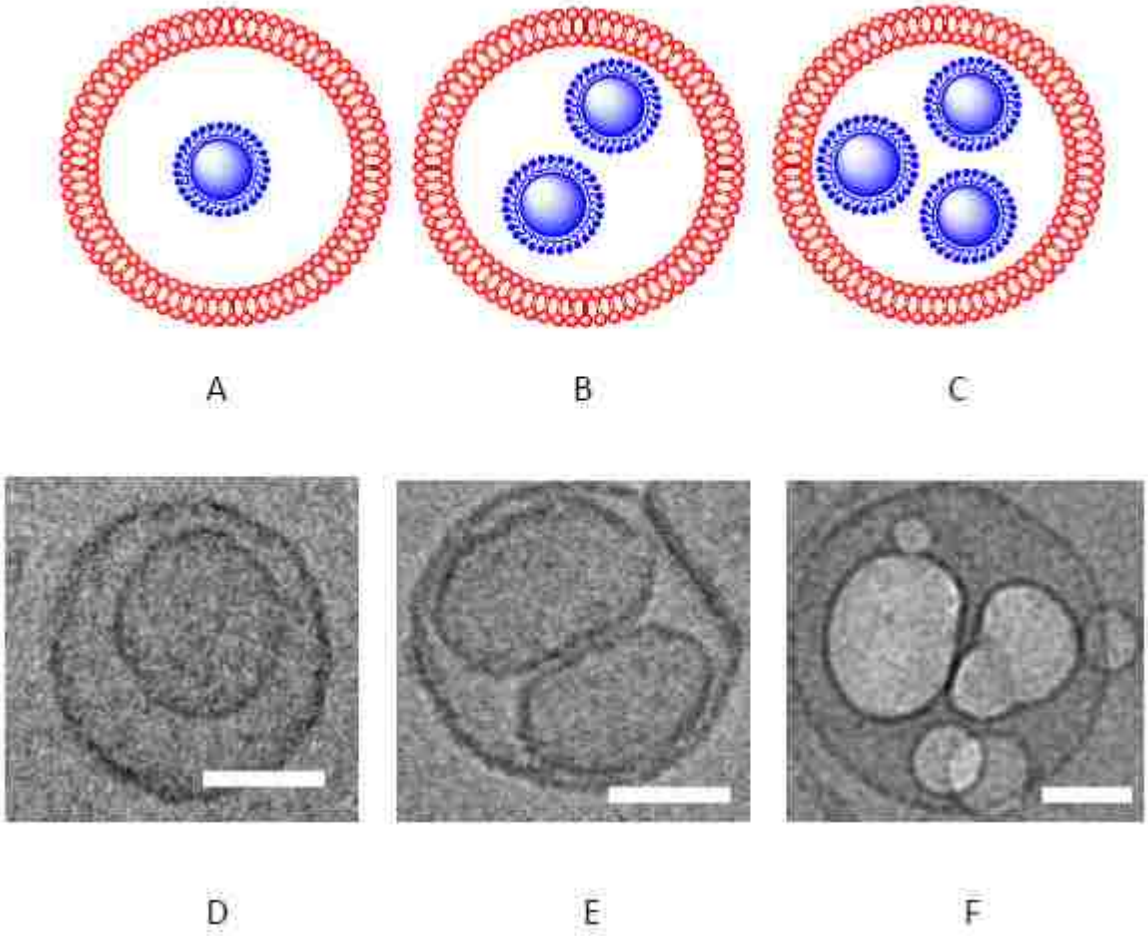

Figure 14: Cartoon pictures of eLiposomes with A) 1 B) 2 and C) 3 emulsion droplets inside. Cryo-TEM picture of eLiposomes with D) 1 E) 2 and F) more than 2 emulsion droplets inside. White bar in each picture indicates 100 nm.

5.2.4 Calcein Delivery to Cells

The eLiposomes made for this research contained self-quenched calcein which enabled quantitation of release [104, 106]. The "ultra method" of preparation was used in experiments of calcein delivery to cells because it is an easier method than the 1-step method, and it does not

have the limitations of compatibility of liposome surfactant and emulsion surfactant as is the case with the 1-step method.

The first set of experiments with cells was designed to examine the need for folate as a targeting ligand to achieve cytosolic delivery. Figure 15 shows HeLa cells exposed to PFC5 eLiposomes containing 30 mM calcein. Panels A and C are light microscopy and B and D are confocal fluorescent microscope images of the same place on the slide. Parallel experiments were conducted using eLiposomes prepared with and without DSPE-PEG2000-folate incorporated into the eLiposome bilayer. 200 μm L of each eLiposome sample were added to HeLa cells in 12-well plates. The plates were incubated at 37°C for about 2 hours and then 20 kHz ultrasound was applied at 1 W/cm^2 for 2 seconds. Finally the cells were washed to remove external calcein and eLiposomes. Figures 15(A, B) shows the resulting calcein fluorescence from eLiposomes without folate, while Figures 15(C, D) shows the parallel experiment having folate incorporated in the eLiposomes. Because the calcein was concentrated (15 mM) in the eLiposomes, it did not fluoresce until released by insonation; but all cells in Figure 15 were insonated. There is very little calcein signal observable in Figure 15B, suggesting that very few calcein-containing eLiposomes were endocytosed when they were not derivatized with folate. In Figure 15D, the calcein fluorescence is originating from the cell cytosol, not the cell surface, suggesting that the folated eLiposomes had been endocytosed and that the calcein had been released to the cytosol. Some of these cells exhibit a granular pattern of calcein fluorescence, perhaps indicating that some calcein remains in endosomes, and although released from the eLiposome and diluted sufficiently to fluoresce, some calcein may not have been released completely from the endosome.

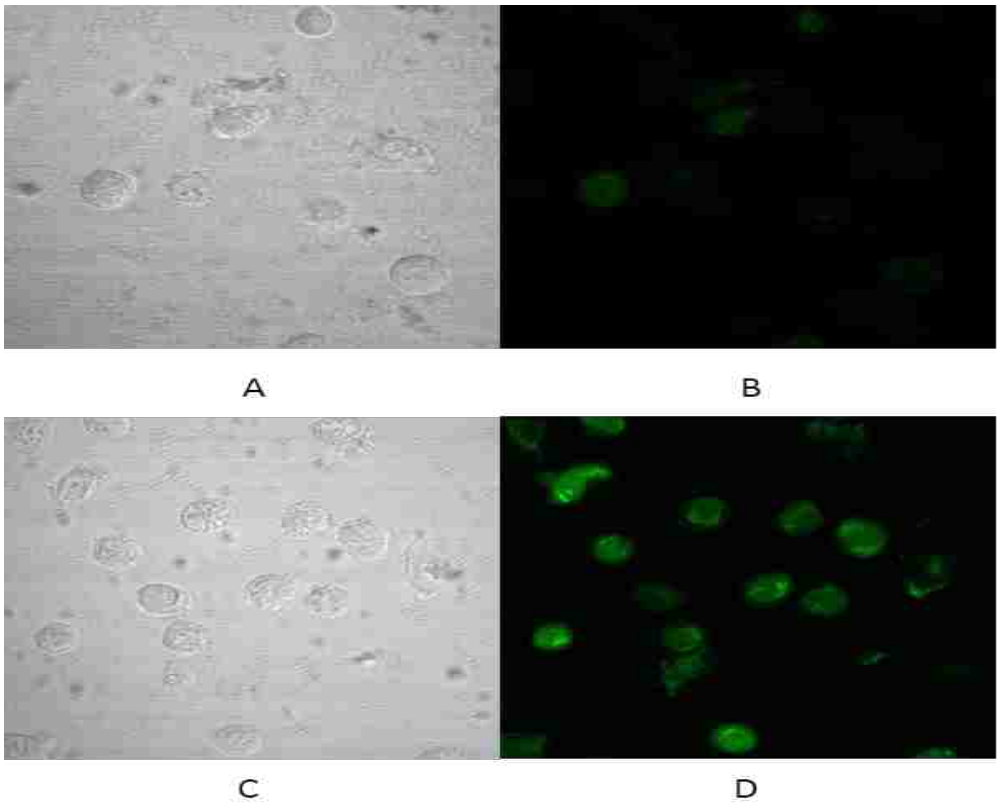

Figure 15: Images of HeLa cells exposed for 2 hours to ultra eLiposomes containing 15 mM calcein, followed by application of 20 kHz ultrasound at 1W/cm^2 for 2 seconds. (A, B) eLiposomes were not folated. (C, D) eLiposomes contained folate in their phospholipid membrane. A and C are light images, B and D are confocal fluorescent images. Taken from [106] with permission.

While Figure 15 shows that folate is necessary, Figure 16 shows that emulsions are also necessary for calcein delivery. Folated ultra eLiposomes with PFC5 emulsions and folated conventional liposomes (without emulsions) were prepared, each containing calcein at 30 mM. Then 200 μL of each sample was added to HeLa cells in 12-well plates. The plates were incubated at 37°C for about 2 hours and then 20 kHz ultrasound was applied to all samples (1 W/cm^2 for 2 s). Figure 16A shows very little release of calcein to the cells exposed to folated conventional liposomes (without emulsion) while Figure 16B shows considerable release of

calcein in the parallel experiment employing folated eLiposomes. Recall that non-released calcein does not show up because it is self-quenched.

Both these images were collected under identical optical conditions with the same gain and other settings on the confocal microscope. Most cells in Figure 16 B show calcein distributed through the cell, but again sometimes calcein appears more intensely in punctate spots which might be ruptured eLiposomes but not unruptured endosomes. The lack of release of calcein from folated conventional liposomes (Figure 16A) implicates the emulsion nanodroplets as a necessary element to obtain ultrasonically-triggered calcein release to the cytosol.

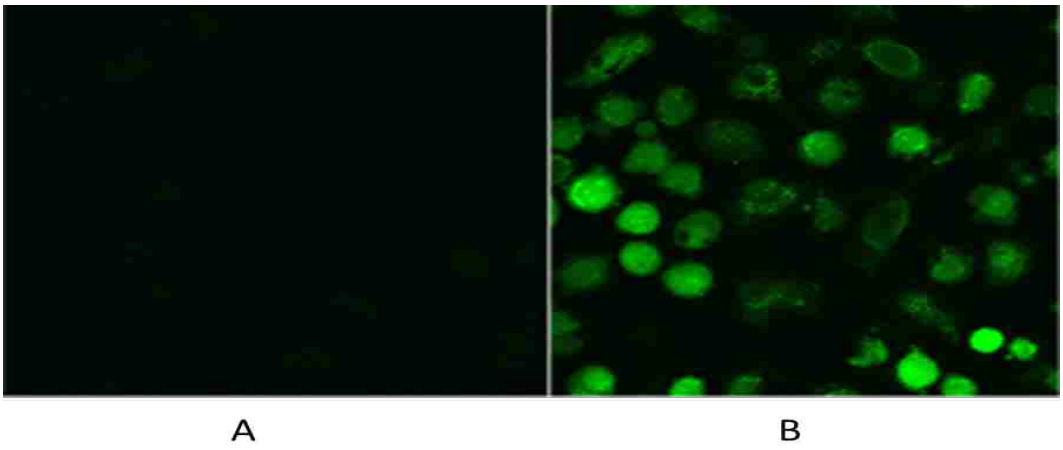

Figure 16: (A) Confocal image of HeLa cells exposed to calcein-containing folated liposomes (no emulsion within) for 2 hours after which ultrasound was applied at 1W/cm^2 for 2 seconds. (B) Confocal image of a similar experiment except that folated eLiposomes (containing PFC5 emulsions) were used. Taken from [106] with permission.

5.2.5 Discussion

Bubbles, bubble liposomes and echogenic liposomes have been used in drug and gene delivery for several years [110-116]. However, these bubble constructs are usually not small

enough to take advantage of the EPR effect and extravasate into tumors. Ultrasound has been used to cause release from drug carriers and make the cell permeable to the drug at targeted locations [41, 117, 118]. However liposomes are not inherently responsive to ultrasound. Drug release from liposomes may occur in the presence of microbubbles undergoing cavitation; release also depends on lipid composition as well [119-121]. The key advantages of these new eLiposomes are that they are small enough to extravasate and that they are responsive to low intensity ultrasound.

Cryo-TEM showed that the majority of eLiposomes had one emulsion droplet inside, fewer had 2 droplets and about 1% had more than 2 droplets inside. This distribution is consistent with our hypothesis that the possibility of 3 droplets finding themselves in the same location is much less than the probability of 2 droplets being in the same location.

We propose that our eLiposomes can be used in ultrasonically activated drug delivery as follows. The eLiposomes could be loaded with drugs, such as Doxorubicin, using conventional or pH gradient techniques [122]. Upon exposure to ultrasound, the local pressure oscillates above and below ambient pressure. At sufficiently high acoustic amplitudes, the local pressure decreases below the vapor pressure of the PFC emulsion inside the eLiposome. During this short time, the PFC may start to boil to a gas phase.

The physics underlying ultrasonically induced phase change may be very complex. Boiling is suppressed by the additional pressure imposed on the interior of the nanoemulsion, called the Laplace pressure (ΔP_{Lp}), created by the interfacial energy (γ_l) and the small radius (R) of the emulsion: $\Delta P_{Lp} = 2\ (\gamma/r)$. The local pressure inside the emulsion is the sum of the atmospheric pressure (P_{atm}), the hydrostatic pressure (P_{hyd}) due to the depth under the liquid

surface, the Laplace pressure, and the imposed dynamic ultrasonic pressure, $P_{US}(t)$. In many cases the ultrasonic pressure is approximately sinusoidal: $P_{US}(t) = P^{-} \sin \omega t$ where P^{-} is the peak rarefactional pressure. For gas to form, the total pressure inside the nanoemulsion must drop below the vapor pressure of the PFC, $P_{vap}(T)$. Thus gas expansion may occur when

$$P_{tot} = P_{atm} + P_{hyd} + \Delta P_{Lp} + P_{US}(t) \leq P_{vap}(T) \quad \textbf{(3)}$$

Obviously, a phase change will occur more readily for PFCs with higher vapor pressure (i.e. PFC5) and larger droplet diameters. By rearranging equation (3), we see that the dynamic ultrasound pressure must drop to a fairly low value, perhaps even a negative absolute pressure value:

$$P_{US}(t) \leq P_{vap}(T) - P_{atm} - \Delta P_{Lp} - P_{hyd} \quad \textbf{(4)}$$

As an example, PFC6 boils at 57°C; at this temperature its vapor pressure is 1 atm. At 37° PFC6 has a vapor pressure of 0.48 atm. In this example, we assume the hydrostatic pressure is negligible. Thus an ultrasonic peak rarefactional pressure of only 0.52 atm less the Laplace pressure would be sufficient to allow boiling in the PFC6. We emphasize “allow”, and not “cause”, because this requirement is necessary but not sufficient for boiling, since nucleation must also occur. For now we will assume that nucleation occurs, and we note that initially the gas forms as the local pressure of the ultrasonic wave decreases below the emulsion vapor pressure less the Laplace pressure. When the oscillating pressure wave reverses and increases in pressure, the gas condenses back into PFC liquid [46]. However, during that short time of gas formation, a large volume expansion occurs, sufficient to rupture the eLiposomes and the endosome.

Lipid bilayers can only sustain about 3% area expansion before they rupture [123, 124]. For the PFC6 and PFC5 of this research, the liquid to gas expansion ratios are 125.9-fold and 137.0-fold, respectively (vapor to liquid volume ratio, 1 atm, boiling temperature, no Laplace pressure). For a 250-nm-diameter eLiposome containing a single 100-nm-diameter PFC6 emulsion droplet, less than 0.2% of the PFC liquid is required to vaporize to achieve the 3% area expansion for eLiposome lysis. We expect that once nucleated, the droplet will completely vaporize, based on recently published models showing that the window for partial vaporization is very narrow [125]. Nucleation of the vapor phase may or may not occur on the first negative pressure cycle of the ultrasonic wave. There are reports of gas-phase nucleation occurring in only a few cycles [126], but these were conditions of much higher acoustic amplitude (8 MPa) than employed in our research (0.2 MPa). More study remains to be done on the nucleation kinetics of the gas phase under these conditions.

Although any liquid of high vapor pressure could be employed in eLiposomes, PFCs are useful for making emulsion droplets within eLiposomes because the phospholipids and PFCs are biocompatible and non-toxic [127]. The boiling point of PFC6 is above the body temperature so it will not be vaporized in the body before application of the ultrasound, and it will return to liquid afterwards. Furthermore it remains stable in the liposomes during heating and hydration (in the 1-step process) to form the eLiposomes containing PFC6.

Although PFC5 has a boiling point (29°C) lower than body temperature, it has some advantages over PFC6 for use at body temperature (37°C). First of all, we and others have formed PFC5 emulsions that are stable at body temperature or higher [128-131], which stability is attributed to the Laplace pressure imposed on the emulsion. The interfacial tension of a phospholipid-coated PFC/water interface is about 3.8 dyn/cm [132]; but despite the small value

of this interfacial tension the small radius of the emulsions is sufficient to stabilize the emulsion above its normal boiling point. In fact, we can carefully heat our PFC5 nanoemulsions to 50°C for a short time without boiling them. However, once expanded by ultrasound into a gas bubble at body temperature, the 5-fold larger radius of the gas bubble and reduced interfacial tension (~3.8 dyn/cm for DPPC [133]) will decrease the Laplace pressure by more than a factor of 5 and preclude condensation back to a liquid at body temperature. The PFC5 nanobubbles will be above their boiling point and remain in the gas phase indefinitely, although they may eventually dissolve into the surrounding liquid. Continued application of ultrasound will cause the nanobubbles to cavitate and cause shear stress on the endosome and other cellular membranes, causing endosomal escape and promoting increased intracellular drug or gene distribution [30, 134, 135].

6 CALCEIN AND PLASMID DELIVERY USING ELIPOSOMES

6.1 Introduction

In chapter 5 we developed 1-step eLiposomes and "ultra" eLiposomes. We also did some preliminary experiments to deliver calcein to HeLa cells using eLiposomes.

By applying ultrasound to eLiposomes, emulsion droplets can transform from liquid to gas and rupture the lipid bilayer of the eLiposome to release its contents. This chapter presents the results of experiments showing that PFC5 eLiposomes could be taken up by HeLa cells. It shows the effect of PFC5 emulsion droplets, ultrasound and folate on delivery of a model drug (calcein) and successful transfection of plasmids to produce a green fluorescent protein.

The eLiposomes used in this chapter were made using the "ultra" method. In brief eLiposomes were formed by mixing emulsion droplets and liposomes using ultrasound. Calcein or plasmid was present when ultrasound was applied to form the eLiposomes. Pillow density separation was done before using eLiposomes. This work has been published in the *Journal of Controlled Release* [136].

Confocal microscopy was used to quantify calcein delivery and the level of plasmid transfection into HeLa cells.

6.2 **Results**

6.2.1 Effect of Ultrasound

The first set of experiments reported in this chapter was designed to establish that application of low intensity ultrasound could release calcein to the interior of the cell and deliver plasmids in a manner to promote expression of the plasmid by the production of a green fluorescent protein.

Figures 17A and B show HeLa cells incubated with calcein eLiposomes for 2 hours, to which no ultrasound was applied, while Figures 17C and D show similarly incubated cells exposed to 20 kHz ultrasound for 2 s at 1 W/cm^2.

A few cells in panel B show barely visible calcein fluorescence, while cells exposed to US show the green color indicative of calcein released from the eLiposome. Although the intensity of green fluorescence varies from cell to cell, every cell in panel C displays some green fluorescence in panel D. The application of ultrasound apparently caused release of the calcein from the eLiposomes, and upon dilution, the fluorescence of the unquenched calcein appeared as a green color. Panel D also shows that the calcein was released and distributed throughout the cells, suggesting that if the eLiposomes were taken into endosomes, the calcein had escaped from most of the endosomes into the cytosol. Some calcein may have entered the nucleus. There are a few punctate spots of bright green color, which might indicate that calcein was released from the eLiposome, but not from the endosome.

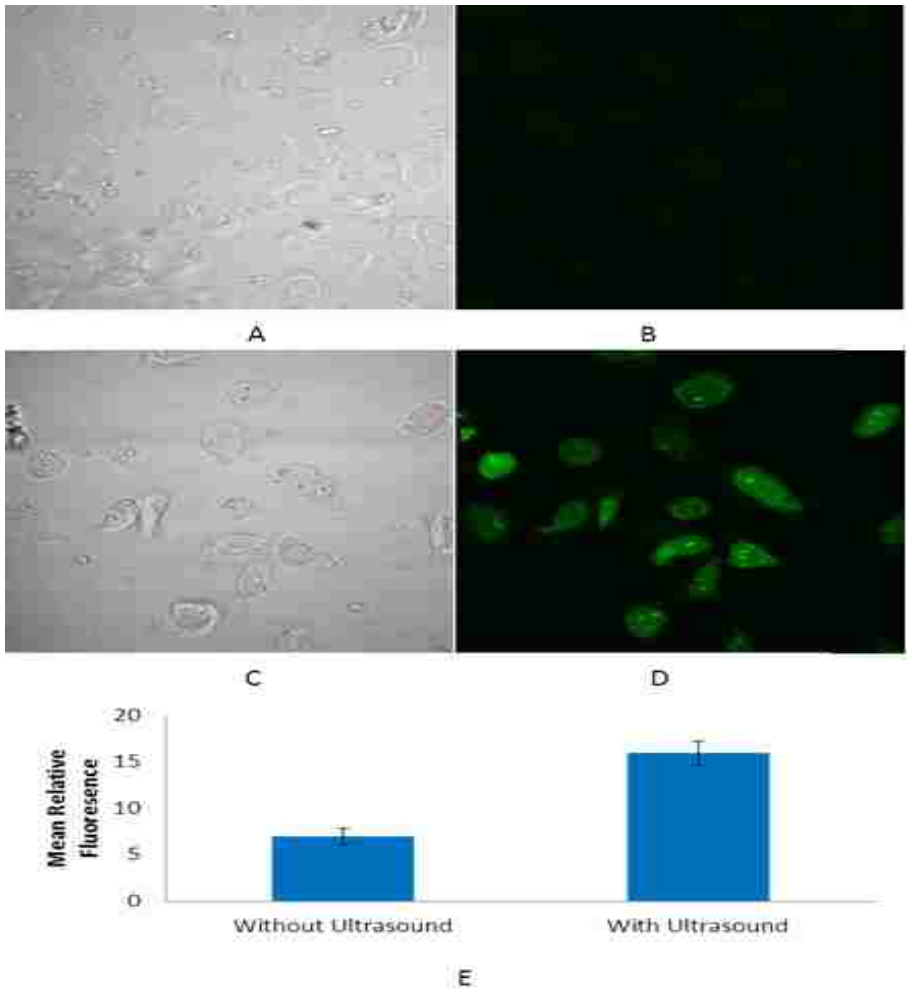

Figure 17: Light (A) and confocal images (B) of HeLa cells exposed to PFC5 folated-eLiposomes containing calcein but not insonated. Light (C) and confocal (D) images of cells exposed to ultrasound at 1W/cm2 for 2 s. (E) Average fluorescence intensity from confocal images of HeLa cells. Error bars represent 95% confidence intervals. Taken from [136] with permission.

The average relative intensities of green fluorescence and 95% confidence intervals were calculated and are presented in Figure 17E. The average fluorescence per cell is significantly greater ($p < 0.05$) when ultrasound was applied.

Similar experiments were done with eLiposomes containing the AFP plasmid. This time instead of calcein we encapsulated plasmid inside the eLiposomes. Figure 18A shows negligible plasmid transfection at 48 hours in cells exposed to eLiposomes but without insonation, while

Figure 18B shows considerable transfection and expression of plasmid in the parallel experiment 48 hours after application of 20 kHz ultrasound for only 2 sesonds. The expression of fluorescent protein is significantly greater ($p < 0.05$) when ultrasound was applied. We note that the green fluorescent protein does not appear in the nucleus, as expected for the production of large protein that cannot traverse the nuclear membrane.

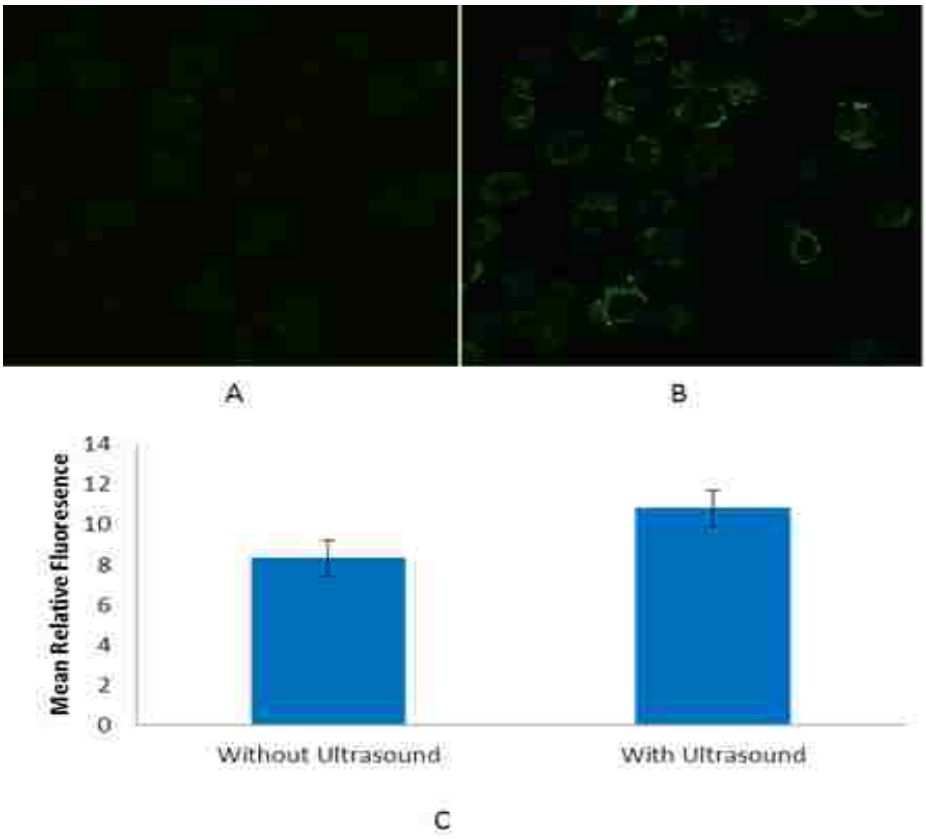

Figure 18: (A) Confocal image of HeLa cells exposed to plasmid-containing folated eLiposomes 48 hours after adding eLiposome droplets. (B) Confocal image of the same experiment except that ultrasound was applied. C) Average fluorescence intensity from confocal images of HeLa cells. Error bars represent 95% confidence intervals. Taken from [136] with permission.

6.2.2 Effect of Emulsion

While Figures 17 and 18 show that ultrasound is necessary for release from the eLiposome to the interior of the cell, Figures 19 and 20 indicate the requirement of PFC5 emulsion droplets for efficient calcein release and plasmid delivery and expression. In these experiments, folated eLiposomes containing PFC5 emulsion droplets and folated conventional liposomes (without emulsions) were prepared, each containing calcein at 15 mM. Figure 19A shows very little release of calcein into the cells from folated conventional liposomes (without emulsion), while Figure 19B shows considerable release of calcein in parallel experiments employing eLiposomes receiving the same ultrasonic exposure (2 seconds at 1 W/cm^2). Figures 19A and B were collected under identical optical conditions, so their relative fluorescence can be directly compared (Figure 19C). Most of the cells show calcein distributed through the whole cell, but in some cells calcein appears more intensely in punctate spots that might indicate that some endosomes may not have been ruptured even though the eLiposomes with PFC5 droplets were ruptured.

Similar experiments were done for eLiposomes containing the GFP plasmid. Figure 20A shows much less transfection and protein expression in the cells exposed to ultrasound and conventional folated liposomes (without emulsion), while Figure 20B shows gene expression of plasmid in the parallel experiment employing ultrasound and folated eLiposomes. In Figure 20B, the protein expression appears to be localized in the cytosol as expected for a large protein unable to diffuse into the nucleus.

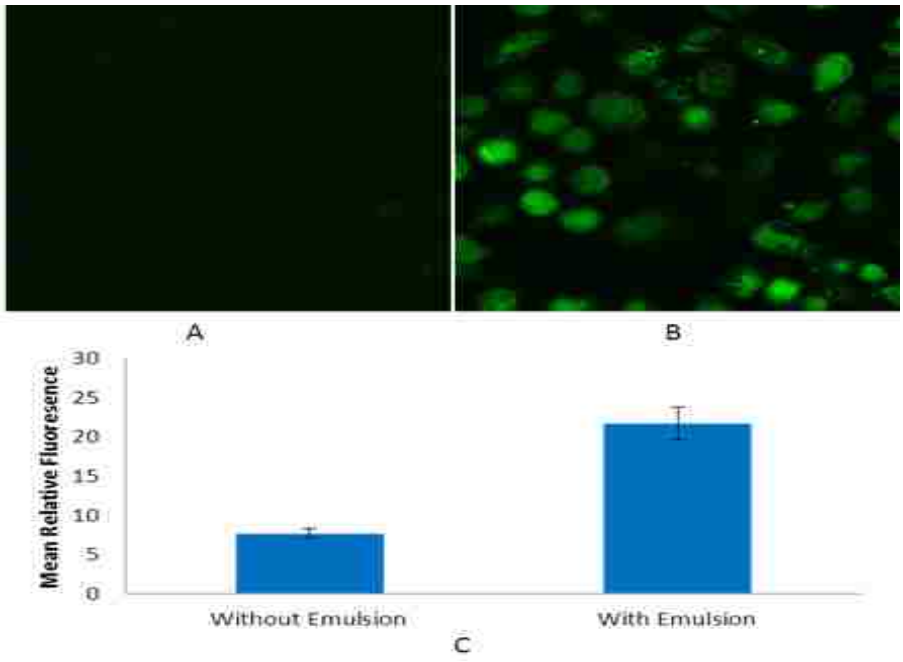

Figure 19: (A) Confocal image of HeLa cells exposed to folated liposomes (containing 15 mM calcein but not emulsion droplets) for 2 hours after which ultrasound was applied. (B) Confocal image of the parallel experiment except that folated eLiposomes (containing calcein and emulsion droplets) were used. (C) Average fluorescence intensity from confocal images. Error bars represent 95% confidence intervals. Taken from [136] with permission.

6.2.1 Effect of Folate

Having established the requirement for both ultrasound and emulsions within the eLiposome to produce calcein delivery and plasmid protein expression, the next set of experiments investigated the role of folate as a necessary ligand. Parallel experiments were conducted using eLiposomes containing calcein, which were prepared with and without DSPE-PEG2000-folate incorporated into the eLiposome bilayer. The same size aliquot (200 μL) and procedure were used in these experiments, including the same ultrasonic exposure

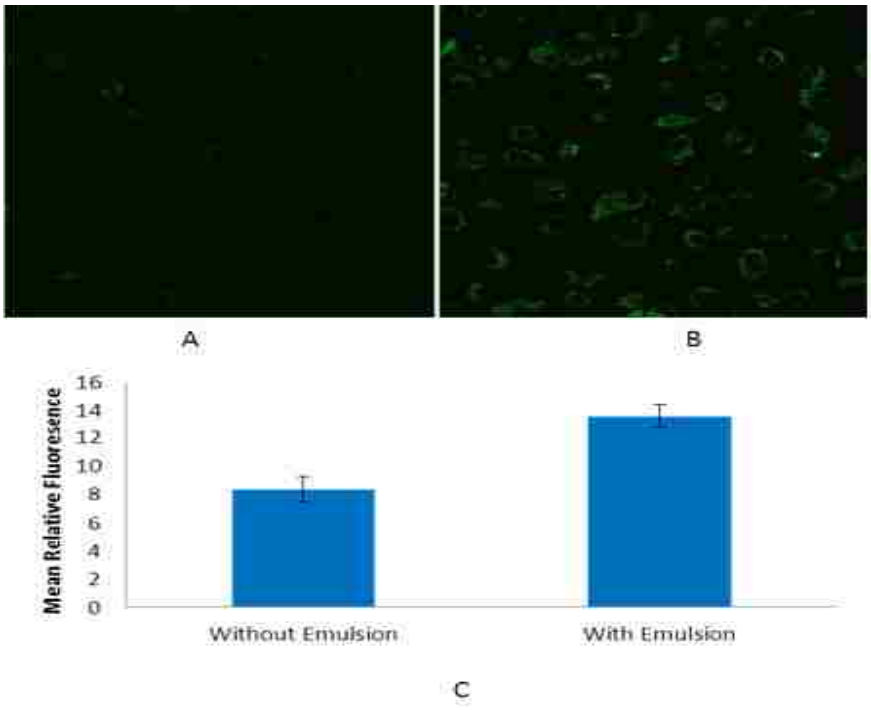

Figure 20: (A) Confocal image of HeLa cells exposed to folated liposomes containing plasmid (but not emulsion droplets) 48 hours after ultrasound was applied. (B) Confocal image of the parallel experiment except that folated eLiposomes (containing plasmid and emulsion droplets) were used. (C) Average fluorescence intensity from confocal images of HeLa cells. Error bars represent 95% confidence intervals. Taken from [136] with permission.

(1 W/cm^2 for 2 seconds). Figure 21A shows the resulting calcein fluorescence from eLiposomes without folate, while Figure 21B shows the same experiment with folated eLiposomes. In Figure 21A, very little calcein signal was observed, even though ultrasound was applied to the cells with PFC5 eLiposomes.

These data suggest that when folate was absent, comparatively few calcein-containing eLiposomes were endocytosed and thus not many calcein-containing eLiposomes were within the cell when they were induced to release their payload. On the other hand, when folate ligands were present, there was a significant increase (p<0.05) in the calcein intensity following

insonation (Figure 21B). Furthermore these confocal images show a slice through the interior of the cell. Thus the calcein fluorescence originates from the cell interior, not the cell surface, indicating that the eLiposomes were more than just bound to the surface – they were taken into the cell, most probably through endocytosis.

In a control experiment, before adding the eLiposomes some soluble folate (6-8 mg/mL) was added to the folate-starved cells to fill their folate receptors thus blocking the receptors from binding folated eLiposomes. In this case, as shown in Figure 21C, very little calcein fluorescence was observed after insonation, suggesting that relatively few calcein-containing eLiposomes were endocytosed under conditions of competitive inhibition by free folate. These data indicate that both folate attached to the eLiposome and available folate receptors on the cells are required for cytosolic calcein release upon insonation of the cells.

Similar experiments using eLiposomes containing the AFP2 plasmid (Figure 22) exhibited similar results. Figure 22A shows the resulting green fluorescent protein 48 hours after insonating eLiposomes without folate, while Figure 22B shows the parallel experiment using folated eLiposomes. In Figure 22B, the fluorescence is again originating from the cell cytosol, not the cell surface or cell nucleus, suggesting that the folated eLiposomes had been endocytosed and the plasmid released and delivered to the cytosol where it apparently entered the nucleus and elicited protein expression in the cytosol.

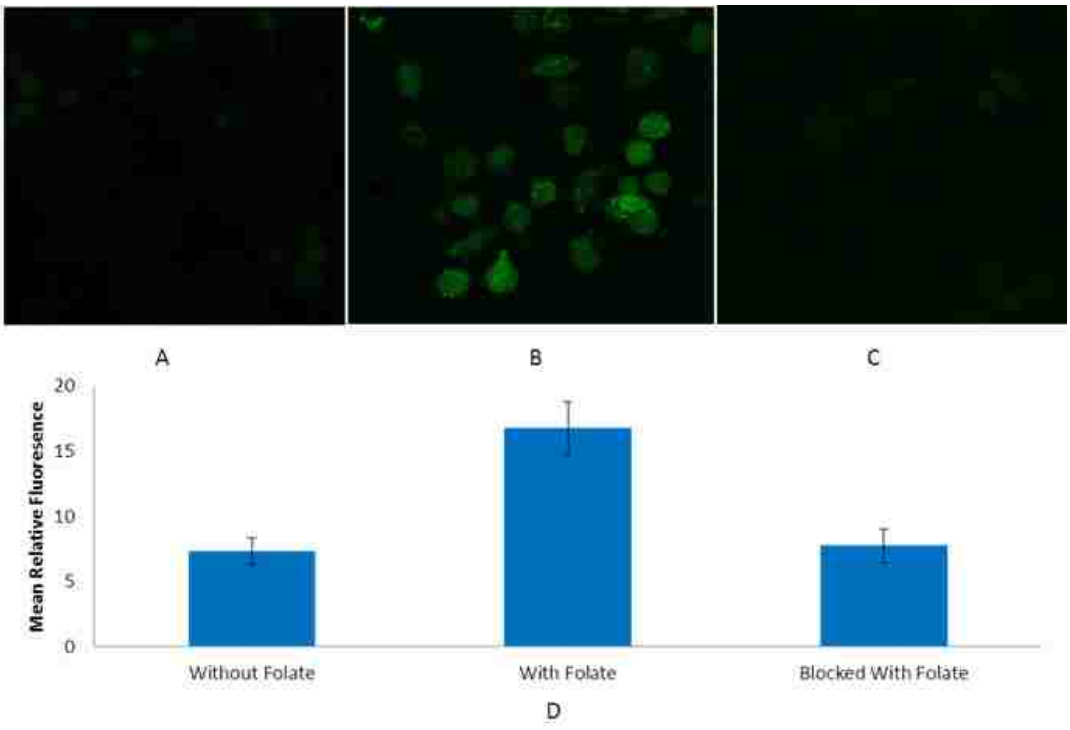

Figure 21: Confocal images of HeLa cells after being exposed to eLiposomes containing 15 mM calcein for 2 h, followed by application of 20 kHz ultrasound for 2 s at 1W/cm^2. (A) Cells incubated with non-folated eLiposomes. (B) Cells incubated with folated eLiposomes (C) Cells that were exposed to free folate (6-8 mg/mL) prior to adding folated eLiposomes. (D) Average fluorescence intensity from confocal images of HeLa cells. Error bars represent 95% confidence intervals. Taken from [136] with permission.

Again in competitive inhibition experiments, free folate (6-8 mg/mL) was added to the cells just prior to addition of the eLiposomes. The lack of green fluorescence (see Figure 22C) suggests that very few plasmid-containing eLiposomes were endocytosed when folate receptors were blocked with free folate. Images 22A, B and C were obtained 50 hours after addition of eLiposomes and 48 hours after insonation.

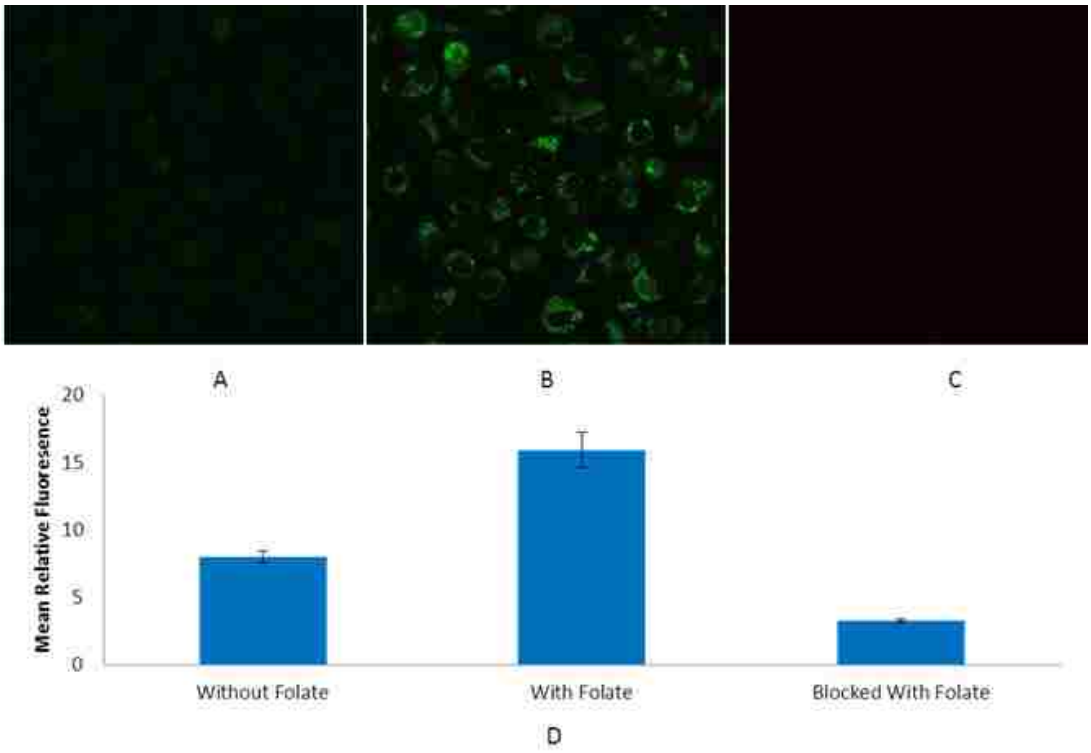

Figure 22: Confocal image of HeLa cells after being exposed to eLiposomes containing AFP plasmid and followed 2 h later by application of 20 kHz ultrasound. (A) Non-folated eLiposomes. (B) Folated eLiposomes. (C) Folate receptors were blocked with free folate (6-8 mg/mL) prior to adding the folated eLiposomes. All images were collected 48 h after applying the ultrasound at 1W/cm^2 for 2 seconds (D) Average fluorescence intensity from confocal images of HeLa cells. Error bars represent 95% confidence intervals. Taken from [136] with permission.

6.2.2 Effect of Time and Intensity of Ultrasound

Several miscellaneous experiments were conducted to explore the effects of various ultrasonic exposure times and intensities. In each case, 200 μL of folated eLiposomes with PFC5 emulsions containing calcein at 15 mM were added to HeLa cells in 12-well plates. Exposure times were varied from 2 to 6.4 seconds and the intensities were varied from 0.25 to 1 W/cm^2 to test the hypothesis that longer times and higher intensities would produce more calcein release or transfection. Figure 23 shows confocal images of representative fields of cells. As the times and

intensities were varied (see captions of Figures 23 and 24), there did not appear to be great differences in calcein fluorescence. Figure 23G compares the relative mean fluorescence ranked according to the energy density, which is the product of the exposure time and the power density. I could find no statistically significant correlations within this data set.

Similar experiments were conducted using folated and plasmid-containing eLiposomes. Again there was not any significant correlation between time, intensity and the amount of protein expression (see Figure 24).

6.3 **Discussion**

We have shown that a model drug (calcein) and a model plasmid can be delivered to cells *in vitro* and released upon application of low frequency and low intensity ultrasound. These eLiposomes were easily made by adding nanosized emulsion droplets (50 to 100 nm) to 200-nm phosphatidylcholine liposomes and mixing with a probe sonicator on ice [106]. PFC5 was chosen for making emulsions because of its high vapor pressure and superior release [104].

Although acoustic droplet vaporization is not new [45, 48-51, 137, 138], to our knowledge this research is the first demonstration of using perfluorocarbon emulsion vaporization to deliver a plasmid for gene expression via escape from the endosome to the cytosol and eventually to the nucleus.

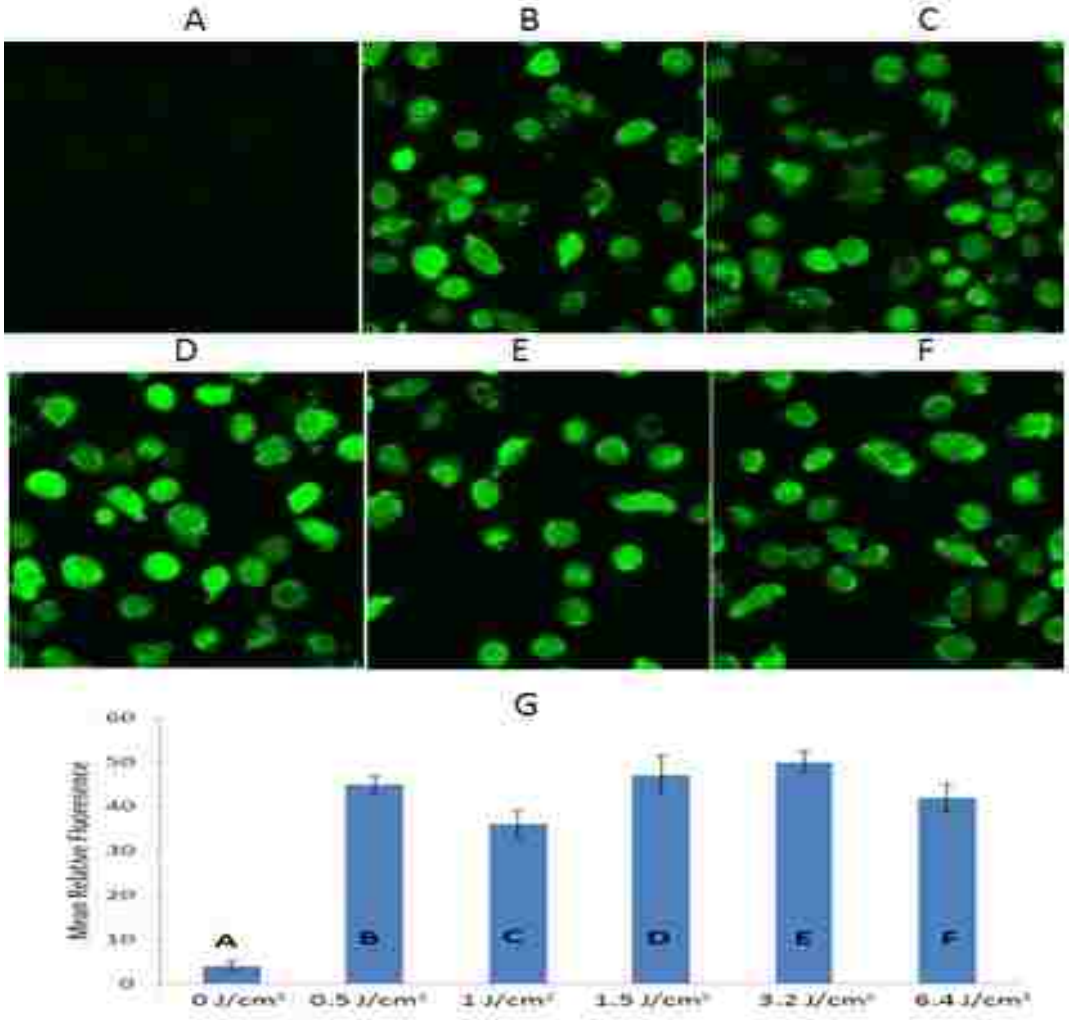

Figure 23: Confocal images of HeLa cells exposed to eLiposomes containing calcein after applying ultrasound as follows:(A) 0 J/cm^2 , (B) 0.25W/cm^2 × 2s = 0.5 J/cm^2, (C) 0.25W/cm^2 × 4s = 1 J/cm^2, (D) 0.75W/cm^2 × 2s = 1.5 J/cm^2, (E) 1W/cm^2 × 3.2s = 3.2 J/cm^2, and (F) 1W/cm^2 × 6.4s= 6.4 J/cm^2. (G) Average fluorescence intensity from confocal images of HeLa cells. Error bars represent 95% confidence intervals. Taken from [136] with permission.

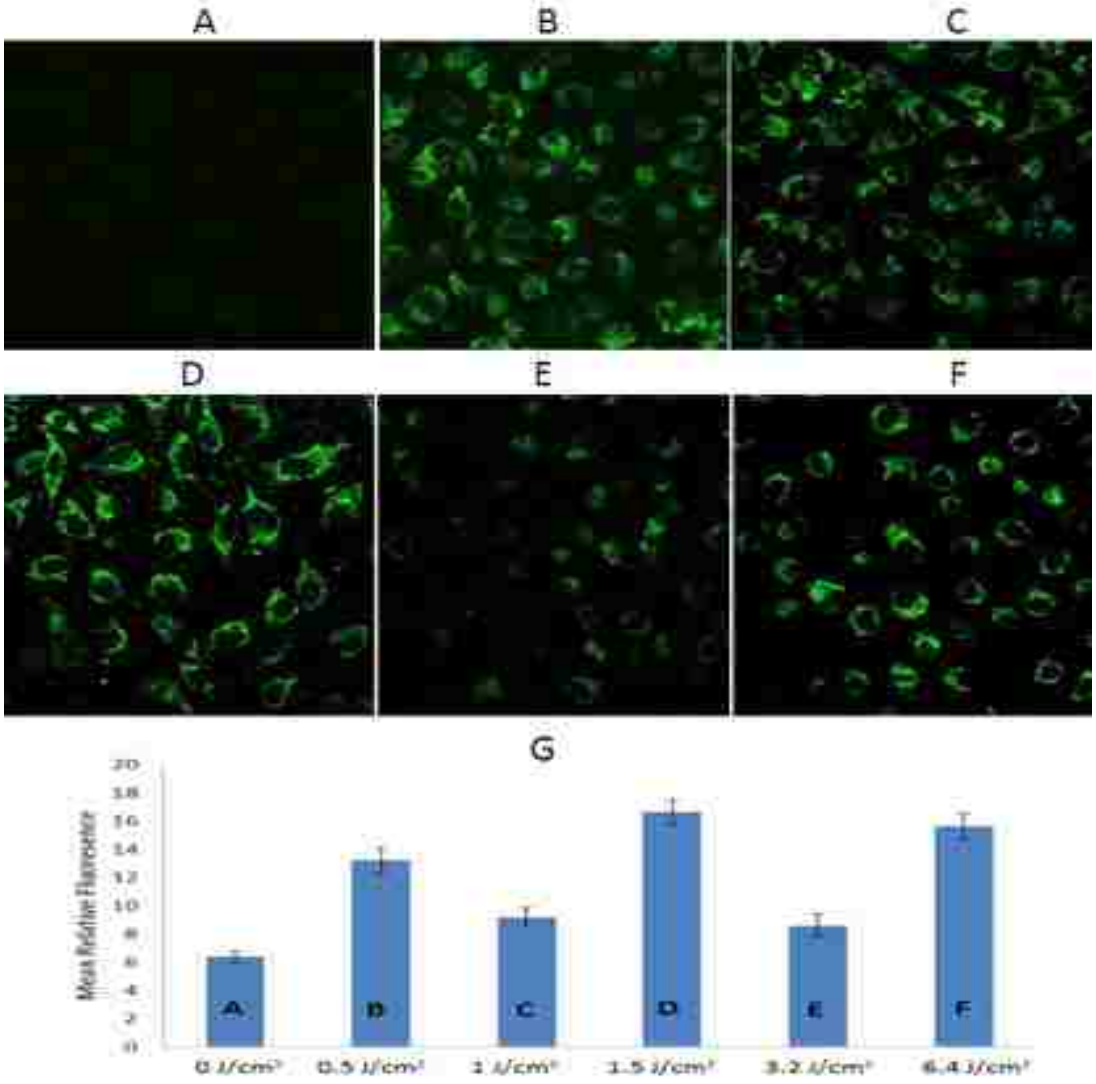

Figure 24: Confocal images of HeLa cells exposed to eLiposomes containing plasmid after applying ultrasound as follows: (A) 0 J/cm^2 , (B) 0.25W/cm^2 × 2s = 0.5 J/cm^2, (C) 0.25W/cm^2 × 4s = 1 J/cm^2, (D) 0.75W/cm^2 × 2s = 1.5 J/cm^2, (E) 1W/cm^2 × 3.2s = 3.2 J/cm^2, and (F) 1W/cm^2 × 6.4s= 6.4 J/cm^2. (G) Average fluorescence intensity from confocal images of HeLa cells. Error bars represent 95% confidence intervals. Taken from [136] with permission.

One of the most novel aspects of this therapeutic delivery device is that emulsions are placed inside the liposome that carries the therapeutic. The quantitative results of this study have

shown that the release of calcein or plasmid from this eLiposome package was significantly less in the absence of ultrasound (Figures 17 and 18). Such a tight and secure delivery vehicle is required for the site-specific delivery of toxic therapeutics that should not be released indiscriminately in the body.

In addition to retaining therapeutics within the vesicle, we posit that our eLiposomes also keep lytic molecules from entering and degrading the payload. For example, our eLiposomes were sufficiently tight that the plasmids were not degraded after uptake by the endosome, even though we loaded naked plasmids that were not condensed with any protective polymers or cationic lipid molecules. Endosomes degrade plasmids as they mature toward lysosomes.

Furthermore, none of the components of this delivery system involve any cationic polymers, cationic lipids, or any other molecules that are toxic to cells. Only natural phospholipids are used to build the eLiposomes; and the perfluoropentane is safe and readily cleared from the body through the lungs [139].

To achieve delivery to the cytosol, folate was attached to a phospholipid and inserted into the outer membrane of the eLiposome. Folate was selected as it is the substrate for folate receptors that are over-expressed in many cancerous cell lines, including the HeLa cells used in this research [140]. While there are other ligand-receptor pairs that can be used to actively target cancerous cells, folate was selected because its binding also induces endocytosis of the folate, and in this case, endocytosis of the attached eLiposome, a scenario supported in this study (see Figures 21 and 22). For example, when non-folated eLiposomes were exposed to cells, which were subsequently insonated, calcein release or GFP expression was not nearly as great as with folated eLiposomes, indicating that folate binding increased the uptake of eLiposomes by folate-starved cells. Furthermore when eLiposome uptake was competitively inhibited by blocking

folate receptors with free folate, there was much less calcein release or gene expression after insonation.

These results are consistent with those of prior investigators who showed that folate attachment to conventional liposomes containing doxorubicin increased *in vitro* cell toxicity, which was attributed to increased endocytotic uptake [69]. It was also previously observed that folated liposomes had 45 times higher uptake into KB cells compared to uptake of non-targeted liposomes [70]. Gabizon et al. found that folated liposomal doxorubicin is much more effective than non-folated liposomes [141]. Folate also has been used in gene delivery and showed 1.6-fold increase in binding and internalization compared to non-targeted liposomes in a mouse model of breast cancer [142].

We speculate that attachment of other ligands that induce endocytosis would be effective in promoting uptake of eLiposomes, including carbohydrates and protein ligands (i.e. antibodies) designed to selectively bind to cancer cells. For example we would expect that the attachment of trastuzumab to an eLiposome would stimulate endocytosis via attachment to the HER2/neu receptor [143-145].

Some of the cells exhibit a granular pattern of calcein fluorescence, perhaps indicating that some calcein remains in endosomes, and while released from the eLiposome and diluted sufficiently to fluoresce, not all of the calcein may have been released from the endosome. In such cases it is possible that the emulsion expansion may have been large enough to rupture the eLiposome, but was not sufficiently large to rupture the endosome.

Direct delivery to the cytosol through rapid bursting of the endosome is advantageous for delivery of therapeutics whose targets are in the cytosol. Such therapeutics include siRNA (and other therapeutics that interfere with protein translation) or drugs that interfere with actin

assembly or other required processes of cell replication. Delivery of small molecules whose targets are not in the cytosol is also feasible if the diffusion and organelle membrane permeability is sufficient. The nucleus and mitochondria are obvious targets. The charged molecule calcein appears to easily penetrate into the nucleus as seen in Figures 17, 19, and 21.

It was a bit surprising that there was sufficient plasmid delivery to demonstrate significant GFP expression. Plasmid delivery to the cytosol does not guarantee delivery to the nucleus, particularly since the transport of a plasmid through the cytosol is negligible due to interactions with stationary structures [146]. The successful nuclear delivery and gene expression might have occurred because some endosomes were very near the nucleus. An additional hypothesis is that the formation of PFC5 gas bubbles and subsequent oscillation (cavitation) during the pulse of ultrasound could have created microconvection in the cytosol that transported plasmids to the vicinity of the nucleus. The cavitation may have even breached the nuclear membrane to allow direct entry of plasmid; but if this happened the membrane healed sufficiently that the cell was not damaged in a way to prevent plasmid transcription and GFP protein production. Inspection of Figures 20 and 22 show that in most if not all cells, the GFP is excluded from the nucleus. Such exclusion implies that if the nuclear membrane was damaged to allow plasmid entry, the membrane was intact again by the time the protein was produced by mRNA in the cytosol.

In any event, the plasmid was successfully delivered and the protein produced using eLiposomes and ultrasound. A more detailed mechanistic understanding of plasmid delivery should be the subject of future research.

Studies by others suggested that there should have been some correlation between calcein and plasmid delivery and time and intensity of ultrasound [147]. However, data in Figures 23

and 24 show that within the time and intensity parameters studied herein, there was not a statistically significant correlation. It is possible that the threshold for release might occur at a much lower intensity than we used, or that even our short insonation pulse was sufficiently long to burst all eLiposomes. More research should be done to identify any such thresholds.

As to the mechanisms of eLiposome delivery, this study showed convincingly that the internal nanoemulsion droplet is required. The data revealed that the amount of calcein or plasmid delivery increases significantly when emulsions are incorporated inside the eLiposomes (see Figures 19 and 20), suggesting that emulsions droplets rupture the eLiposome bilayer and allow the encapsulated therapeutics to escape.

The ultrasound intensity used in this study (1 W/cm^2) was much more than needed to transform the liquid PFC5 to gas. This intensity corresponds to a pressure amplitude of 173 kPa, assuming a plane wave. A 100 nm emulsion droplet of PFC5, stabilized with a phosphatidyl choline is estimated to have an interfacial energy of 3.5 mN/m [132] and a Laplace pressure of 140 kPa. At 37°C and 1 atm external pressure, the vapor pressure of PFC5 is 132,253 Pa [148], which is still less than the internal pressure of 241,000 Pa, the local external pressure (101,000 Pa) plus the Laplace pressure. Such a droplet could boil only if the local temperature were increased to 55.8°C. However, if an ultrasound wave of more than 108,747 Pa amplitude were imposed, at some point the pressure inside the nanodroplet would drop below the vapor pressure of 132,253 at 37°C. The boiling would expand the volume of the emulsion by 138 fold, to a gas bubble with a diameter of 517 nm ($200 \times (138)^{1/3} = 517$). Assuming the same interfacial energy, the Laplace pressure on the PFC gas bubble would be only 27,092 Pa, and at 37°C the PFC5 would remain as a gas bubble after the insonation stopped (132,253 Pa > 101,000 Pa + 27,092 Pa). The theoretical expansion to a gas is sufficient to burst the eLiposome bilayer membrane,

and apparently in our experiments it is also sufficient to burst some of the endosomes. The acoustic amplitude used in my experiments is both theoretically sufficient, and experimentally proven to burst eLiposomes.

As yet we do not know all of the detailed intricacies of the mechanisms and physics of delivery via eLiposomes, but we have shown that drug and plasmid delivery is feasible and fairly easy to accomplish.

7 OTHER PARAMETERS CONTROLLING OF ULTRASONIC RELEASE FROM ELIPOSOMES

7.1 Introduction

We have seen that eLiposomes can be made by three different methods, one of which was studied extensively in this research. Ultrasound, emulsion droplets and folate are essential elements for delivering calcein and plasmid to the cell cytosol. In this study our objective was to find other parameters that control release from eLiposomes.

Even though there has been comprehensive research about the effect of ultrasound on release from liposomes, no previous studies have systematically examined the effect of ultrasound amplitude, insonation time, temperature, or emulsion formulation on release from eLiposomes.

In this study our objective was to examine the effect of intensity, insonation time, and different perfluorocarbon composition on release from eLiposomes.

The results show that by increasing the ultrasound amplitude and insonation time, the release from eLiposomes increases. It also shows that changing the composition of emulsion droplets from perfluorohexane to perfluoropentane increases release. The release of calcein does not appear to correlate linearly with vapor pressure of the perfluorocarbon liquids forming the emulsion droplets.

To produce a drug carrier system that can target tumors and induce endocytosis, folate was attached to the outer leaflet of the eLiposome bilayer. Poly ethylene glycol (PEG) was attached to the eLiposomes to increase the circulation time for future *in vivo* studies. Calcein was used as a model drug and ultrasound was applied to expand the liquid droplets to gas, rupture the bilayer and release the calcein from eLiposomes.

7.1.1 Effect of Ultrasound Intensity on Release from eLiposomes

The effect of acoustic intensity was examined by applying 20 kHz ultrasound at intensities from 0.5 W/cm^2 to 5 W/cm^2 for 200 milliseconds (ms), following which the percentage of release was measured. It was hypothesized that by increasing the ultrasound intensity, calcein release should increase. As Figure 25 shows, increasing the intensity of ultrasound increases the release of calcein from eLiposomes which is always about 3-fold greater than the control that uses conventional liposomes. At 0.5 W/cm^2 the percentage of release was about 10%, and increased to 60% when the intensity increased to 5 W/cm^2. This is a remarkably high percentage of release for this short time of insonation (200 ms). The release increased fairly linearly with intensity up to 3 W/cm^2, after which point there was less change in release as intensity increased.

For comparison with numbers in the previous chapter, an intensity of 5 W/cm^2 corresponds to pressure amplitude of 387.3 kPa, assuming a plane wave. This is significantly greater than the value of 108.7 kPa, the minimum calculated to put the PFC5 droplets in a state in which they could change to a gas.

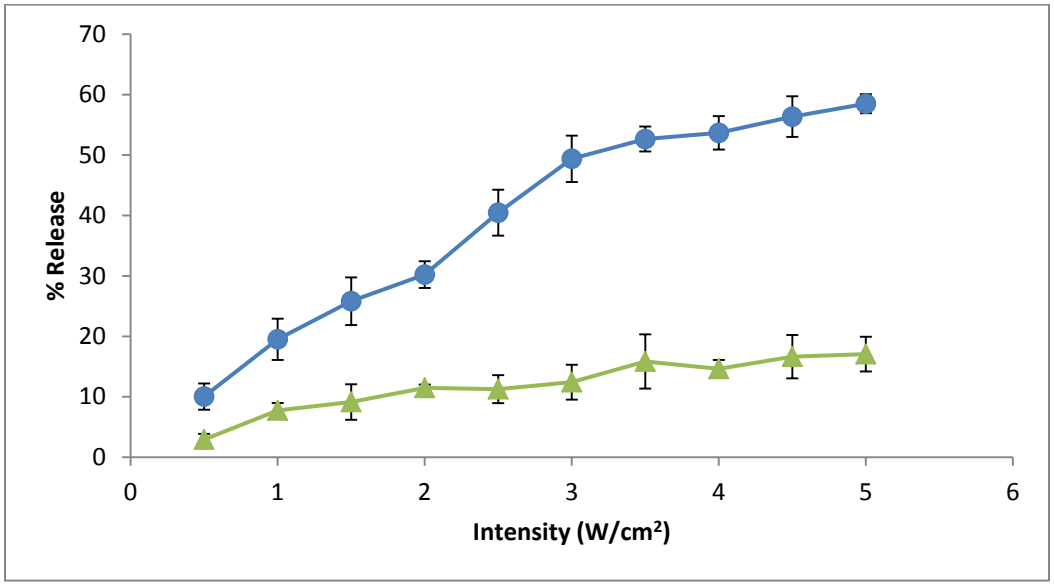

Figure 25: Calcein release from conventional liposomes (▲) and eLiposomes (●). Error bars indicate the standard deviation of repeat experiments (n≥3). Ultrasound was applied for 200 ms. eLiposomes and conventional liposomes were about 200 nm and had PEG in their bilayer.

7.1.2 Effect of Insonation Time on Release from eLiposomes

Figure 26 shows the effect of insonation time on the release from eLiposomes exposed to 3 different acoustic intensities. In this experiment the insonation time was varied from 200 ms to 20 seconds and intensity was applied at 0.5 W/cm^2 (Figure 26A), 1.0 W/cm^2 (Figure 26B) and 1.5 W/cm^2 (Figure 26C). As can be seen in Figures 26A-C, increasing the insonation time increased the amount of release from eLiposomes. In Figure 26A, the amount of release increased from 6.5% to 59% at 23°C and from 20 % to 73 % at 37°C as insonation time reached 20s. The maximum release from the negative control (conventional liposomes, without emulsion droplets) increased from 11% to 23% which is less than half of the release from eLiposomes at

the same condition (37°C), and this difference is statistically significant ($p < 0.05$). The same trend was observed in the data shown in Figures 26B and 26C.

As was presented in section 3.2, increasing the insonation intensity increased the amount of release; in this study it was observed that the maximum amount of release was at 1.5 W/cm^2 (both at 23°C and 37°C) and the minimum was at 0.5 W/cm^2. The increase in calcein release from eLiposomes at each point was statistically significant from 0.5 W/cm^2 to 1.5 W/cm^2 point ($p < 0.05$).

A negative control was also conducted in which eLiposomes containing calcein were submitted to the entire release procedure, except that no ultrasound was applied. These sham experiments showed no evidence of calcein leakage in the absence of insonation (see Figure 26A-C).

Figures 26A-C show significant release at 200 ms, suggesting that the rate of release is very high in the initial time of exposure. The rate of release was calculated as the difference in % release divided by the time span. These rates are plotted in Figures 26D-F with the rate as the ordinate point and the midpoint of the time interval as the abscissa. It is seen that the release rates are very high at the commencement of insonation. At longer times, the rate and amount of release are independent of ultrasound intensity and insonation time.

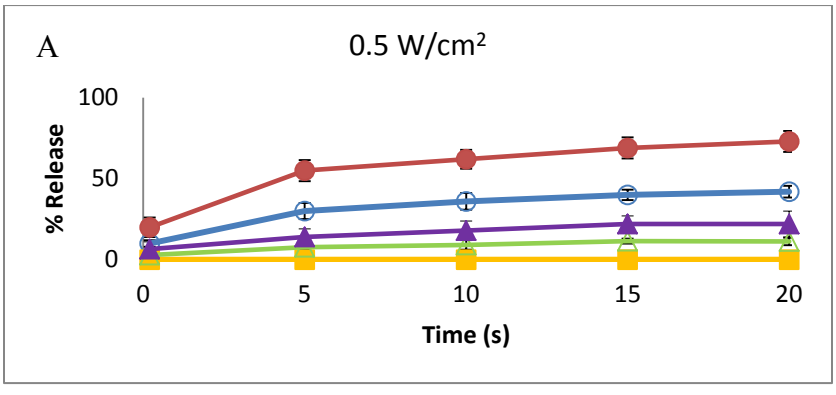

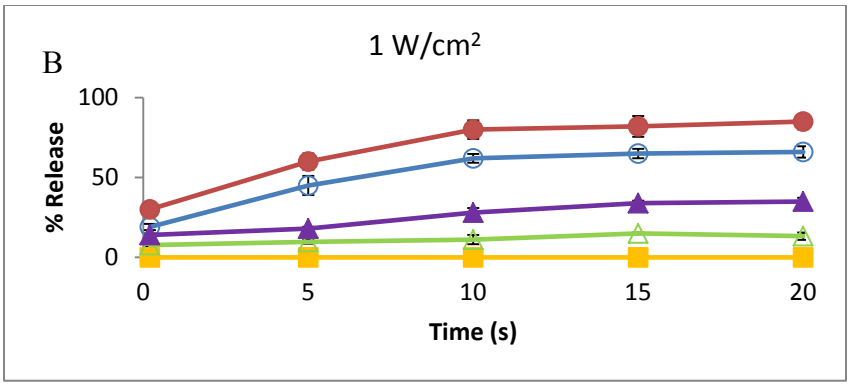
B
1 W/cm2
100
50
0
% Release
0
5
10
15
20
Time (s)

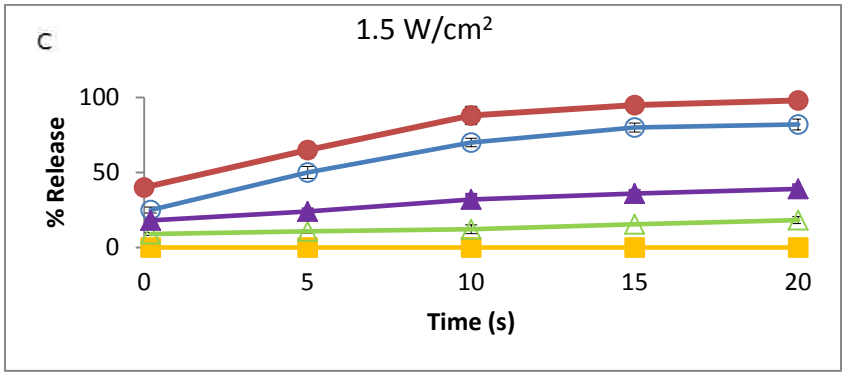
C
1.5 W/cm2
100
50
0
% Release
0
5
10
15
20
Time (s)

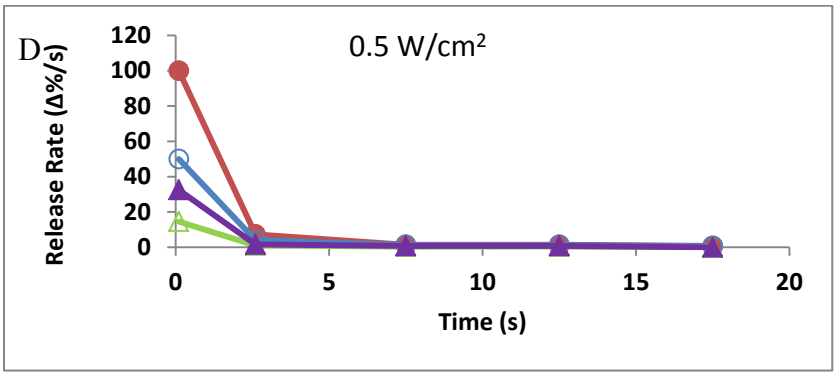
D
0.5 W/cm2
120
100
80
60
40
20
0
Release Rate (Δ%/s)
0
5
10
15
20
Time (s)

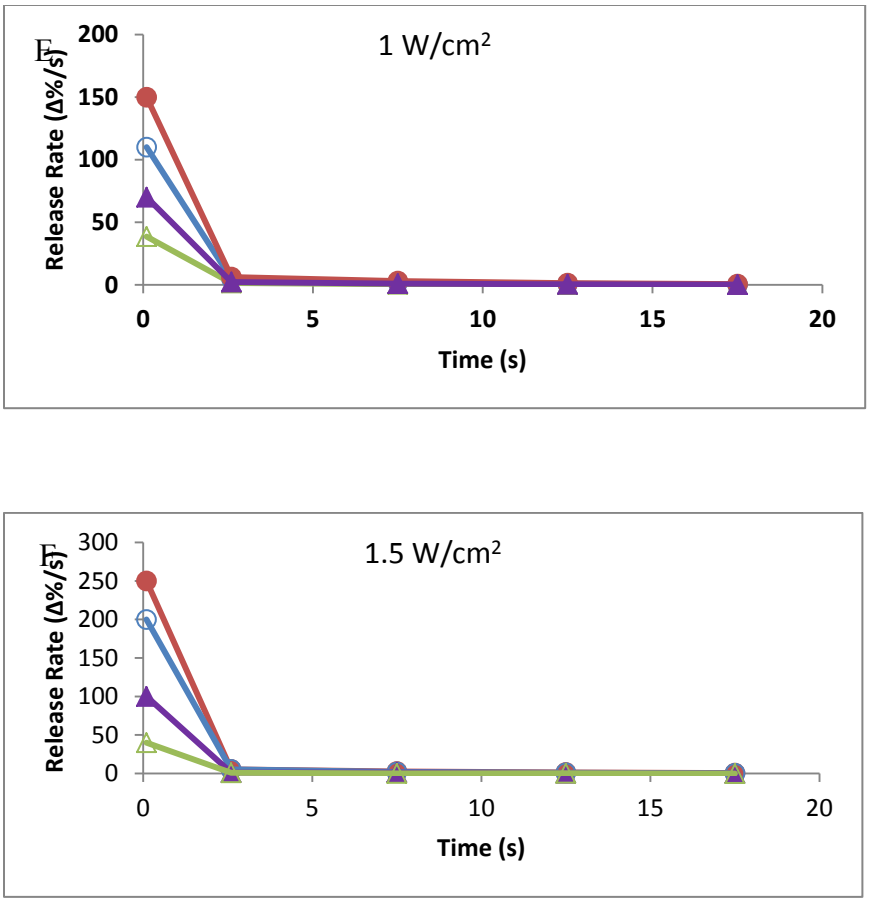

Figure 26: Calcein release and release rates from liposomes (Δ) and eLiposomes (O) at 23°C, and liposomes (▲) and eLiposomes (●) at 37°C, and negative control (■). Figures A-C show the accumulated release at A) 0.5 W/cm^2, B) 1 W/cm^2, C) 1.5 W/cm^2. Error bars indicate the standard deviation of repeat experiments (n≥3). eLiposomes and conventional liposomes were about 200 nm and had PEG in their bilayer. Figures D-F plot the release rate estimated by numerical differentiation of the cumulative release, using a central difference algorithm. E) 0.5 W/cm^2, F) 1 W/cm^2, G) 1.5 W/cm^2. In E, F and G, the x-axis values indicate the center of the time interval in which release happened.

7.1.3 Effect of Temperature on Release from eLiposomes

Several experiments were conducted to examine the role of PFC vapor pressure in the acoustically activated release. The first set of experiments was done to test the hypothesis that more release would occur at higher temperature because the PFC5 vapor pressure is higher. 20 kHz ultrasound was applied for 200 ms at 0.5 W/cm^2 to 5 W/cm^2 on samples at 23°C and 37°C,

and the release was measured (see Figure 27). Although changing the temperature increased the release, increase was not as large as would be attributed to the increase in vapor pressure of PFC5 from 79.4 KPa at 23°C to 132.3KPa at 37°C. The amount of release from eLiposomes was at least 2-fold higher than from conventional liposomes at both temperatures. Each point represents the average of at least 3 experiments.

Although temperature has a statistically significant effect, the increase in release is not proportional to the increase in vapor pressure as the temperature changed.

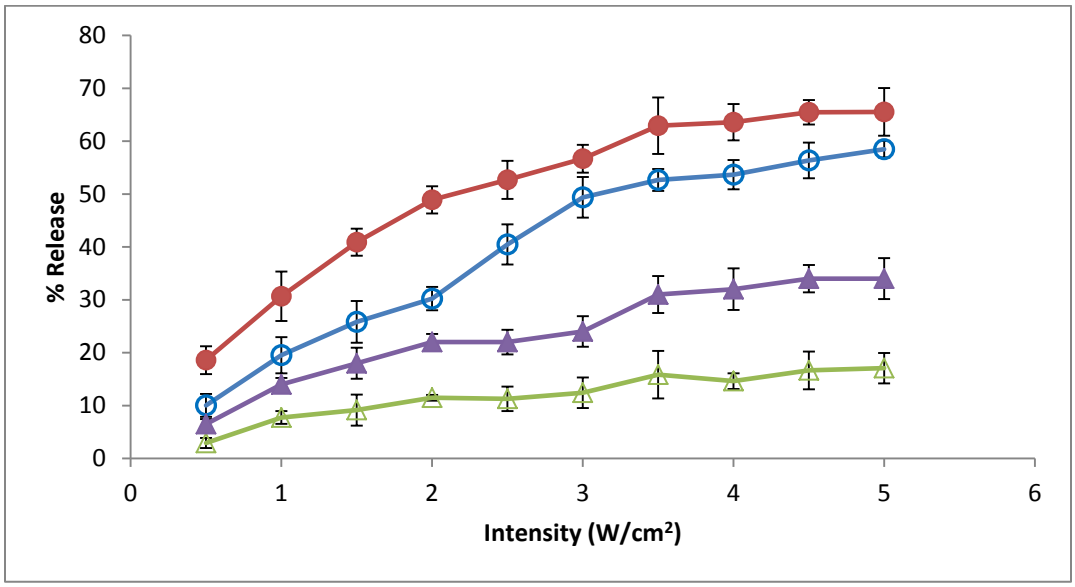

Figure 27: Calcein release from liposomes (Δ) and PFC5 eLiposomes (o) at 23°C and liposomes (▲) and PFC5 eLiposomes (●) 37°C. Error bars indicate the standard deviation of repeat experiments (n≥3). Ultrasound was applied for 200 ms to eLiposomes and conventional liposomes were about 200 nm and had PEG in their bilayer.

7.1.4 Effect of Perfluorocarbon Composition on Release from eLiposomes

The second set of experiments varied the vapor pressure of the emulsion droplets by varying the composition between pure PFC5 and pure PFC6. While previous studies were done to observe the effect of different compositions of acoustically active nanodroplets of PFC5 and PFC6 on their size [149], no studies have examined the effect of mixed perfluorocarbons on the release from eLiposomes. Five different mixtures were prepared in mole ratios of PFC5/PFC6: 100/0, 75/25, 50/50, 25/75 and 0/100. These different formulations of emulsion droplets were encapsulated inside the eLiposomes, and ultrasound intensity was varied between 1.25 W/cm^2 and 5 W/cm^2. Figure 28 shows the calcein released from these eLiposomes. Ultrasound was applied for 500 ms in each experiment, and each experiment was repeated at least 3 times.

As expected, increasing intensity enlarged the release for all droplet formulations. Those with highest vapor pressure released more calcein than those with lower vapor pressure. By increasing the intensity from 1.25 W/cm^2 to 5 W/cm^2 the release from PFC6 increased from 10% to 24%. Release from PFC5 increased from 29% to 53% by changing the intensity from 1.25 W/cm^2 to 5 W/cm^2. The total amount of release from PFC5 was much higher than PFC6 (29% release from PFC5 compared to 10% release from PFC6 at 1.25 W/cm^2). Similar trends were observed in different combinations. By increasing the molar percentage of PFC5 the amount of release increased which is attributed to the high vapor pressure of PFC5. It was also observed that the mixture of 50 mol% PFC5 and 50 mol% PFC6 produced release somewhere between pure PFC6 and PFC5. The data were replotted in Figure 29 to look for correlations with vapor pressure. This will be discussed later.

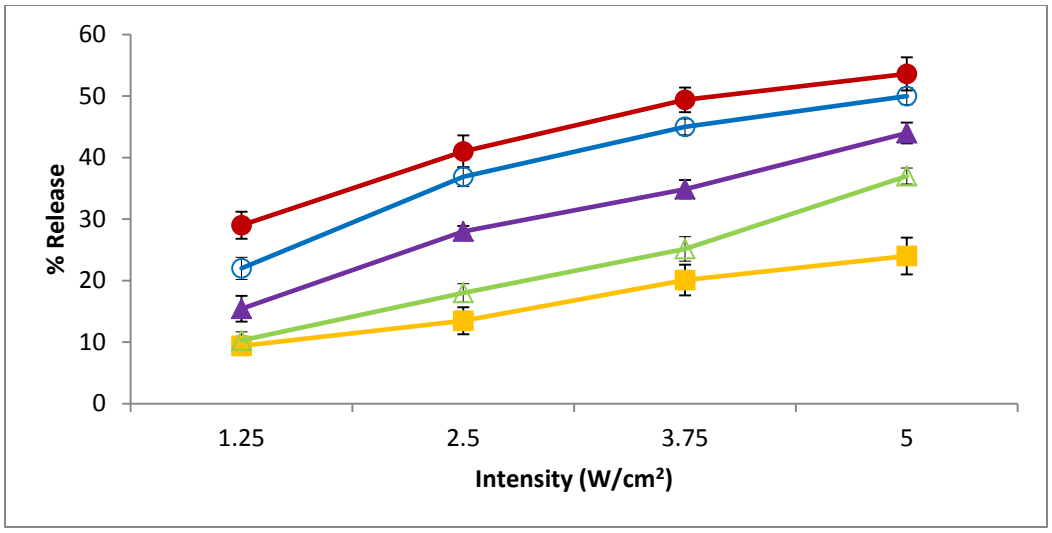

Figure 28: Calcein release from eLiposomes containing droplets of various mole ratios of PFC5/PFC6: 100/0 (●), 75/25 (o), 50/50 (▲), 25/75 (Δ), and 0/100 (■). Error bars indicate the standard deviation of repeat experiments (n≥3). Ultrasound was applied for 500 ms to eLiposomes that were about 200 nm in diameter and had PEG in their bilayer.

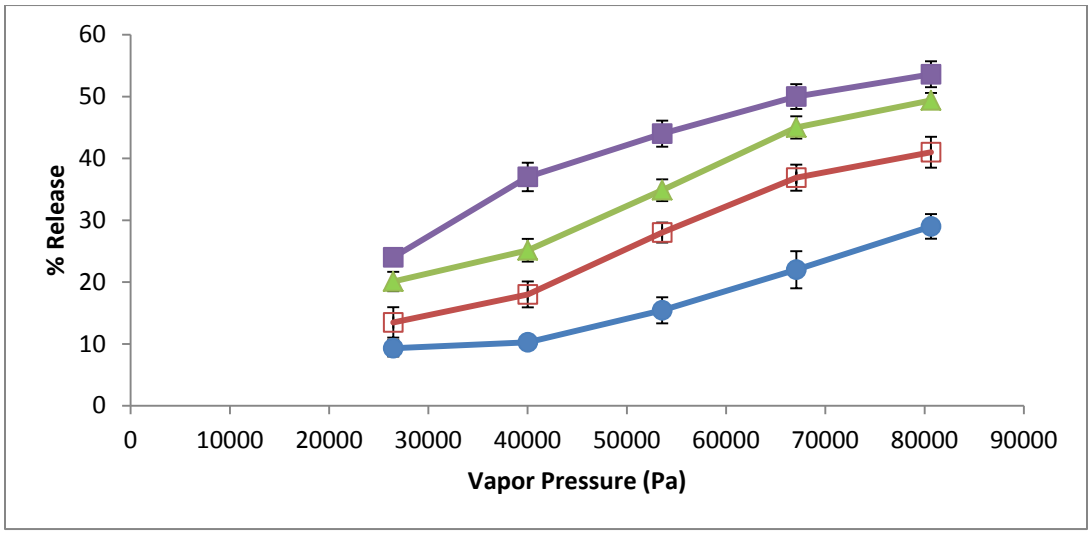

Figure 29: Calcein release from eLiposomes as a function of the calculated vapor pressure of the PFC droplets and the ultrasound intensity. 1.25 W/cm^2 (●) 2.5 W/cm^2 (□), 3.75 W/cm^2 (▲) and, 5 W/cm^2 (■) Error bars indicate the standard deviation of repeat experiments (n≥3). Ultrasound was applied for 500 ms. The eLiposomes were about 200 nm in diameter and had PEG in their bilayer.

7.1.5 Effect of Storage Time on Release from eLiposomes

Liposomes are one of the promising candidates for drug carrier systems. However, the practical application of liposomes in a drug delivery system is dependent upon the stability of the vesicles over long time periods during storage. Aggregation, degradation and coalescent processes might change the properties of the eLiposomes to store and release drugs. The stability of eLiposomes was determined by measuring amount of calcein escape from eLiposomes for 7 weeks at room temperature and at 4°C (see Figure 30).

Measurement of the release (without insonation) of calcein from eLiposomes shows that eLiposomes release less calcein at 4°C compared to eLiposomes at 23°C, suggesting that cold temperature increases the integrity of the eLiposomal bilayer.

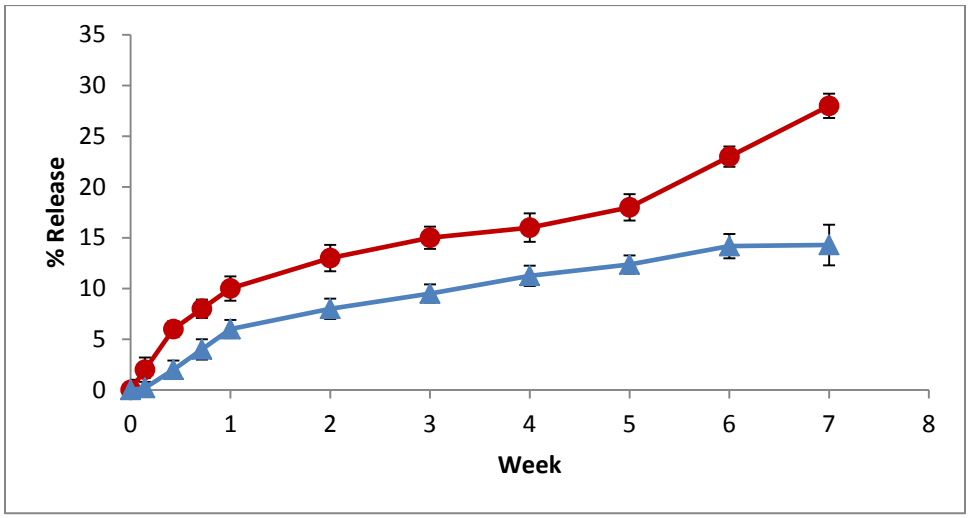

Figure 30: Premature release (without any insonation) of calcein from eLiposome at 4°C (▲) and 23°C (●). Error bars indicate the standard deviation of repeat experiments (n≥3). eLiposomes and conventional liposomes were about 200 nm in diameter and had PEG in their bilayer.

7.2 **Discussion**

The objectives of this study were to observe the effect of ultrasound amplitude, sonication time, temperature and emulsion compositions on release from eLiposomes.

eLiposomes were successfully made with PFC5 or with PFC6 emulsion droplets encapsulated within; cryo-TEM micrographs taken with a tilting stage showed that liquid PFCs droplets are inside the liposomes, not above or below the image of the liposome's bilayer. Dynamic light scattering was used to measure the size of emulsions and eLiposomes. In most experiments PFC5 emulsions were used because of their high vapor pressure, low toxicity, low solubility and stability in an aqueous phase [103, 104]. PFC6 emulsions also have low toxicity and solubility, and appear to be stable. However, the vapor pressure of PFC6 is about one third that of PFC5. For example the vapor pressure of PFC6 at 37°C is the same as that of PFC5 at 11°C.

The percentage of calcein release was measured at 23°C for eLiposomes and conventional liposomes (no emulsion droplet inside). Results suggested that emulsion droplets play an essential role in release from eLiposomes because release from eLiposomes was much higher than from conventional liposomes without droplets.

Figure 26 shows that increasing the intensity increased the release from eLiposomes. At 37°C and 20 seconds of insonation at 0.5 W/cm^2, calcein release was about 73%; this number increases to 85% and 98% at 1 W/cm^2 and 1.5 W/cm^2. This observation suggests that increasing the intensity makes more emulsion droplets vaporize and disrupts more eLiposomes. Similar results were observed at 23°C. In all these experiments, the negative control conventional liposomes showed less release compared to eLiposomes containing liquid PFC5 droplets inside. These observations show the important role of emulsions in producing release. Negative control

experiment did not show any release within the time frame of the experiment, suggesting that not only is ultrasound necessary to release calcein from eLiposomes, but these vesicles do not leak in the absence of ultrasound.

It was hypothesized that temperature change can alter three things; vapor pressure, membrane stiffness and rate of nucleation. The effect of temperature on release from eLiposomes was examined in this research (see Figure 27) by measuring release at 23°C and 37°C. The normal boiling point of PFC5 is 29°C, but because of the high Laplace pressure within these very small droplets, they can still be stable at temperatures higher than their normal boiling point [48, 52]. This creates a metastable PFC5 emulsion droplet that is easily disrupted by ultrasound. Results did not show a large difference between release at 23°C and 37°C, indicating that increasing the vapor pressure by 66% did not increase the release by this same amount.

The release from eLiposomes at 23°C changed from 10% at 0.5 W/cm^2 to 60% at 5 W/cm^2. By increasing the temperature to 37°C the release started at 20% at 1 W/cm^2 and went up to 65% at 5 W/cm^2 respectively for eLiposomes. At 5 W/cm^2 release from control experiment increased from 17% at 23°C to 35% at 37°C, which suggests that at higher temperature DMPC chains are not as tight, independent of the presence of emulsion droplets. However, this release was in the presence of ultrasound, so cavitating bubbles that naturally occur in fluid may have stressed the membranes. It is unknown if the same amount of "natural" cavitation occurs at both temperatures or if there is more "natural" cavitation at 37°C. Gas is less soluble in water at higher temperature so it is possible that there is more cavitational activity at 37°C.

As it was shown in this dissertation, emulsion droplets potentially can increase the release form eLiposomes. Understanding how the formulation variables influence release may help predict the *in vivo* behavior of targeted eLiposomes and the design of successful preparations.

Figure 28 shows release from different formulations of emulsion droplets. It was shown that by increasing the portion of PFC5 in emulsion formulations, the release was increased, which might be due to higher vapor pressure of emulsion droplets.

Figure 29 shows the relationship between vapor pressure and release from eLiposomes containing different compositions of emulsion droplets. If calcein release were only a function of vapor pressure, then all lines would go linearly through zero. This was not the case and the lack of strict correlation between vapor pressure and release suggests that other physical phenomena might be involved, such as the rate of nucleation of PFC bubbles or the presence of "natural" bubbles causing additional cavitation.

A liquid (such as PFC droplets) that has a vapor pressure above the surrounding local pressure already has a thermodynamic driving force to vaporize to gas. There are some reasons that this phase change might not happen immediately when the local pressure drops below the vapor pressure. First, a phase change from liquid to gas requires energy (enthalpy of vaporization); and second, a nucleation event must occur to initiate the formation of the gas phase. Nucleation is a stochastic event, so even when there is a thermodynamic potential for vaporization, the liquid droplets may not instantly boil. We hypothesize that the rate of nucleation of a gas phase might only have a small increase from 23°C to 37°C, so that vaporization and subsequent calcein release is not very different at these two temperatures even though the vapor pressure has been raised significantly.

The eLiposomes appear to be very stable at 4°C up to seven weeks (Figure 30); more leakage from vesicles at room temperature may correlate with the DMPC phase change from the ordered gel phase to the disordered liquid crystalline phase. At temperatures above the lipid transition temperature, lipid bilayer is not as mechanically rigid so it may become more

permeable and the contents inside the bilayer may be released slowly overtime. In this experiment no sonication was done so all the release was from bilayer leakage, from spontaneous gas formation and subsequent rupture, or from coalescence of aggregating eLiposomes. Having PEG in the bilayer of liposomes may reduce the transition temperature to less than 23°C [150]. In such a case (reduced T_m), the lipid physical state will change from the ordered gel phase (where the hydrocarbon chains are fully extended and closely packed), to the disordered liquid crystalline phase, (where the hydrocarbon chains are more randomly oriented), and that change will increase the permeability of the eLiposomes at room temperature.

8 DELIVERY OF PACLITAXEL, DOXORUBICIN AND SIRNA USING ELIPOSOMES

8.1 Introduction

Paclitaxel (PTX) is one of the major anti-cancer drugs that is used widely for lung, ovarian and breast cancer. Paclitaxel is hydrophobic and is not soluble in water. To inject PTX into a patient, it must first be dissolved in Cremophor EL (polyethoxylated castor oil) and ethanol, which causes serious side effects [151]. To avoid the side effects and provide delivery of PTX directly to the cytosol, we are developing eLiposomes as a triggerable carrier. eLiposomes containing PTX (eLipoTax) were prepared as described in section 4.2.7, and HeLa cell lines were used for measuring cell viability after adding the formulation to cells. We studied the effect of PFC5 eLipoTax, ultrasound and folate on cell viability.

Doxorubicin (Dox) is an anticancer drug which is slightly soluble in water. This drug is also used in treatment of a wide variety of cancers, including lung, breast, thyroid, stomach, and bladder. Patients who are receiving free Dox show very serious side effects such as cardiotoxicity. However, Dox encapsulated in DMPC liposomes have much less cardiotoxicity and other side effects, and it is more effective against tumors than free Dox [152]. We encapsulated Dox inside the eLiposomes (eLipoDox) to avoid the side effects of free Dox and provide a triggerable release mechanism for cytosolic delivery.

In this chapter we show necessary elements for delivering PTX to cells. Some experiments in delivering siRNA were also done. siRNA with a sequence complementary to a section of mRNA of the phosducin-like protein (PhLP) [153] was encapsulated inside the eLiposomes to knockdown the expression of PhLP inside the HeLa cells. These experiments are also described in this chapter.

8.2 Delivery of Paclitaxel to Cells Using eLiposomes

8.2.1 Effect of Ultrasound in Delivery of eLipoTax

The first set of PTX experiments was designed to establish that the application of low intensity ultrasound could release PTX to the interior of the HeLa cells and reduce cell viability. eLipoTax samples were prepared with PFC5 nanodroplets and PTX nanoparticles. Folate was attached to the outer surface of the eLipoTax using the same DSPE-PEG-folate used previously. After preparation of eLiposomes, the DSPE-PEG-folate (1.2 mol%) was added and the mixture was incubated for an hour . HeLa cells were grown in 12-well plates. Ultrasound (20 kHz, 2 seconds at 1 W/cm^2) was applied to 3 wells containing eLipoTax and was not applied to 3 other wells. Cell viability was counted using a hemocytometer at 6, 24 and 48 hours after applying the ultrasound.

As shown in Figure 31, cell viability was highest with no PTX added to the cells and was lowest with cells exposed to eLipoTax and ultrasound. The control is a liposome empty of all drug and emulsion. Percentage of cell viability was calculated by dividing the cell count at zero hour. The data show that addition of eLipoTax without applying US was less toxic than free PTX, which suggests that encapsulating the PTX particles in the eLiposomes reduced the toxicity

of the PTX. Furthermore, application of ultrasound was beneficial, perhaps by breaking open the endosome membrane and releasing the drug to the cytosol. Each result is the average of at least 3 experiments.

At 24 and 48 hours post insonation, the decreased viability following insonation is statically significant. Viability appears 5% within 48 hours of sonication after incubation with folated eLipoTax.

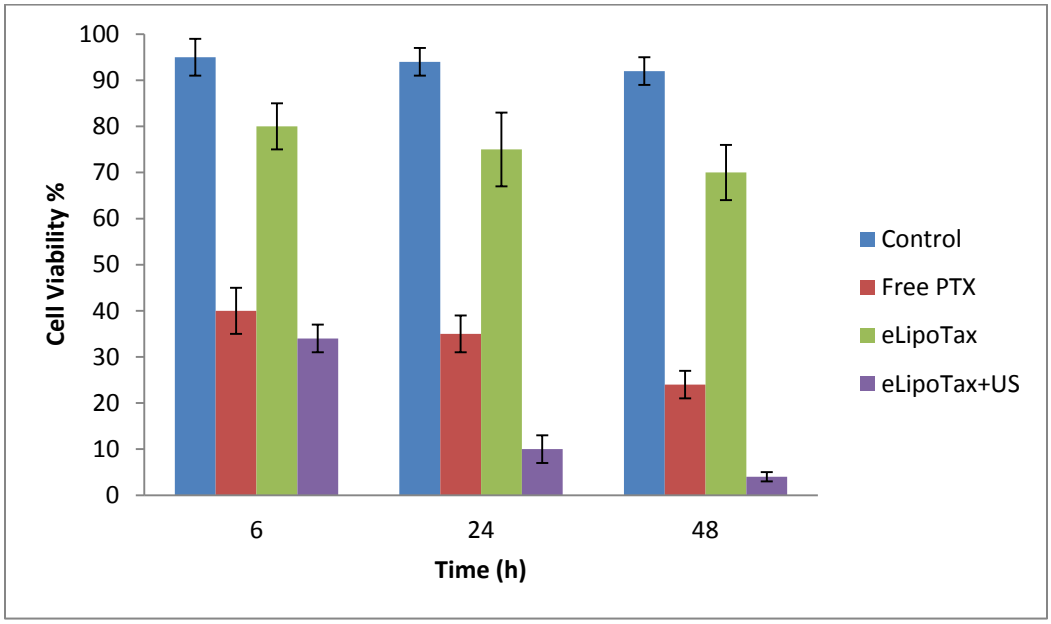

Figure 31: Effect of ultrasound on cell viability of HeLa cells after incubation with various formulations for 15 min before insonation. Insonation was done at 1 W/cm^2 for 2 seconds. Error bars show the standard deviations (n≥ 3).

8.2.2 Effect of Emulsion on PTX release

While Figure 31 shows that ultrasound is necessary to reduce cell viability after exposure to folated eLipoTax, Figure 32 indicates the requirement of PFC5 emulsion droplets for increased toxicity. In these experiments, folated eLipoTax containing PFC5 emulsion droplets,

and folated conventional liposomes containing PTX (without emulsions) were prepared. 200 uL of each sample was added to cells and cells were incubated for 6, 24 and 48 hours before counting for cell viability. In experiments with ultrasound, insonation occurred 15 min after addition of eLipoTax.

Again cell viability was measured as a function of incubation time, and the results are shown in Figure 32. Each bar is the average of at least 3 experiments and error bars are standard deviations.

Figure 32 shows the cell viability of control, free PTX (the same concentration as added to eLiposomes), liposomes containing PTX, and eLipoTax. It was observed that not only is ultrasound necessary to deliver PTX, but also emulsion droplets inside the eLiposome play an important role. Each result is the average of at least 3 experiments. The control had the highest percentage of cell viability, most probably due to absence of any PTX.

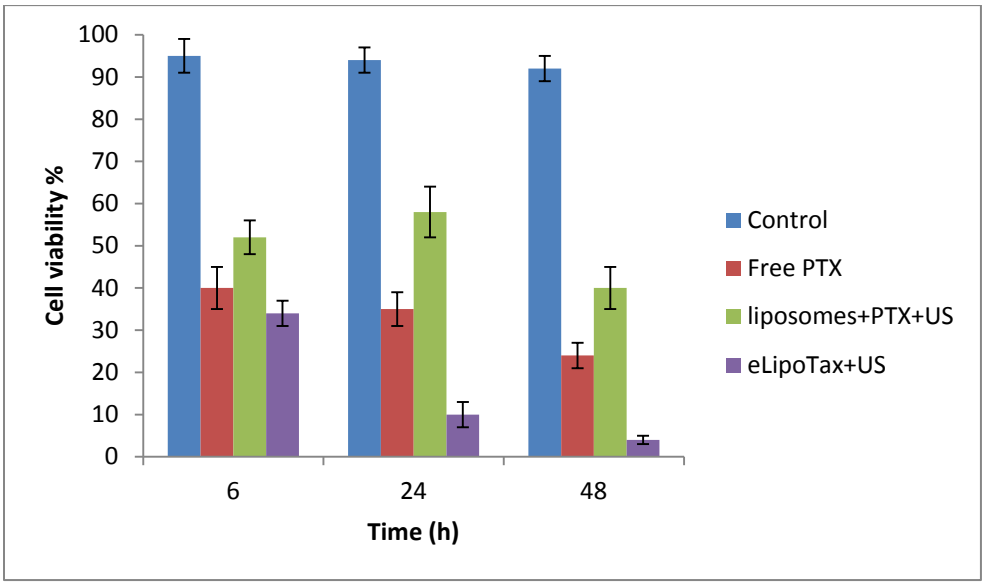

Figure 32: Effect of emulsion droplets on cell viability of HeLa cells after incubation with various formulations at various times. Insonation was done at 1W/cm^2 for 2 seconds. Error bars are standard deviations (n=3).

8.2.3 Effect of Folate

Having established the requirement for both ultrasound and emulsions within the eLipoTax to produce delivery of PTX, the next set of experiments investigated the role of folate as a necessary ligand. Parallel experiments were conducted using eLiposomes containing PTX, which were prepared with and without DSPE-PEG2000-folate incorporated into the eLipoTax bilayer. The same size aliquot (200 μL) and procedure were used in these experiments, including the same ultrasonic exposure (1 W/cm^2 for 2seconds). As shown in Figure 33, the control cells were not exposed to any drugs or US and there was nearly 100% cell viability. Samples exposed to free PTX showed 20 to 40% viability, which decreased with time. eLiposomes without folate showed 40 to 60% viability. Cells exposed to folated eLipoTax and ultrasound had 5 to 30% viability, which decreased with time. Viability was similar ($p>0.05$) for eLipoTax without folate and folated eLipoTax applied to cells competitively blocked folate receptors.

These observations suggest that when folate was absent, comparatively few PTX-containing eLiposomes were endocytosed and thus not many PTX-containing eLiposomes were within the cell to release their payload and kill cells. On the other hand, when folate ligands were present, there was a statistically significant decrease in cell viability following insonation.

In a control experiment before adding the eLipoTax, some soluble folate (6-8 mg/mL) was added to the folate-starved cells to fill their folate receptors. In this case, high cell viability was observed after insonation, suggesting that relatively few PTX-containing eLiposomes were endocytosed under conditions of competitive inhibition by free folate. This data set is not different from viability of cell exposed to non-folated eLipoTax and ultrasound. These data indicate that both folate on the eLiposome and available folate receptors on the cells are required for PTX release within the cells upon insonation of the cells.

The results from studies of the cell viability after exposure to with eLipoTax support the hypothesis that emulsion droplets are necessary to break open the eLiposome and endosome and release PTX inside the cells (Figure 32). Without having emulsion droplets inside the eLiposomes, the high viability of exposure to conventional liposomes containing PTX suggests that the drug was not released inside the cell when the cell was insonated. Also when emulsion droplets were encapsulated inside the liposomes but there was no insonation to change their phase from liquid to gas, the PTX had little effect, suggesting that it was not released to the cytosol (Figure 31). We suppose it remained in the endosome and was digested.

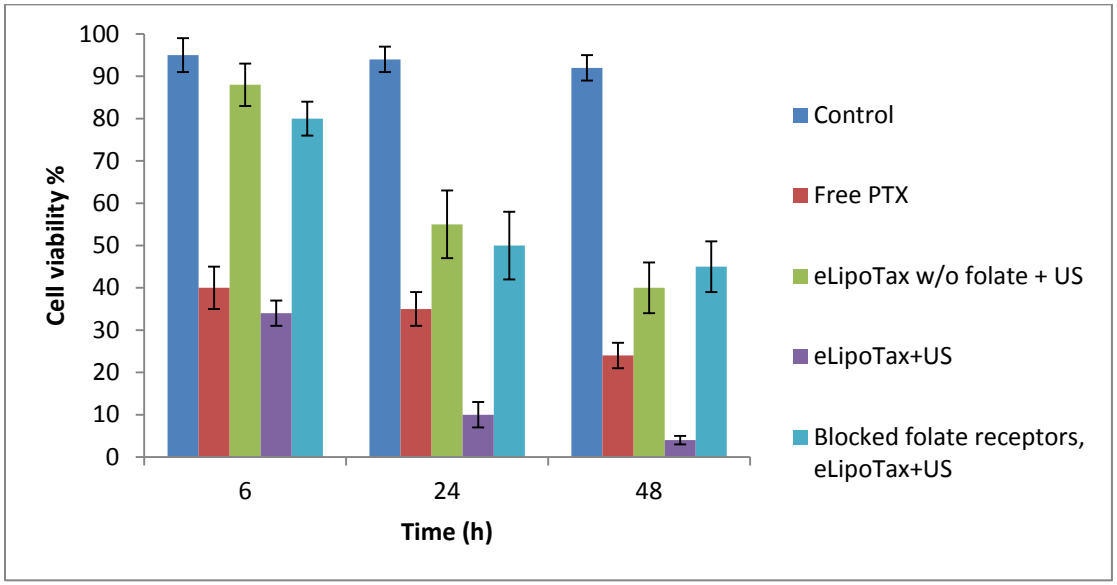

Figure 33: Effect of folate on cell viability of HeLa cells after incubation with eLiposomes at various times. Insonation was done at 1 W/cm^2 for 2 seconds. Error bars are standard deviations (n=3).

Folate is also another important ligand required for efficient delivery from eLipoTax. Folate attached to the outside of the eLiposome bilayer binds to the folate receptors of the cell and induces the endocytosis. When folate receptors of cells are blocked (by adding an extra

amount of free folate) before adding the folated eLipoTax, we posit that less of eLipoTax was endocytosed, which means there was less eLipoTax inside the endosome when it was insonated.

In all of these data, we posit that cell viability correlates with the delivery of intact PTX to the cell cytosol, which is the compartment where PTX acts on the cell by stabilizing the filaments and arresting cell division. Thus these viability experiments are proposed to correlate with cytosolic delivery of PTX.

8.3 **Delivery of Doxorubicin to the Cells Using eLiposomes**

As part of my lab responsibilities, I assisted Dr. Chung-Yin Lin in (a postdoc in our group) and Erika Handly (an undergraduate) in developing a procedure to load Dox into eLiposomes. Dox is loaded commercially into conventional liposomes by a "remote" loading technique employing a Dox concentration gradient. It is based on the commercial loading procedure, but differs because the presence of PFC5 precludes heating eLiposomes to high temperatures. The method developed with Dr. Lin has been published with myself as a co-author [154]. It differs slightly from the method developed with Erika Handly in that Dr. Lin runs the Dowex column equilibrated with and eluted with ammonium sulfate, while Erika Handly equilibrates and elutes with PBS. Dr. Lin also does the final Dox loading incubation at 4°C while Erika does Dox loading at room temperature and achieves a much higher loading efficiency.

Because I assisted in the development of the eLipoDox and not the generation of the data of Dox loading and Dox delivery to cells, those results are not presented as part of my dissertation. Erika Handly plans to present her results in a BYU Honors Thesis at a later date.

Successful encapsulation of Dox in eLiposomes was verified by Dr. Lin using UV-vis spectroscopy and HPLC [154]. Dr. Lin also showed successful release of Dox using fluorescent

spectroscopy and delivery to HeLa cells as evidenced by confocal microscopy and reduced cell viability.

8.4 **Delivery of siRNA to HeLa cells using eLiposomes**

We prepared some eLiposomes with siRNA encapsulated inside. The siRNA sequence was designed to knockdown Phosducin-like protein (PhLP) in the cell. We used the same siRNA that Chris Tracy has used to successfully knockdown PhLP in Dr. Willardson's lab at BYU. As was mentioned earlier, exquisite cleanliness in siRNA preparation and delivery is very important. All chemicals and equipment that were used for siRNA delivery must be RNAse free (RNAse enzymes destroy RNA.). eLiposomes with specific siRNA to knockdown PhLP and nonspecific siRNA (scrambled siRNA that does not knockdown PhLP) were obtained from the lab of Dr. Willardson. Positive and negative controls were prepared as well; positive and negative controls were specific and non-specific siRNA that were delivered using Lipofectamine® instead of eLiposomes.

eLiposomes containing siRNA inside (siRNA concentration of 100 nM) were added to HeLa cells and were incubated for 2 hours before applying ultrasound. 20 kHz ultrasound ($1W/cm^2$) was used for 2 seconds. After adding eLiposomes containing siRNA, all the subsequent experiments to identify the knockdown of proteins were done by Christopher Tracy (PhD candidate in Dr. Willardson's lab).

Figure 34 shows a polyacrylamide gel of the protein from the various experiments. The first column on the left is the ladder (molecular-weight size marker), which is a set of standard proteins of known sizes that are used to identify the approximate size of proteins in the other columns. Columns 2-4 are proteins extracted from cells exposed to non-specific siRNA

encapsulated in eLiposomes, columns 5-7 are proteins from experiments using specific (anti-PhLP) siRNA encapsulated in eLiposomes, column 8 is the negative Lipofectamine control, and column 9 is the positive Lipofectamine control.

The second row from the bottom is where we are looking for the knock down. As it was shown on the photograph of the gel, all columns except the last one (column 9) has some grey color indicating that PhLP knockdown did not happen successfully. Column 9 shows very little grey which indicates the knockdown was successful with the Lipofectamine positive control. This experiment shows that delivery of siRNA was successful with the Lipofectamine positive control but not with siRNA encapsulated in eLiposomes. This indicates that delivery of siRNAs with eLiposomes was not successful, or that if delivery occurred, it was not as efficient as the positive control.

As was described above, the knockdown experiments involving eLiposomes were not successful. It was hypothesized that not enough siRNA was delivered to the cells. Lack of delivery might have been due to several reasons: 1. In this experiment eLiposomes encapsulating siRNA were incubated with HeLa cells for 2 hours before sonication which might have resulted in some degradation of free (and unprotected) siRNA. We incubated our eLiposomes for two hours to be consistent with the plasmid experiment that we did before. 2. Some siRNA might have been delivered, but it was not enough to knockdown the mRNA and PhLP production sufficiently to be detected on the blot. 3. Encapsulation efficiency of eLiposomes might be low, so less siRNA than expected was encapsulated. 4. In eLiposomes preparation, some RNAse might be present which may have degraded the siRNA.

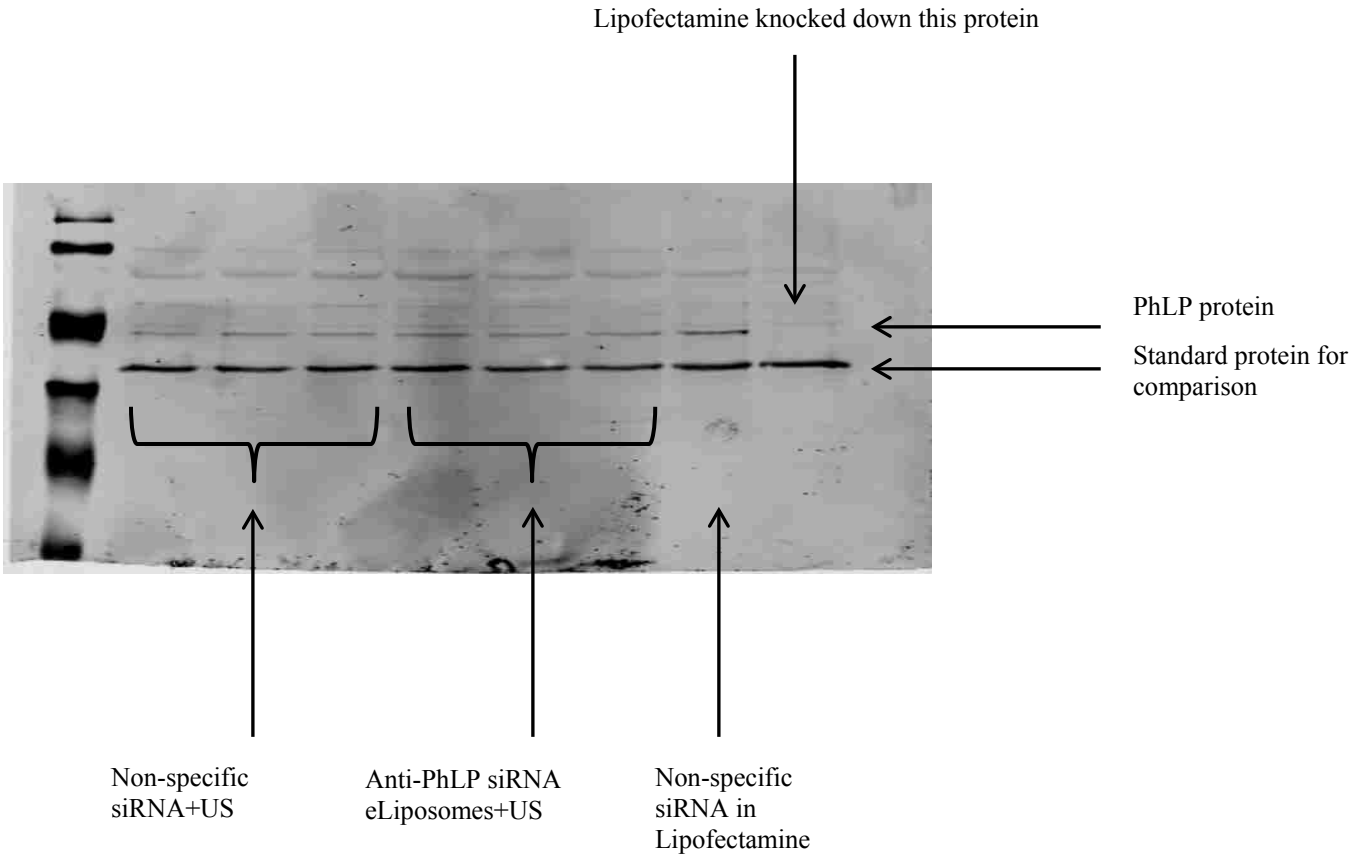

Figure 34: PhLP blot. First column on left is the ladder (molecular-weight size marker), columns 2-4 are non-specific siRNA encapsulated in eLiposomes, columns 5-7 are specific siRNA encapsulated in eLiposomes, column 8 is the negative non-specific Lipofectamine control, and column 9 is the positive Lipofectamine control.

9 CONCLUSIONS AND RECOMMENDATIONS

9.1 Conclusions

In this dissertation research I have constructed two new types of eLiposomes (1-step and ultra) containing both PFC5 and PFC6 emulsions. The 1-step eLiposome method requires the use of a phosphoacid to stabilize the emulsion and a phosphatidylcholine to form the eLiposome bilayer; but we have found no such restrictions in the production of ultra eLiposomes. Preparation of eLiposomes in 1-step is faster than the 2-step method of Lattin et al. [104], but it has its own limitations. For example emulsion droplets prepared with negatively charged surfactants and liposomes with negatively charged surfactants cannot produce eLiposomes. Preparation of eLiposomes in ultra method is faster and it has no limitations with respect to surfactants that we have tried to date.

We have shown that emulsions encapsulated within the eLiposome and folate attached to the surface of the eLiposomes, are required to deliver significant amounts of calcein to the cytosol of these cells. This strongly supports our hypothesis that folated eLiposomes are taken into endosomes, and that insonation ruptures both the eLiposome and endosome.

We have successfully encapsulated several compounds inside the new eLiposomes. These are a model drug (calcein), DNA plasmid, PTX, and Dox. The eLiposomes could be

modified with folate and PEG respectively on their outer surface as an active targeting ligand to bind to the receptors of HeLa cancer cells and as stealth polymer chains to reduce clearance in blood. Successful folate targeting and subsequent endocytosis were demonstrated in several experiments.

Upon exposure to ultrasound, the emulsion droplets are postulated to change their phase from liquid to gas and cause the lipid bilayer to rupture in a manner to release drug or gene payload. This study supports this hypothesis and shows release from eLiposomes upon insonation and much less delivery of calcein, plasmid and PTX when no ultrasound was applied.

This study revealed the essential components of the eLiposome delivery vehicle. Internal emulsions in combination with ultrasound were found to be necessary to obtain measurable release of calcein or protein expression from a GFP plasmid. Without either ultrasound or internal PFC5 emulsion droplets, delivery was significantly lower ($p < 0.05$). Delivery appeared to be fairly independent of the time and intensity of the applied ultrasound, at least within the parameters explored in this study.

eLiposomes can be formed that are small enough to be extravasated within the leaky capillary network of many tumors. In my work, the sizes ranged from 200-500 nm in diameter. Optimal size for extravasation is 50-300 nm [155]. Thus this delivery technique is triple targeting: extravasation employs passive targeting to allow collection of eLiposomes at a tumor site; and active folate targeting attaches the eLiposome to the target cell. The attachment induces endocytosis; both of these are modes of spatial targeting. Most importantly, ultrasonically triggered targeting, a form of both temporal and spatial targeting, causes acoustic droplet vaporization only at the focal point of the ultrasound and releases the therapeutic payload from the eLiposome and endosome directly to the cytosol of triple-targeted cells. Although spatial

targeting was not demonstrated in this work, we posit that focused insonation at higher frequencies can provide spatial triggered targeting as well as temporal targeting.

As presented in previous chapters, ultrasound-sensitive eLiposomes were made which encapsulate emulsion droplets and calcein. These exhibited more calcein release when insonated than did conventional liposomes without emulsions. Release from eLiposomes was measured and showed that increasing the insonation time and intensity increases release from eLiposomes. Some subsequent experiments were done to test the hypothesis that changing the temperature, which changes the vapor pressure, will proportionally change the release. Surprisingly increasing temperature did not produce an effect that was directly proportional to the increase in vapor pressure. To test the hypothesis that vapor pressure is the only driving force, a set of experiments were done using mixtures of perfluorocarbons; it was concluded that other factors such as nucleation may also play a large role in the phase change of emulsion droplets. I have not changed the emulsion droplet size to examine the effect of Laplace pressure on vaporization. The results from this study show the importance of structure of the eLiposome and its effect in drug delivery.

Ultrasound sensitive eLipoTax and eLipoDox were made. Using eLipoTax and ultrasound increased the cytotoxicity of the PTX compared to free PTX, supporting the hypothesis that this carrier was endocytosed and the PTX released to the cytosol by insonation.

Ultrasound sensitive eLiposomes containing siRNA were made. Results did not show protein knockdown which indicates the need for further investigation.

9.2 Recommendations

In this dissertation research, two new therapeutic systems were developed and one was studied extensively. However, more research needs to be done to increase the understanding of the physics and chemistry of this technology to increase the usefulness and efficiency of these nanoparticles.

I suggest further study in the following areas.

1. In 1-step preparation, we found out negatively charged emulsion droplets and positively charged liposomes can make eLiposomes, but we were not sure why other combinations did not make eLiposomes. More investigation needs to be done to discover the reason and potentially exploit those chemical principles to make better eLiposomes.
2. The encapsulation efficiency of the eLiposomes is still very low, only around 4% for calcein and plasmid. Theory and experiments need to be developed to explore techniques to increase the encapsulation efficiency.
3. The pillow density separation is still a very complicated method for separating empty liposomes, non-encapsulated emulsions, and the eLiposomes. An easier method for separation should be developed.
4. More quantitative methods to measure the encapsulation efficiency of therapeutics (such as PTX and siRNA) should be developed. This might include using some analytical instruments such as HPLC.
5. All these studies were done using 20 kHz ultrasound. This ultrasound is difficult to focus and cannot be used in clinical applications. Higher frequency ultrasound like 1 MHz and 3 MHz should be considered. However, according to Lattin [156] the

release at higher frequency will be lower. Techniques to increase release at higher frequency should be explored.

6. The effects of cholesterol, PEG chains, and new combination of various lipids for making liposome bilayers should be explored, as this might affect encapsulation and also release efficiency from eLiposomes. Cholesterol is usually required for *in vivo* applications. It was used to make eLipoTax, but was not used in other constructs.
7. Follow up experiments could to be done to find out the reason that siRNA delivery form eLiposomes was not successful in knocking down PhLP.
8. The biological mechanisms by which these nanoparticles are endocytosed still remain unknown. This should be explored further by using inhibitors for various endocytosis pathways.
9. Even though numerous experiments were conducted with cells and confocal microscopy, the best way to keep the cells healthy while doing confocal microscopy can be improved. It would also be very useful to grow cells on a slide that can be insonated and also inserted directly into the confocal microscope.
10. The amount of release of calcein and PTX from eLiposomes to the cell is unknown. Some more detailed experiments should be done to more quantitatively measure uptake.
11. In the long run, all the experiments conducted *in vitro* should be done *in vivo*, preferably in mouse or rat models of tumors.

10 REFERENCES

[1] V. Torchilin, Passive and Active Drug Targeting: Drug Delivery to Tumors as an Example, in: M. Schäfer-Korting (Ed.) Drug Delivery, Springer Berlin Heidelberg, 2010, pp. 3-53.

[2] D.M. McDonald, P. Baluk, Significance of Blood Vessel Leakiness in Cancer, Cancer Research, 62 (2002) 5381-5385.

[3] H. Maeda, T. Sawa, T. Konno, Mechanism of tumor-targeted delivery of macromolecular drugs, including the EPR effect in solid tumor and clinical overview of the prototype polymeric drug SMANCS, Journal of Controlled Release, 74 (2001) 47-61.

[4] S. Jin, K. Ye, Nanoparticle-Mediated Drug Delivery and Gene Therapy, Biotechnology Progress, 23 (2007) 32-41.

[5] Y.H. Bae, K. Park, Targeted drug delivery to tumors: myths, reality and possibility, J Control Release, 153 (2011) 198-205.

[6] S.V. Vinogradov, T.K. Bronich, A.V. Kabanov, Nanosized cationic hydrogels for drug delivery: preparation, properties and interactions with cells, Advanced Drug Delivery Reviews, 54 (2002) 135-147.

[7] D.E. Owens, N.A. Peppas, Opsonization, biodistribution, and pharmacokinetics of polymeric nanoparticles, International Journal of Pharmaceutics, 307 (2006) 93-102.

[8] A.N. Lukyanov, V.P. Torchilin, Micelles from lipid derivatives of water-soluble polymers as delivery systems for poorly soluble drugs, Advanced Drug Delivery Reviews, 56 (2004) 1273-1289.

[9] G.A. Husseini, M.A. Diaz de la Rosa, E.S. Richardson, D.A. Christensen, W.G. Pitt, The role of cavitation in acoustically activated drug delivery, Journal of Controlled Release, 107 (2005) 253-261.

[10] H.A.H. Rongen, A. Bult, W.P. van Bennekom, Liposomes and immunoassays, Journal of Immunological Methods, 204 (1997) 105-133.

[11] A.D. Bangham, Liposomes: the Babraham connection, Chemistry and Physics of Lipids, 64 (1993) 275-285.

[12] A. Sharma, U.S. Sharma, Liposomes in drug delivery: Progress and limitations, International Journal of Pharmaceutics, 154 (1997) 123-140.

[13] H. Lv, S. Zhang, B. Wang, S. Cui, J. Yan, Toxicity of cationic lipids and cationic polymers in gene delivery, Journal of Controlled Release, 114 (2006) 100-109.

[14] C.-H. Huang, Phosphatidylcholine vesicles. Formation and physical characteristics, Biochemistry, 8 (1969) 344-352.

[15] E.S. Richardson, W.G. Pitt, D.J. Woodbury, The Role of Cavitation in Liposome Formation, Biophysical Journal, 93 (2007) 4100-4107.

[16] G. Gregoriadis, Immunological adjuvants: a role for liposomes, Immunology Today, 11 (1990) 89-97.

[17] G. Gregoriadis, N. Garcon, H. da Silva, B. Sternberg, Coupling of ligands to liposomes independently of solute entrapment: observations on the formed vesicles, Biochimica et Biophysica Acta (BBA) - Biomembranes, 1147 (1993) 185-193.

[18] H. Schreier, J. Bouwstra, Liposomes and niosomes as topical drug carriers: dermal and transdermal drug delivery, Journal of Controlled Release, 30 (1994) 1-15.

[19] J.N. Herron, C.A. Gentry, S.S. Davies, W. Ai-ping, L. Jinn-nan, Antibodies as targeting moieties: affinity measurements, conjugation chemistry and applications in immunoliposomes, Journal of Controlled Release, 28 (1994) 155-166.

[20] C.B. Hansen, G.Y. Kao, E.H. Moase, S. Zalipsky, T.M. Allen, Attachment of antibodies to sterically stabilized liposomes: evaluation, comparison and optimization of coupling procedures, Biochimica et Biophysica Acta (BBA) - Biomembranes, 1239 (1995) 133-144.

[21] E.T. Kisak, B. Coldren, C.A. Evans, C. Boyer, J.A. Zasadzinski, The vesosome - A multicompartment drug delivery vehicle, Current Medicinal Chemistry, 11 (2004) 199-219.

[22] M.S. Inayat, A.C. Bernard, V.S. Gallicchio, B.A. Garvy, H.L. Elford, O.R. Oakley, Oxygen carriers: A selected review, Transfus Apher Sci, 34 (2006) 25-32.

[23] M.P. Krafft, A. Chittofrati, J.G. Riess, Emulsions and microemulsions with a fluorocarbon phase, Curr Opin Colloid In, 8 (2003) 251-258.

[24] J. Bibette, F. Leal-Calderon, Surfactant-stabilized emulsions, Current Opinion in Colloid & Interface Science, 1 (1996) 746-751.

[25] S.M. Moghimi, A.C. Hunter, T.L. Andresen, Factors Controlling Nanoparticle Pharmacokinetics: An Integrated Analysis and Perspective, Annu Rev Pharmacol, 52 (2012) 481-503.

[26] W.H. De Jong, P.J. Borm, Drug delivery and nanoparticles:applications and hazards, Int J Nanomedicine, 3 (2008) 133-149.

[27] R. Kenneth S. Schmitz and George D. J. Phillies, An Introduction to Dynamic Light Scattering by Macromolecules, American Institute of Physics, 1990.

[28] K. Tachibana, S. Tachibana, The Use of Ultrasound for Drug Delivery, Echocardiography, 18 (2001) 323-328.

[29] S. Mitragotri, Healing sound: the use of ultrasound in drug delivery and other therapeutic applications, Nat Rev Drug Discov, 4 (2005) 255-260.

[30] G.A. Husseini, W.G. Pitt, Micelles and nanoparticles for ultrasonic drug and gene delivery, Advanced Drug Delivery Reviews, 60 (2008) 1137-1152.

[31] W.G. Pitt, G.A. Husseini, B.J. Staples, Ultrasonic drug delivery – a general review, Expert Opinion on Drug Delivery, 1 (2004) 37-56.

[32] L.D. Johns, Nonthermal effects of therapeutic ultrasound: the frequency resonance hypothesis, Journal of athletic training, 37 (2002) 293-299.

[33] K. Ferrara, R. Pollard, M. Borden, Ultrasound microbubble contrast agents: Fundamentals and application to gene and drug delivery, Annu Rev Biomed Eng, 9 (2007) 415-447.

[34] E.A. Brujan, T. Ikeda, Y. Matsumoto, Jet formation and shock wave emission during collapse of ultrasound-induced cavitation bubbles and their role in the therapeutic applications of high-intensity focused ultrasound, Phys Med Biol, 50 (2005) 4797-4809.

[35] D.P. Guo, X.Y. Li, P. Sun, Y.B. Tang, X.Y. Chen, Q. Chen, L.M. Fan, B. Zang, L.Z. Shao, X.R. Li, Ultrasound-targeted microbubble destruction improves the low density lipoprotein receptor gene expression in HepG(2) cells, Biochemical and Biophysical Research Communications, 343 (2006) 470-474.

[36] A. Lawrie, A.F. Brisken, S.E. Francis, D.C. Cumberland, D.C. Crossman, C.M. Newman, Microbubble-enhanced ultrasound for vascular gene delivery, Gene Therapy, 7 (2000) 2023-2027.

[37] K. Tachibana, T. Uchida, K. Tamura, H. Eguchi, N. Yamashita, K. Ogawa, Enhanced cytotoxic effect of Ara-C by low intensity ultrasound to HL-60 cells, Cancer Letters, 149 (2000) 189-194.

[38] V.G. Zarnitsyn, M.R. Prausnitz, Physical parameters influencing optimization of ultrasound-mediated DNA transfection, Ultrasound in Medicine and Biology, 30 (2004) 527-538.

[39] T.G. Leighton, What is ultrasound?, Progress in Biophysics & Molecular Biology, 93 (2007) 3-83.

[40] S. Miura, K. Tachibana, T. Okamoto, K. Saku, In vitro transfer of antisense oligodeoxynucleotides into coronary endothelial cells by ultrasound, Biochemical and Biophysical Research Communications, 298 (2002) 587-590.

[41] P. Prentice, A. Cuschierp, K. Dholakia, M. Prausnitz, P. Campbell, Membrane disruption by optically controlled microbubble cavitation, Nature Physics, 1 (2005) 107-110.

[42] R.K. Schlicher, H. Radhakrishna, T.P. Tolentino, R.P. Apkarian, V. Zarnitsyn, M.R. Prausnitz, Mechanism of intracellular delivery by acoustic cavitation, Ultrasound in Medicine and Biology, 32 (2006) 915-924.

[43] Z. Gao, A.M. Kennedy, D.A. Christensen, N.Y. Rapoport, Drug-loaded nano/microbubbles for combining ultrasonography and targeted chemotherapy, Ultrasonics, 48 (2008) 260-270.

[44] N. Rapoport, Z.G. Gao, A. Kennedy, Multifunctional nanoparticles for combining ultrasonic tumor imaging and targeted chemotherapy, J Natl Cancer I, 99 (2007) 1095-1106.

[45] P.S. Sheeran, S.H. Luois, L.B. Mullin, T.O. Matsunaga, P.A. Dayton, Design of ultrasonically-activatable nanoparticles using low boiling point perfluorocarbons, Biomaterials, 33 (2012) 3262-3269.

[46] R. Singh, G.A. Husseini, W.G. Pitt, Phase transitions of nanoemulsions using ultrasound: Experimental observations, Ultrasonics Sonochemistry, 19 (2012) 1120-1125.

[47] B.D. Spiess, Perfluorocarbon emulsions as a promising technology: a review of tissue and vascular gas dynamics, Journal of Applied Physiology, 106 (2009) 1444-1452.

[48] P.S. Sheeran, S. Luois, P.A. Dayton, T.O. Matsunaga, Formulation and Acoustic Studies of a New Phase-Shift Agent for Diagnostic and Therapeutic Ultrasound, Langmuir, 27 (2011) 10412-10420.

[49] P.S. Sheeran, V.P. Wong, S. Luois, R.J. McFarland, W.D. Ross, S. Feingold, T.O. Matsunaga, P.A. Dayton, Decafluorobutane as a Phase-Change Contrast Agent for Low-Energy Extravascular Ultrasonic Imaging, Ultrasound in Medicine and Biology, 37 (2011) 1518-1530.

[50] M.L. Fabiilli, Ultrasound-triggered Drug Delivery Using Acoustic Droplet Vaporization, in: Biomedical Engineering, Univeristy of Michigan, 2012.

[51] M.L. Fabiilli, K.J. Haworth, N.H. Fakhri, O.D. Kripfgans, P.L. Carson, J.B. Fowlkes, The role of inertial cavitation in acoustic droplet vaporization, IEEE Trans Ultrason Ferroelectr Freq Control, 56 (2009) 1006-1017.

[52] T. Giesecke, K. Hynynen, Ultrasound-mediated cavitation thresholds of liquid perfluorocarbon droplets in vitro, Ultrasound Med Biol, 29 (2003) 1359-1365.

[53] K. Maruyama, O. Ishida, T. Takizawa, K. Moribe, Possibility of active targeting to tumor tissues with liposomes, Advanced Drug Delivery Reviews, 40 (1999) 89-102.

[54] V.P. Torchilin, Multifunctional nanocarriers, Advanced Drug Delivery Reviews, 58 (2006) 1532-1555.

[55] A. VertutDoi, H. Ishiwata, K. Miyajima, Binding and uptake of liposomes containing a poly(ethylene glycol) derivative of cholesterol (stealth liposomes) by the macrophage cell line J774: Influence of PEG content and its molecular weight, Bba-Biomembranes, 1278 (1996) 19-28.

[56] A. Jain, S.K. Jain, In vitro and cell uptake studies for targeting of ligand anchored nanoparticles for colon tumors, European Journal of Pharmaceutical Sciences, 35 (2008) 404-416.

[57] T.M. Allen, Ligand-targeted therapeutics in anticancer therapy, Nature Reviews Cancer, 2 (2002) 750-763.

[58] L. Brannon-Peppas, J.O. Blanchette, Nanoparticle and targeted systems for cancer therapy, Advanced Drug Delivery Reviews, 64, Supplement (2012) 206-212.

[59] N. Kasahara, A. Dozy, Y. Kan, Tissue-specific targeting of retroviral vectors through ligand-receptor interactions, Science, 266 (1994) 1373-1376.

[60] P. Holliger, P.J. Hudson, Engineered antibody fragments and the rise of single domains, Nat Biotech, 23 (2005) 1126-1136.

[61] C. Brignole, D. Marimpietri, C. Gambini, T.M. Allen, M. Ponzoni, F. Pastorino, Development of Fab' fragments of anti-GD2 immunoliposomes entrapping doxorubicin for experimental therapy of human neuroblastoma, Cancer Letters, 197 (2003) 199-204.

[62] F. Marcucci, F. Lefoulon, Active targeting with particulate drug carriers in tumor therapy: fundamentals and recent progress, Drug Discovery Today, 9 (2004) 219-228.

[63] M.R. Safarnejad, G.S. Jouzani, M. Tabatabaie, R.M. Twyman, S. Schillberg, Antibody-mediated resistance against plant pathogens, Biotechnology Advances, 29 (2011) 961-971.

[64] B. Stella, S. Arpicco, M.T. Peracchia, D. Desmaële, J. Hoebeke, M. Renoir, J. D'Angelo, L. Cattel, P. Couvreur, Design of folic acid-conjugated nanoparticles for drug targeting, Journal of Pharmaceutical Sciences, 89 (2000) 1452-1464.

[65] A. Gabizon, H. Shmeeda, A.T. Horowitz, S. Zalipsky, Tumor cell targeting of liposome-entrapped drugs with phospholipid-anchored folic acid-PEG conjugates, Advanced Drug Delivery Reviews, 56 (2004) 1177-1192.

[66] S.A. Kularatne, P.S. Low, Targeting of nanoparticles: folate receptor, Methods Mol Biol, 624 (2010) 249-265.

[67] R.J. Lee, L. Huang, Folate-targeted, Anionic Liposome-entrapped Polylysine-condensed DNA for Tumor Cell-specific Gene Transfer, Journal of Biological Chemistry, 271 (1996) 8481-8487.

[68] A.D. Miller, Cationic Liposomes for Gene Therapy, Angewandte Chemie International Edition, 37 (1998) 1768-1785.

[69] R.J. Lee, P.S. Low, Folate-Targeted Liposomes for Drug Delivery, Journal of Liposome Research, 7 (1997) 455-466.

[70] R.J. Lee, P.S. Low, Folate-Mediated Tumor-Cell Targeting of Liposome-Entrapped Doxorubicin in-Vitro, Bba-Biomembranes, 1233 (1995) 134-144.

[71] J.M. Saul, A. Annapragada, J.V. Natarajan, R.V. Bellamkonda, Controlled targeting of liposomal doxorubicin via the folate receptor in vitro, Journal of Controlled Release, 92 (2003) 49-67.

[72] Y.J. Lu, P.S. Low, Folate-mediated delivery of macromolecular anticancer therapeutic agents, Advanced Drug Delivery Reviews, 54 (2002) 675-693.

[73] S.C. Kim, D.W. Kim, Y.H. Shim, J.S. Bang, H.S. Oh, S.W. Kim, M.H. Seo, In vivo evaluation of polymeric micellar paclitaxel formulation: toxicity and efficacy, Journal of Controlled Release, 72 (2001) 191-202.

[74] C. Dumontet, B.I. Sikic, Mechanisms of action of and resistance to antitubulin agents: Microtubule dynamics, drug transport, and cell death, J Clin Oncol, 17 (1999) 1061-1070.

[75] K.C. Nicolaou, J.J. Liu, Z. Yang, H. Ueno, E.J. Sorensen, C.F. Claiborne, R.K. Guy, C.K. Hwang, M. Nakada, P.G. Nantermet, Total Synthesis of Taxol .2. Construction of a-Ring and C-Ring Intermediates and Initial Attempts to Construct the Abc Ring-System, Journal of the American Chemical Society, 117 (1995) 634-644.

[76] K.C. Nicolaou, P.G. Nantermet, H. Ueno, R.K. Guy, E.A. Couladouros, E.J. Sorensen, Total Synthesis of Taxol .1. Retrosynthesis, Degradation, and Reconstitution, Journal of the American Chemical Society, 117 (1995) 624-633.

[77] K.C. Nicolaou, H. Ueno, J.J. Liu, P.G. Nantermet, Z. Yang, J. Renaud, K. Paulvannan, R. Chadha, Total Synthesis of Taxol .4. The Final Stages and Completion of the Synthesis, Journal of the American Chemical Society, 117 (1995) 653-659.

[78] K.C. Nicolaou, Z. Yang, J.J. Liu, P.G. Nantermet, C.F. Claiborne, J. Renaud, R.K. Guy, K. Shibayama, Total Synthesis of Taxol .3. Formation of Taxols Abc Ring Skeleton, Journal of the American Chemical Society, 117 (1995) 645-652.

[79] K.C. Nicolaou, Z. Yang, J.J. Liu, H. Ueno, P.G. Nantermet, R.K. Guy, C.F. Claiborne, J. Renaud, E.A. Couladouros, K. Paulvannan, E.J. Sorensen, Total Synthesis of Taxol, Nature, 367 (1994) 630-634.

[80] A.K. Singla, A. Garg, D. Aggarwal, Paclitaxel and its formulations, Int J Pharm, 235 (2002) 179-192.

[81] Y. Liu, J. Sun, W. Cao, J. Yang, H. Lian, X. Li, Y. Sun, Y. Wang, S. Wang, Z. He, Dual targeting folate-conjugated hyaluronic acid polymeric micelles for paclitaxel delivery, Int J Pharm, 421 (2011) 160-169.

[82] P. Crosasso, M. Ceruti, P. Brusa, S. Arpicco, F. Dosio, L. Cattel, Preparation, characterization and properties of sterically stabilized paclitaxel-containing liposomes, J Control Release, 63 (2000) 19-30.

[83] M.L. Immordino, F. Dosio, L. Cattel, Stealth liposomes: review of the basic science, rationale, and clinical applications, existing and potential, Int J Nanomedicine, 1 (2006) 297-315.

[84] M. Ceruti, P. Crosasso, P. Brusa, S. Arpicco, F. Dosio, L. Cattel, Preparation, characterization, cytotoxicity and pharmacokinetics of liposomes containing water-soluble prodrugs of paclitaxel, J Control Release, 63 (2000) 141-153.

[85] O. Tacar, P. Sriamornsak, C.R. Dass, Doxorubicin: an update on anticancer molecular action, toxicity and novel drug delivery systems, The Journal Of Pharmacy And Pharmacology, 65 (2013) 157-170.

[86] C. Carvalho, R.X. Santos, S. Cardoso, S. Correia, P.J. Oliveira, M.S. Santos, P.I. Moreira, Doxorubicin: The Good, the Bad and the Ugly Effect, Curr. Med. Chem., 16 (2009) 3267-3285.

[87] A. Trouet, D. Deprez-De Campeneere, Daunorubicin-DNA and doxorubicin-DNA a review of experimental and clinical data, Cancer Chemotherapy and Pharmacology, 2 (1979) 77-79.

[88] A. Coates, S. Abraham, S.B. Kaye, T. Sowerbutts, C. Frewin, R.M. Fox, M.H.N. Tattersall, On the receiving end--patient perception of the side-effects of cancer chemotherapy, European Journal of Cancer and Clinical Oncology, 19 (1983) 203-208.

[89] D.D. Von Hoff, M.W. Layard, P. Basa, H.L. Davis, A.L. Von Hoff, M. Rozencweig, F.M. Muggia, Risk factors for doxorubicin-induced congestive heart failure, Annals of internal medicine, 91 (1979) 710-717.

[90] X. Chen, X. Wang, Y. Wang, L. Yang, J. Hu, W. Xiao, A. Fu, L. Cai, X. Li, X. Ye, Y. Liu, W. Wu, X. Shao, Y. Mao, Y. Wei, L. Chen, Improved tumor-targeting drug delivery and therapeutic efficacy by cationic liposome modified with truncated bFGF peptide, Journal of Controlled Release, 145 (2010) 17-25.

[91] A.A. Gabizon, Liposome circulation time and tumor targeting: implications for cancer chemotherapy, Advanced Drug Delivery Reviews, 16 (1995) 285-294.

[92] A. Wei, J.G. Mehtala, A.K. Patri, Challenges and opportunities in the advancement of nanomedicines, Journal of Controlled Release, 164 (2012) 236-246.

[93] K.A. Whitehead, R. Langer, D.G. Anderson, Knocking down barriers: advances in siRNA delivery, Nat Rev Drug Discov, 8 (2009) 129-138.

[94] A. Reynolds, D. Leake, Q. Boese, S. Scaringe, W.S. Marshall, A. Khvorova, Rational siRNA design for RNA interference, Nature biotechnology, 22 (2004) 326-330.

[95] J.M. Layzer, A.P. McCaffrey, A.K. Tanner, Z. Huang, M.A. Kay, B.A. Sullenger, In vivo activity of nuclease-resistant siRNAs, RNA, 10 (2004) 766-771.

[96] X. Pan, R. Thompson, X. Meng, D. Wu, L. Xu, Tumor-targeted RNA-interference: functional non-viral nanovectors, Am J Cancer Res, 1 (2011) 25-42.

[97] D.W. Bartlett, M.E. Davis, Insights into the kinetics of siRNA-mediated gene silencing from live-cell and live-animal bioluminescent imaging, Nucleic Acids Res, 34 (2006) 322-333.

[98] A. Muratovska, M.R. Eccles, Conjugate for efficient delivery of short interfering RNA (siRNA) into mammalian cells, FEBS Letters, 558 (2004) 63-68.

[99] I. Mellman, Endocytosis and molecular sorting, Annual Review of Cell and Developmental Biology, 12 (1996) 575-625.

[100] C.S. Pillay, E. Elliott, C. Dennison, Endolysosomal proteolysis and its regulation, Biochem. J., 363 (2002) 417-429.

[101] B.D. Chithrani, W.C.W. Chan, Elucidating the mechanism of cellular uptake and removal of protein-coated gold nanoparticles of different sizes and shapes, Nano Letters, 7 (2007) 1542-1550.

[102] A.K. Varkouhi, M. Scholte, G. Storm, H.J. Haisma, Endosomal escape pathways for delivery of biologicals, Journal of Controlled Release, 151 (2011) 220-228.

[103] J.R. Lattin, W.G. Pitt, D.M. Belnap, G.A. Husseiniz, Ultrasound-Induced Calcein Release from Eliposomes, Ultrasound in Medicine and Biology, 38 (2012) 2163-2173.

[104] J.R. Lattin, D.M. Belnap, W.G. Pitt, Formation of eLiposomes as a drug delivery vehicle, Colloid Surface B, 89 (2012) 93-100.

[105] C. Boyer, C. Evans, J.A. Zasadzinski, Encapsulation of colloidal materials in lipid membranes, Biophysical Journal, 82 (2002) 34A-34A.

[106] M. Javadi, W.G. Pitt, D.M. Belnap, N.H. Tsosie, J.M. Hartley, Encapsulating nanoemulsions inside eLiposomes for ultrasonic drug delivery, Langmuir, 28 (2012) 14720-14729.

[107] P.P. Constantinides, K.J. Lambert, A.K. Tustian, B. Schneider, S. Lalji, W. Ma, B. Wentzel, D. Kessler, D. Worah, S.C. Quay, Formulation development and antitumor activity of a filter-sterilizable emulsion of paclitaxel, Pharm Res, 17 (2000) 175-182.

[108] H. Ogawa, S. Inouye, F.I. Tsuji, K. Yasuda, K. Umesono, Localization, trafficking, and temperature-dependence of the Aequorea green fluorescent protein in cultured vertebrate cells, Proc Natl Acad Sci U S A, 92 (1995) 11899-11903.

[109] R.C. Weast, Handbook of Chemistry and Physics. , CRC Press, 1980-1981.

[110] R. Suzuki, Y. Oda, N. Utoguchi, K. Maruyama, [Development of ultrasonic cancer therapy using ultrasound sensitive liposome], Yakugaku Zasshi: Journal Of The Pharmaceutical Society Of Japan, 130 (2010) 1665-1670.

[111] K.D. Buchanan, S. Huang, H. Kim, R.C. Macdonald, D.D. McPherson, Echogenic liposome compositions for increased retention of ultrasound reflectivity at physiologic temperature, Journal of Pharmaceutical Sciences, 97 (2008) 2242-2249.

[112] Y. Ueno, S. Sonoda, R. Suzuki, M. Yokouchi, Y. Kawasoe, K. Tachibana, K. Maruyama, T. Sakamoto, S. Komiya, Combination of ultrasound and bubble liposome enhance the effect of doxorubicin and inhibit murine osteosarcoma growth, Cancer Biology & Therapy, 12 (2011) 270-277.

[113] D.A.B. Smith, S.S. Vaidya, J.A. Kopechek, S.-L. Huang, M.E. Klegerman, D.D. McPherson, C.K. Holland, Ultrasound-triggered release of recombinant tissue-type plasminogen activator from echogenic liposomes, Ultrasound In Medicine & Biology, 36 (2010) 145-157.

[114] J.A. Kopechek, T.M. Abruzzo, B. Wang, S.M. Chrzanowski, D.A.B. Smith, P.H. Kee, S. Huang, J.H. Collier, D.D. McPherson, C.K. Holland, Ultrasound-Mediated Release of Hydrophilic and Lipophilic Agents From Echogenic Liposomes, J Ultras Med, 27 (2008) 1597-1606.

[115] A.L. Klibanov, T.I. Shevchenko, B.I. Raju, R. Seip, C.T. Chin, Ultrasound-triggered release of materials entrapped in microbubble-liposome constructs: a tool for targeted drug delivery, Journal Of Controlled Release: Official Journal Of The Controlled Release Society, 148 (2010) 13-17.

[116] B. Geers, I. Lentacker, N.N. Sanders, J. Demeester, S. Meairs, S.C. De Smedt, Self-assembled liposome-loaded microbubbles: The missing link for safe and efficient ultrasound triggered drug-delivery, Journal Of Controlled Release: Official Journal Of The Controlled Release Society, 152 (2011) 249-256.

[117] E.C. Unger, T.P. McCreery, R.H. Sweitzer, V.E. Caldwell, Y.Q. Wu, Acoustically active lipospheres containing paclitaxel - A new therapeutic ultrasound contrast agent, Invest Radiol, 33 (1998) 886-892.

[118] Y.Y. Liu, H. Miyoshi, M. Nakamura, Encapsulated ultrasound microbubbles: Therapeutic application in drug/gene delivery, J Control Release, 114 (2006) 89-99.

[119] A. Schroeder, Y. Avnir, S. Weisman, Y. Najajreh, A. Gabizon, Y. Talmon, J. Kost, Y. Barenholz, Controlling liposomal drug release with low frequency ultrasound: Mechanism and feasibility, Langmuir, 23 (2007) 4019-4025.

[120] A. Schroeder, J. Kost, Y. Barenholz, Ultrasound, liposomes, and drug delivery: principles for using ultrasound to control the release of drugs from liposomes, Chem Phys Lipids, 162 (2009) 1-16.

[121] T.J. Evjen, E.A. Nilssen, S. Barnert, R. Schubert, M. Brandl, S.L. Fossheim, Ultrasound-mediated destabilization and drug release from liposomes comprising dioleoylphosphatidylethanolamine, Eur. J. Pharm. Sci., 42 (2011) 380-386.

[122] G.H. Yechezkel Barenolz, Method of Amphiphatic Drug Loading in Liposomes by PH Gradient, in: United States Patent, Yissum Research Development Company of the Hebrew University of Jerusalem, USA, 1993.

[123] E.A. Evans, R. Waugh, L. Melnik, Elastic Area Compressibility Modulus of Red-Cell Membrane, Biophysical Journal, 16 (1976) 585-595.

[124] R.R. Netz, M. Schick, Pore formation and rupture in fluid bilayers, Physical Review E, 53 (1996) 3875-3885.

[125] W.G. Pitt, R.N. Singh, K.X. Perez, G.A. Husseini, D.R. Jack, Phase transitions of perfluorocarbon nanoemulsion induced with ultrasound: A mathematical model, Ultrason Sonochem, (2013).

[126] S.-T. Kang, C.-K. Yeh, Intracellular Acoustic Droplet Vaporization in a Single Peritoneal Macrophage for Drug Delivery Applications, Langmuir, 27 (2011) 13183-13188.

[127] M. Nieuwoudt, G.H.C. Engelbrecht, L. Sentle, R. Auer, D. Kahn, S.W. van der Merwe, Non-toxicity of IV Injected Perfluorocarbon Oxygen Carrier in an Animal Model of Liver Regeneration Following Surgical Injury, Artificial Cells, Blood Substitutes and Biotechnology, 37 (2009) 117-124.

[128] O.D. Kripfgans, J.B. Fowlkes, D.L. Miller, O.P. Eldevik, P.L. Carson, Acoustic droplet vaporization for therapeutic and diagnostic applications, Ultrasound In Medicine & Biology, 26 (2000) 1177-1189.

[129] K. Shiraishi, R. Endoh, H. Furuhata, M. Nishihara, R. Suzuki, K. Maruyama, Y. Oda, J.-i. Jo, Y. Tabata, J. Yamamoto, M. Yokoyama, A facile preparation method of a PFC-containing nano-sized emulsion for theranostics of solid tumors, International Journal of Pharmaceutics, 421 (2011) 379-387.

[130] P.S. Sheeran, S. Luois, P.A. Dayton, T.O. Matsunaga, Formulation and acoustic studies of a new phase-shift agent for diagnostic and therapeutic ultrasound, Langmuir : the ACS journal of surfaces and colloids, 27 (2011) 10412-10420.

[131] P.S. Sheeran, V.P. Wong, S. Luois, R.J. McFarland, W.D. Ross, S. Feingold, T.O. Matsunaga, P.A. Dayton, Decafluorobutane as a phase-change contrast agent for low-energy extravascular ultrasonic imaging, Ultrasound in medicine & biology, 37 (2011) 1518-1530.

[132] A. Kabalnov, J. Weers, R. Arlauskas, T. Tarara, Phospholipids as Emulsion Stabilizers. 1. Interfacial Tensions, Langmuir, 11 (1995) 2966-2974.

[133] M.C. Johnson, L. Saunders, Time dependent interfacial tensions of a series of phospholipids, Chemistry and Physics of Lipids, 10 (1973) 318-327.

[134] R.K. Schlicher, J.D. Hutcheson, H. Radhakrishna, R.P. Apkarian, M.R. Prausnitz, Changes in Cell Morphology Due to Plasma Membrane Wounding by Acoustic Cavitation, Ultrasound in Medicine & Biology, 36 (2010) 677-692.

[135] R.K. Schlicher, H. Radhakrishna, T.P. Tolentino, R.P. Apkarian, V. Zarnitsyn, M.R. Prausnitz, Mechanism of intracellular delivery by acoustic cavitation, Ultrasound in Medicine & Biology, 32 (2006) 915-924.

[136] M. Javadi, W.G. Pitt, C.M. Tracy, J.R. Barrow, B.M. Willardson, J.M. Hartley, N.H. Tsosie, Ultrasonic gene and drug delivery using eLiposomes, Journal of Controlled Release, 167 (2013) 92-100.

[137] M.L. Fabiilli, K.J. Haworth, I.E. Sebastian, O.D. Kripfgans, P.L. Carson, J.B. Fowlkes, Delivery of chlorambucil using an acoustically-triggered perfluoropentane emulsion, Ultrasound Med Biol, 36 (2010) 1364-1375.

[138] M.L. Fabiilli, J.A. Lee, O.D. Kripfgans, P.L. Carson, J.B. Fowlkes, Delivery of water-soluble drugs using acoustically triggered perfluorocarbon double emulsions, Pharm Res, 27 (2010) 2753-2765.

[139] J.M. Correas, A.R. Meuter, E. Singlas, D.R. Kessler, D. Worah, S.C. Quay, Human pharmacokinetics of a perfluorocarbon ultrasound contrast agent evaluated with gas chromatography, Ultrasound Med Biol, 27 (2001) 565-570.

[140] J.R. Masters, HeLa cells 50 years on: the good, the bad and the ugly, Nat Rev Cancer, 2 (2002) 315-319.

[141] A. Gabizon, D. Tzemach, J. Gorin, L. Mak, Y. Amitay, H. Shmeeda, S. Zalipsky, Improved therapeutic activity of folate-targeted liposomal doxorubicin in folate receptor-expressing tumor models, Cancer Chemotherapy and Pharmacology, 66 (2010) 43-52.

[142] E. Bruckheimer, P. Harvie, J. Orthel, B. Dutzar, K. Furstoss, E. Mebel, P. Anklesaria, R. Paul, In vivo efficacy of folate-targeted lipid-protamine-DNA (LPD-PEG-Folate) complexes in an immunocompetent syngeneic model for breast adenocarcinoma, Cancer Gene Therapy, 11 (2004) 128-134.

[143] J.V. Abella, M. Park, Breakdown of endocytosis in the oncogenic activation of receptor tyrosine kinases, Am J Physiol-Endoc M, 296 (2009) E973-E984.

[144] K. Roepstorff, L. Grovdal, M. Grandal, M. Lerdrup, B. van Deurs, Endocytic downregulation of ErbB receptors: mechanisms and relevance in cancer, Histochem Cell Biol, 129 (2008) 563-578.

[145] J. Baulida, M.H. Kraus, M. Alimandi, P.P. DiFiore, G. Carpenter, All ErbB receptors other than the epidermal growth factor receptor are endocytosis impaired, Journal of Biological Chemistry, 271 (1996) 5251-5257.

[146] G.L. Lukacs, P. Haggie, O. Seksek, D. Lechardeur, N. Freedman, A.S. Verkman, Size-dependent DNA mobility in cytoplasm and nucleus, The Journal of biological chemistry, 275 (2000) 1625-1629.

[147] M. Afadzi, C.d.L. Davies, Y.H. Hansen, T. Johansen, Ø.K. Standal, R. Hansen, S.-E. Måsøy, E.A. Nilssen, B. Angelsen, Effect of Ultrasound Parameters on the Release of Liposomal Calcein, Ultrasound in Medicine and Biology, 38 (2012) 476-486.

[148] R.L. Rowley, W.V. Wilding, J.L. Oscarson, N.F. Giles, DIPPR® Data Compilation of Pure Chemical Properties, in, Design Institute for Physical Properties, AIChE, Brigham Young University, Provo, Utah, 2012, pp. R. L. Rowley, W. V. Wilding, J. L. Oscarson, N. F. Giles, DIPPR® Data Compilation of Pure Chemical Properties, Design Institute for Physical Properties, AIChE, http://dippr.byu.edu, Brigham Young University, Provo, Utah (2011).

[149] J.-Y. Fang, C.-F. Hung, M.-H. Liao, C.-C. Chien, A study of the formulation design of acoustically active lipospheres as carriers for drug delivery, European Journal of Pharmaceutics and Biopharmaceutics, 67 (2007) 67-75.

[150] M. Caffrey, J. Hogan, LIPIDAT: a database of lipid phase transition temperatures and enthalpy changes. DMPC data subset analysis, Chem Phys Lipids, 61 (1992) 1-109.

[151] H. Gelderblom, J. Verweij, K. Nooter, A. Sparreboom, Cremophor EL: the drawbacks and advantages of vehicle selection for drug formulation, European Journal of Cancer, 37 (2001) 1590-1598.

[152] L. Harris, G. Batist, R. Belt, D. Rovira, R. Navari, N. Azarnia, L. Welles, E. Winer, T.D.S. Group, Liposome-encapsulated doxorubicin compared with conventional doxorubicin in a randomized multicenter trial as first-line therapy of metastatic breast carcinoma, Cancer, 94 (2002) 25-36.

[153] G.L. Lukov, T. Hu, J.N. McLaughlin, H.E. Hamm, B.M. Willardson, Phosducin-like protein acts as a molecular chaperone for G protein beta gamma dimer assembly, Embo J, 24 (2005) 1965-1975.

[154] C.Y. Lin, M. Javadi, D.M. Belnap, J.R. Barrow, W.G. Pitt, Ultrasound sensitive eLiposomes containing doxorubicin for drug targeting therapy, Nanomedicine : nanotechnology, biology, and medicine, (2013).

[155] O. Ishida, K. Maruyama, K. Sasaki, M. Iwatsuru, Size-dependent extravasation and interstitial localization of polyethyleneglycol liposomes in solid tumor-bearing mice, Int J Pharm, 190 (1999) 49-56.

[156] J.R. Lattin, Ultrasound induced phase change of emulsion drplets for targeted gene and drug delivery in: Chemical Engineering, Brigham Young University, 2012.